Leon Diniz Alves

Weather-driven mathematical models of dengue transmission dynamics in twelve Brazilian sites

Brasil

2021

Leon Diniz Alves

Weather-driven mathematical models of dengue transmission dynamics in twelve Brazilian sites

Tese apresentada como requisito parcial
para obtenção do título de
Doutor em Ciências.

Fundação Oswaldo Cruz (Fiocruz)

Instituto Oswaldo Cruz (IOC)

Programa de Pós-graduação Stricto Sensu em Biologia Computacional e Sistemas

(pgBCS)

Orientador Flávio Codeço Coelho

Coorientadora Raquel Martins Lana

Brasil

2021

DINIZ ALVES, LEON.

Weather-driven mathematical models of dengue transmission dynamics in twelve Brazilian sites / LEON DINIZ ALVES. - Rio de Janeiro, 2021.
137 f.

Tese (Doutorado) – Instituto Oswaldo Cruz, Pós-Graduação em Biologia Computacional e Sistemas, 2021.

Orientador: Flávio Codeço Coelho.
Co-orientadora: Raquel Martins Lana.

Bibliografia: f. 97-108

1. dengue. 2. Transmission model. 3. Aedes aegypti. 4. environment variables. 5. tropical diseases. I. Título.

Elaborado pelo Sistema de Geração Automática de Ficha Catalográfica da Biblioteca de Manguinhos/Icict/Fiocruz com os dados fornecidos pelo(a) autor(a), sob a responsabilidade de Igor Falce Dias de Lima - CRB-7/6930.

Acknowledgements

Flávio Codeço Coelho e Raquel Martins Lana foram os melhores orientadores que poderia ter, foram respeitosos, atenciosos e sempre buscaram me fazer entender cada momento do método científico. Tenho muito a agradecer por também terem a disposição e calma para lidar com minha cabeça dura em insistir em funções e variáveis que não se mostraram no caminho certo. Fico feliz por terem confiado em mim e me guiado.

Nestes mais de 4 anos de doutorado, minha família, em especial a minha mãe, meu pai, minha noiva e minhas irmãs sempre estiverem comigo, somando às minhas forças e dando todo o oxigênio que precisava para me manter forte e concentrado neste período. Eu não estaria aqui sem seus apoios.

Também gostaria de agradecer a meus amigos e conhecidos que tiveram a paciência e a compreensão quando disse que não podia sair neste tempo de estudo. Foi muito tempo distante e muita saudade, mas o esforço se mostrou frutífero e espero encontrar a todos de agora em diante.

Resumo

Esta tese investiga modelos matemáticos para avaliar o papel das flutuações climáticas na dinâmica da dengue (DENV) de 2010 a 2019. Os modelos de transmissão propostos foram baseados em um modelo SEIR, que incorpora a transmissão vertical do vetor (mosquito fêmea para ovo) e o compartimento de ovo do vetor, permitindo assim que a chuva seja introduzida para modular a eclosão dos ovos. Dados de satélite de temperatura e precipitação ao longo de dez anos foram utilizados para modular parâmetros dos modelos. Análise de sensibilidade foi realizada para avaliar a importância de cada parâmetro. Os cenários simulados foram comparados à incidência observada de dengue. Os modelos foram capazes de capturar o padrão de incidência da dengue com boa precisão até 2016. De 2016 a 2019, o ajuste do modelo mostrou resultados piores quando comparado aos dados observáveis. Os resultados do primeiro modelo demonstram que as flutuações da transmissão vertical podem afetar a incidência, sugerindo a necessidade de investigar mais a fundo esta dinâmica. O segundo modelo apresentou um bom ajuste para 10 de 12 municípios em que foi avaliado. Os dois municípios onde o ajuste não foi satisfatório, são municípios onde houve invasão por um novo sorotipo de dengue dentro do período estudado, demonstrando a necessidade de evoluir os modelos para multi-sorotipos. A melhor compreensão da relação entre as diferentes variáveis ambientais e a dengue alcançada pelos modelos propostos pode contribuir para políticas públicas de saúde em relação às doenças transmitidas por mosquitos.

Palavras-chaves: dengue, Modelo de transmissão, *Aedes aegypti*, variáveis ambientais, doenças tropicais

Abstract

This thesis investigates two models to assess the role of climate fluctuations in dengue dynamics (DENV) from 2010 to 2019. The proposed transmission models were based on a susceptible, infected and recovered (SIR) model, which incorporates vector vertical transmission (from female mosquito to offspring) and the egg compartment of the vector, thus allowing the effect of rain to be introduced to modulate the hatching of eggs. Satellite data of temperature and precipitation over ten years were used to modulate model parameters. Sensitivity analysis was performed to assess the importance of each parameter in the model. The simulated scenarios of the models were compared to the observed incidence of dengue. The two models were able to capture the pattern of dengue incidence with good accuracy through 2016, although higher deviations were observed from 2016 to 2019. The results of the first model demonstrate that fluctuations in vertical transmission can affect rates and patterns of attack transmission, suggesting the need to further investigate this dynamic. The second model showed a good fit for 10 of the 12 municipalities in which it was evaluated. The two municipalities where the adjustment was not satisfactory were municipalities where a new dengue serotype was being re-introduced during the period of the study, demonstrating the need to enhance the models to include multi-serotypes. The better understanding of the relationship between different environmental variables and dengue achieved by the proposed models can contribute to public health policies in relation to mosquito-borne diseases.

Keywords: dengue, Transmission model, *Aedes aegypti*, environment variables, tropical diseases

List of Figures

List of Tables

List of abbreviations and acronyms

DENV	Dengue virus
DHF	Dengue Hemorrhagic Fever
DSS	Dengue Shock Syndrome
ARIMA	Autoregressive Integrated Moving Average
SSE	Sum Square Error
NDVI	Normalized Difference Vegetation Index
MODIS	Aqua Moderate Resolution Imaging Spectroradiometer
IBGE	Instituto Brasileiro de Geografia e Estatística
SI	Susceptible and Infected
SIR	Susceptible, Infected and Recovered
SEI	Susceptible, Exposed and Infected
SEIR	Susceptible, Exposed, Infected and Recovered

Contents

1 Introduction

Dengue is a viral mosquito-borne disease. The Dengue virus (DENV) transmission cycle includes primarily two vectors, *Aedes aegypti* and *Aedes albopictus*, and the transmission is through bites of the female mosquito (GUARNER; HALE, 2019). Dengue is an endemic disease in many countries worldwide, displaying marked seasonality, and its incidence and geographic distribution has been increasing in the past 40 years, particularly in countries with tropical climates where temperatures and humidity favor mosquito proliferation (RACLOZ et al., 2012; FARINELLI et al., 2018). The disease is one of the most important vector-borne diseases in the world (BHATT et al., 2013) and considered by the World Health Organization one of the 20 Neglected Tropical Diseases (NTDs), which consist of a group of diseases that disproportionately impact vulnerable populations and territories (TIDMAN; ABELA-RIDDER; CASTAÑEDA, 2021).

The ecology of the DENV vector has been widely studied and modelled taking into account temperature-dependency, which is regarded as the main seasonality driver of this disease(FOCKS et al., 1993; OTERO; SOLARI; SCHWEIGMANN, 2006; LIMA et al., 2014). Deterministic models, such as the SIR/SEIR (Susceptible (S), Exposed (E), Infectious (I) and Recovered (R)) model have often been employed to model DENV transmission dynamics(SIDE; NOORANI, 2013; HUBER et al., 2018; CHANPRASOPCHAI; TANG; PONGSUMPUN, 2018).

Existing DENV transmission models methodology and parameters vary substantially (ANDRAUD et al., 2012; LAURA et al., 2019), but many recognize that environmental fluctuations are key to understanding mosquito population dynamics. Temperature, for example, modulates oviposition, survival rates, biting rates and the extrinsic incubation period of DENV(RUEDA et al., 1990; TUN-LIN; BURKOT; KAY, 2000; WATTS et al., 1987), whereas rainfall is an egg hatching trigger, as it provides oviposition breeding sites and the development of the mosquito's aquatic stages (LOWE; CHIROMBO; TOMPKINS, 2013). These environmental aspects contribute to mosquito populations displaying strikingly seasonality and geographically distribution between tropical and

subtropical regions, such as Brazil (KRAEMER et al., 2019).

In SIR/SEIR transmission models, the ecology of the dengue vector is modelled taking into account temperature-dependency and the adult stage of the vector. Temperature is regarded as the main driver of the seasonality of this disease (FOCKS et al., 1993; OTERO; SOLARI; SCHWEIGMANN, 2006; LIMA et al., 2014). In this sense, it is noteworthy that rainfall, despite being relevant when predicting dengue cases, is usually not included as a weather variable (SIDE; NOORANI, 2013; HUBER et al., 2018) because of the difficulty of incorporating this variable, since eggs may stay viable after months during dry seasons (TRPIŠ, 1972), excessive and prolonged rain may wash-out larvae from breeding sites(LOWE; CHIROMBO; TOMPKINS, 2013) and there is a lag between the beginning of rainfall season and the increase of dengue cases (HII et al., 2012). In regards to the vector stage, it is noted that, by incorporating only the adult stage, which is the stage responsible for transmitting the DENV to humans(NATAL, 2002; NELSON et al., 1986), the ability to study the effects of environmental factors on specific immature stages of the vector is limited.

Therefore, the following questions are addressed in this thesis: (1) How is the dynamics of DENV transmission modulated by weather variables? and (2) Is vertical mosquito transmission a significant mechanism for the long-term persistence of DENV in a certain area? To answer these questions, two mathematical models were proposed. The first one was recently published in the International Journal of Environmental Research and Public Health (IJERPH), entitled "A Framework for Weather-Driven Dengue Virus Transmission Dynamics in Different Brazilian Regions" (ALVES; LANA; COELHO, 2021). This article proposed a SIR model based on Huber et al. (2018). This new model includes temperature-driven biological responses related to dengue transmission dynamics, while also adding an egg compartment to the *Aedes* population, thus allowing the effect of rainfall to be introduced as a modulating variable in egg-hatching. Vertical transmission of DENV has been demonstrated in the laboratory for *Ae. aegypti* and *Ae. albopictus*, and has the potential to sustain endemic transmission in the long term (ADAMS; BOOTS, 2010), so it is featured in the model as well. Four municipalities in different climate regions in Brazil were chosen as case studies.

In addition to the results published in the article (ALVES; LANA; COELHO, 2021), this Thesis presents additional results by expanding the analysis to include a new model (a SEI-SEI-SEIR model), to compare these two different models, using twelve municipalities as case studies, and to present an improvement of the optimization process.

This thesis addressed limitations of existing models and also presented and discussed scenarios for dengue transmission that are a cause for concern due to environmental changes that may affect temperature, rainfall, and consequently, mosquito ecology (TIDMAN; ABELA-RIDDER; CASTAÑEDA, 2021). This thesis is organized in eight sections, in the following order: Introduction, Objectives, Justification, Literature Review, Methodology, Results, Discussion, and Conclusions and Recommendations.

2 Objectives

This thesis aimed to study the dengue transmission dynamics through weather-driven mathematical models in the period from 2010 to 2019 in different Brazilian municipalities.

The specific objectives were:

- Consolidate a climatic, epidemiological and demographic database to be used in the models;
- Conceive, implement, calibrate, and fit the model to the data, through an incremental process, in the weather-driven dengue transmission dynamic models that have an explicit compartment of mosquito population for a set of Brazilian municipalities;
- Study neglected parameters such as vertical transmission, egg population compartment, egg-hatching modulated by rainfall, and how they influence the dengue transmission dynamic;
- Compare the two different models considering the goodness-of-fit between the model output and the data.

3 Justification

Dengue is considered a public health emergency of international concern (ORGANIZATION, 2008), as it is spreading rapidly and causes serious public health impacts. To make things more pressing, more than half of the global population (3.45–4.09 billion people) have been predicted to live in areas that are suitable for dengue transmission (MESSINA et al., 2019). Several risk determinants of dengue have been identified, including urbanization, population growth, migration to marginalized areas with poor infrastructure, behavioral, and environmental factors (FARINELLI et al., 2018; LAI, 2018). One issue that has received particular attention is the association between climatic factors and vector-borne diseases (LAI, 2018). Considering the expected increase in global temperatures due to climate change, it is predicted that the dengue endemic regions will expand geographically (WILDER-SMITH, 2021; TIDMAN; ABELA-RIDDER; CASTAÑEDA, 2021).

These facts highlight the extreme importance of expanding dengue surveillance in order to support health agents' efforts to control the dengue virus circulation. Mathematical models are a strategic tool to improve virus surveillance through the development of an early warning system, and therefore were the tool chosen to be explored in this Thesis. In spite of several models for dengue transmission dynamic that have been proposed in literature, important challenges remain, such as the establishment of an association between the vector population and environmental and economic determinants, the human population that is susceptible to the virus, and the contribution of vertical transmission to the maintenance of virus circulation.

The models presented in this Thesis took great inspiration from the literature, but brought innovative adaptations. This work aims to contribute to a better understanding of the relationship between environment variables and dengue transmission dynamic, helping to improve dengue surveillance, which ultimately aids public health agents to propose strategies for the control of dengue.

Despite this Thesis focus on Brazilian municipalities, the methodology presented

is replicable since it uses satellite data and the parameters can be optimized for each specific site. Nonetheless, understanding how environmental variables impact dengue transmission dynamic is of extreme importance since the climate change can modify the average temperature and rainfall causing shifts in dengue transmission (TIDMAN; ABELA-RIDDER; CASTAÑEDA, 2021; GAGNON; BUSH; SMOYER-TOMIC, 2001; POLWIANG, 2015).

4 Literature review

4.1 Dengue fever: symptoms, diagnosis and treatment

Dengue fever is an acute febrile disease whose etiologic agent is a virus that belongs to the *Flavivirus* genus of the *Flaviviridae* family. Dengue virus (DENV) has a simple chain of 11 kilobases (kb) of RNA of positive polarity (Positive polarity RNA) (NELSON et al., 1986). This viral complex comprises four serotypes, antigenically distinct: DENV-1, DENV-2, DENV-3 and DENV-4 (TAUIL, 2001). The four serotypes of the dengue virus are phylogenetically distinct and often to the same degree as different "species" of flaviviruses (KUNO et al., 1998). DENV isolation studies have suggested that mixed-serotype infections can occur, but there is competitive suppression between dengue serotypes (KUNO et al., 1998).

Infection of humans with any dengue virus can cause two well-defined syndromes: Dengue Fever (DF) or Dengue Hemorrhagic Fever/Dengue Shock Syndrome (DHF/DSS) (SERVIÇOS., 2019). A range of intermediate responses or no clinical response is also possible (HALSTEAD, 2007), and it is estimated that around 80% of dengue incidence has no clinical response (BHATT et al., 2013).

Overall, patient treatment is composed of oral intake of rehydration solution (ORS). Paracetamol can be prescribed for high fever if the patient is uncomfortable (ORGANIZATION et al., 2015). However, in more severe cases, patients should be admitted to a hospital with access to intensive care facilities, where there is also availability of blood transfusion; fluid therapy is recommended in severe cases (ORGANIZATION et al., 2015), which represents a considerable burden to any health system (SUAYA et al., 2009).

4.2 Dengue transmission

Dengue viruses are transmitted to humans through the bites of infected *Aedes* mosquitoes, mostly by two main vectors: *Ae. aegypti*, the primary vector, and *Ae. albopictus*, the secondary vector. These mosquitoes are widely distributed around the world, mainly in tropical and subtropical regions.

The transmission cycle of *Aedes* is described in Figure 1. The virus enters the skin when an infected female mosquito bites a human for a blood meal (ORGANIZATION et al., 2015). Once infected, symptoms may appear between the 4th and 7th day after the bite, which is the time required for a host to become infectious, that is, capable of transmitting the virus to a new mosquito (GUZMAN et al., 2016). This is also called the intrinsic incubation period. When a new mosquito becomes infected after biting an infectious human, it takes around 8 to 10 days for it to become infectious, this is the extrinsic incubation period (GUZMAN et al., 2016). *Ae. aegypti* females can bite different people during a single blood meal, thus they can be very effective in spreading the virus (GUBLER, 1998).

Vertical transmission of dengue in mosquitoes is reported to be of low probability (JOSHI; MOURYA; SHARMA, 2002; MITCHELL; MILLER, 1990; SERUFO et al., 1993). This mechanism needs to be further studied, as it can be an efficient way to maintain DENV circulation, especially in regions with marked seasonality, where eggs can go into latency during the dry season and develop after, in more humid seasons, already carrying the virus.

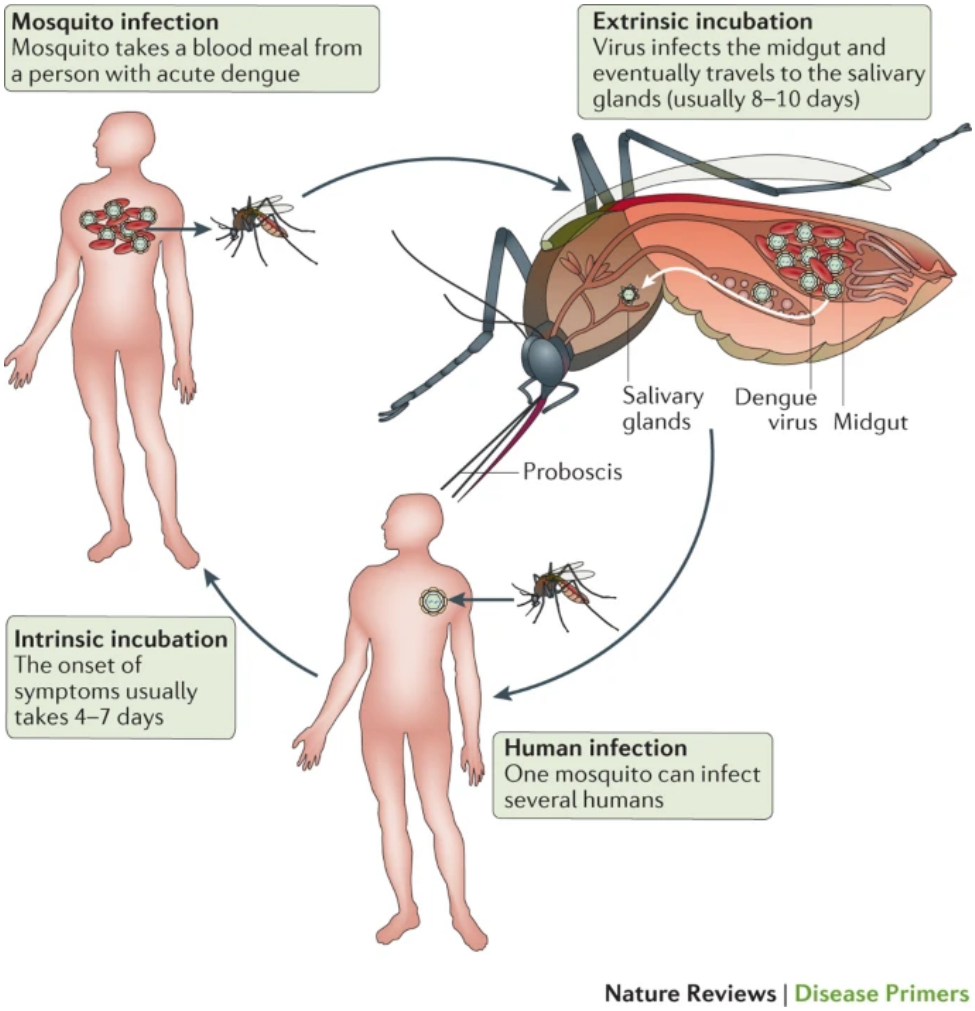

Figure 1 – After an infected *Aedes aegypti* mosquito bites a human, there is a probability that the human will become infected after being exposed to dengue virus. The human host will carry the virus and might pass to susceptible mosquitoes, carrying on the disease. Source: (GUZMAN et al., 2016)

Figure 2 shows three (3) major cycles reported in literature: forest, rural and urban cycles. The primitive forest transmission cycle of dengue viruses involves some *Aedes* species mosquitoes and primates (GUBLER, 1998). Infected primates can invade rural areas carrying the virus and starting a cycle. Humans move between urban and rural areas, bringing the virus to these sites. In Brazil, *Ae. aegypti* is the only main vector in urban sites (GUBLER, 1998).

A great deal of effort is taken to prevent the spread of dengue viruses in infected mosquitoes by implementing mosquito control. Female mosquitoes do not fly far from

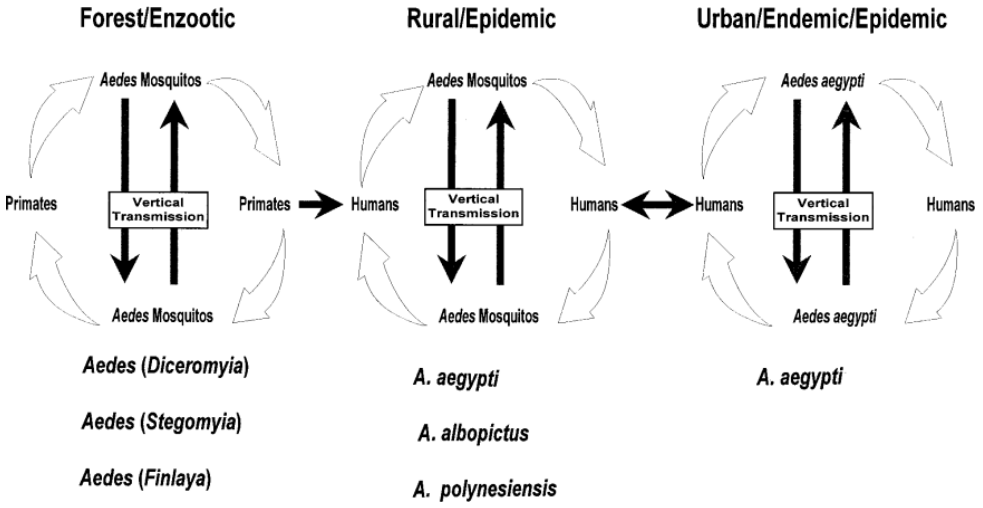

Figure 2 – Major dengue transmission cycles reported: forest/enzootic, related to primates-Aedes-primates mosquitoes cycles; rural, related to human-Aedes-human cycle; and urban areas, where the viruses are maintained in an *Ae. aegypti*-human-*Ae. aegypti* cycle. Source: (GUBLER, 1998)

where they are born. This fact makes human movement an essential key in spreading the virus (ORGANIZATION, 2010; WILDER-SMITH; GUBLER, 2008). Despite these known facts, it is still not clear where or when an epidemic can start. However, since dengue is a vector-borne disease, environmental forcings are important to the vector ecology and the virus transmission. This relation should be carefully studied as determinants of dengue epidemics.

4.3 Dengue burden

Estimates from 2000 to 2010 showed that there were on average 390 million (95% credible interval 284–528) dengue cases per year in the world, of which 96 million (67–136) manifest apparently, with symptons, in any level of disease severity. This results in around 24,000 deaths and an enormous burden in healthcare systems globally (BHATT et al., 2013). Other estimates cite 50 million worldwide cases per year, with 500,000 hospitalized cases and 20,000 deaths caused by dengue (CRUZ, 2002).

According to (ORGANIZATION, 2022), the number of dengue cases is growing,

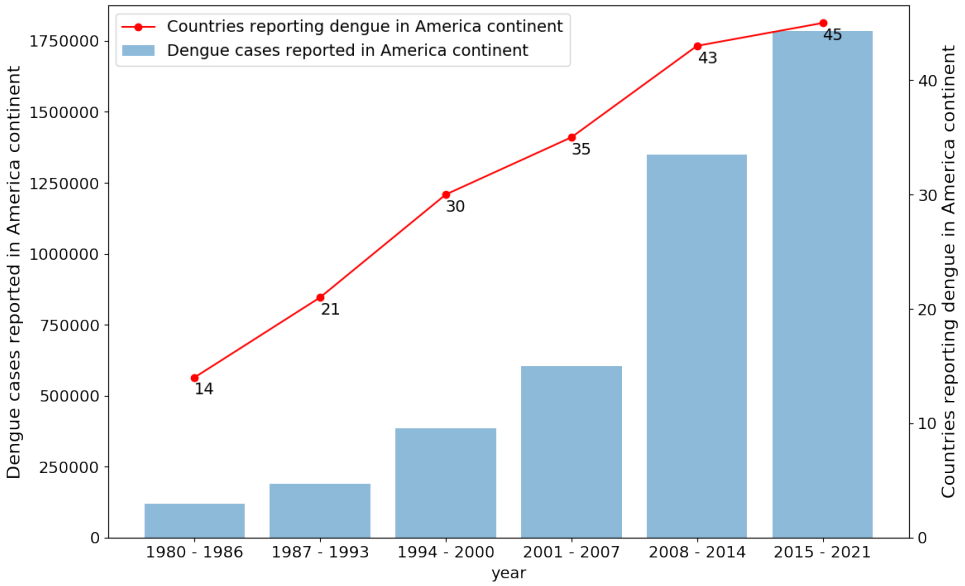

Figure 3 – Average annual number of dengue cases reported to the Panamerican Health Organization and number of countries reporting dengue. Source: (ORGANIZATION, 2022)

as illustrated in Figure 3. This growth has made the World Health Organization revise the International Health Regulations (IHR), including dengue as one of the diseases of public health emergency of international concern (ORGANIZATION et al., 2015). Dengue threatens health security as it can disrupt healthcare systems during rapid epidemic spreads, which may happen beyond national borders (ORGANIZATION et al., 2015).

The metric disability-adjusted life years (DALYs), used to assess health and social impacts, shows a significant burden on the countries in areas where dengue is endemic. Meltzer et al. (1998) estimated that endemic countries lost 580 DALYs/year/million population on average. Similar values caused by other diseases such as malaria, tuberculosis, intestinal helminths, and childhood diseases cluster in all of Latin America.

Few studies have measured the economic impact of dengue. Suaya et al. (2009), in a study conducted more than ten years ago, interviewed 1695 ambulatory and hospitalized patients diagnosed ostensibly with dengue in Latin America and Asia. Of those interviewed, 45% were hospitalized and 78% indeed had dengue. Students

missed an average of 5.6 days of school and workers lost an average of 9.9 days of work, considering days spent in hospital care or at home, with fever. The average opportunity and health cost reached 571 American dollars per case, being opportunity the time lost not working. The total average opportunity and health cost was 149.3 million American dollars per year for the countries Brazil, El Salvador, Guatemala, Panama, and Venezuela (SUAYA et al., 2009). Brazil stands out with an average opportunity and health cost of 135.2 million dollars per year with dengue. The current total cost is probably higher, since it will account for the underreported cases and the substantial costs associated with dengue surveillance and vector control programs (ORGANIZATION et al., 2015).

As evidenced by the study of Suaya et al. (2009), Brazil's dengue burden is worrisome. The country notified 98.5% of all the dengue cases and the highest fatality rate in South America in the 2000-2010 decade (ORGANIZATION et al., 2015). Dengue afflicts all levels of society, but the burden may be higher among the poorest, who more frequently lack access to safe drinking water and proper solid waste collection (ORGANIZATION et al., 2015).

4.4 Dengue history in Brazil

Evidence of occurrence of dengue in Brazil first appears in 1845 (DICK et al., 2012). Dengue was introduced, mainly in port cities which had commercial activities. A possible reason why coastal cities were more susceptible to dengue is that travelers play an essential role in the epidemiology of dengue infections, as travelers with the disease, which can be caused by different serotypes, can carry it into new areas (ORGANIZATION et al., 2015).

In 1945, scientists isolated Dengue viruses for the first time, and laboratory diagnostic was available thereafter (SABIN; SCHLESINGER, 1945). In the same decade, the Pan American Health Conference began to promote prevention and control measures against *Aedes aegypti* in Brazil, by then already known to be the primary vector of dengue (DICK et al., 2012). The measures taken against the vector aimed at their

aquatic and alate stages, using larvicide made of substances with a base of mineral oils, cresols and potassium permanganate (SEVERO, 1955). This campaign was a success in eliminating mosquitoes in vast areas of Brazil (DICK et al., 2012).

However, with the relaxation of a intensive vector control policy, the Americas experienced their first dengue importation in 1963 in Jamaica. DENV-3 caused this epidemic, a virus of Asian origin (DICK et al., 2012). Interestingly, in Asia, only DENV-2 remained in circulation by the middle of the 20th century (HALSTEAD, 2006) Decades of unprecedented human efforts to eradicate *Ae. aegypti* fell apart very rapidly subsequently, and after 1971, a reinfestation of the vector in the Americas brought the spread and expansion of Dengue (DICK et al., 2012). The 80s decade was marked by the re-introduction of DENV-1 in Brazil (SCHATZMAYR et al., 1986); DENV-2 was re-introduced in 1990 (NOGUEIRA et al., 1993); DENV-3 appeared considerably later, in 2001 (NOGUEIRA et al., 2001) and lastly DENV-4 was re-introduced in 2011 (CAMPOS et al., 2013). These introduction timeframes and the resulting number of dengue cases can be seen in Figure 4.

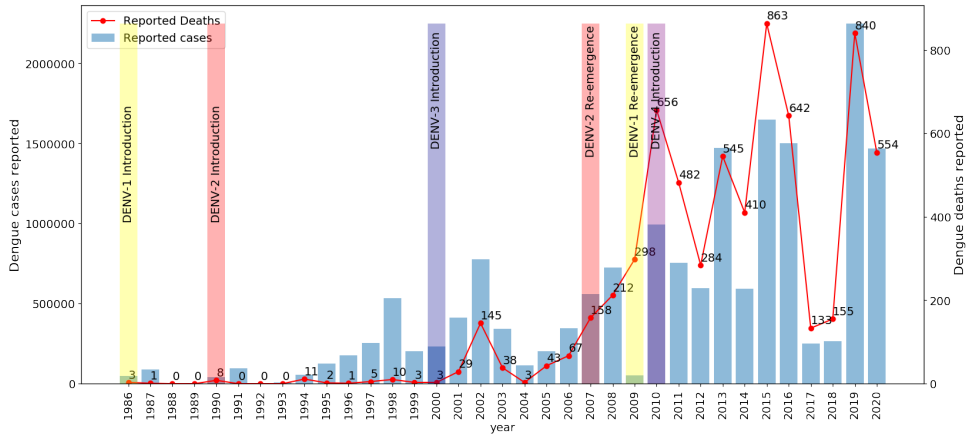

Figure 4 – Dengue cases and dengue fatal cases reported in Brazil in 34 years (1986 to 2020). Colour bars indicate when each dengue strain was introduced or re-emerged. Gray bars indicate number of dengue cases. Line plot indicate number of dengue fatality reported. Source: Salles et al. (2018)

From the 2000s forward, an unprecedented increase in the number of cases is reported in the americas (DICK et al., 2012). All four serotypes have been circulating

since 2011, and the highest record of cases ever reported happened during this decade. Brazil started to reach more than 1 million cases per year, and deaths reportedly reached almost 1,000, as shown in Figure 4. This scenario is worrisome since DHF cases are reported in every epidemic (DICK et al., 2012).

Dengue cases show cyclical variation, with high epidemic years and low epidemic years (ORGANIZATION et al., 2015). Driven by peak transmission of the disease, dengue shows a seasonality influenced by characteristics of the host, the vector and the agent. The history of dengue shows a struggle between humans and virus-vector, but until today researchers still try to fully understand how transmission happens in order to alert health autorities in advance about possible new outbreaks.

4.5 Environmental forcing

Dengue vector's life cycle has four main stages: egg, larvae, pupae, and adult mosquito. Favorable conditions for *Aedes* mosquito development are high temperature and high precipitation. These conditions are found in Tropical and Subtropical regions, classifications made by Köppen-Geiger, which divide Earth into regions as an expression of the prevailing climate (ALVARES et al., 2013). The boundaries between climatic regions were selected using temperature and rainfall data, but they have a high correlation to biome distribution and *Ae. aegypti* population distribution as well.

The tropical region has an average temperature of more than 18 C° during the coldest month (ALVARES et al., 2013). The areas in subtropical zones bordering on tropical zones have similar characteristics. The regions with more rain volume and forest cover in tropical zones can be classified as tropical rainforests. Figure 5 represents mean temperature in Brazil territory. Brazil has a vast territory and thus different climates, almost all favorable to *Ae. aegypti* mosquito (Figure 6).

Environmental factors have been shown to be strong determinants in dengue epidemic behavior. Morin, Comrie e Ernst (2013) bibliographic review give numerous examples of how environmental factors impact dengue transmission: habitat availability for mosquito larvae is influenced by temperature and incoming precipitation; and tem-

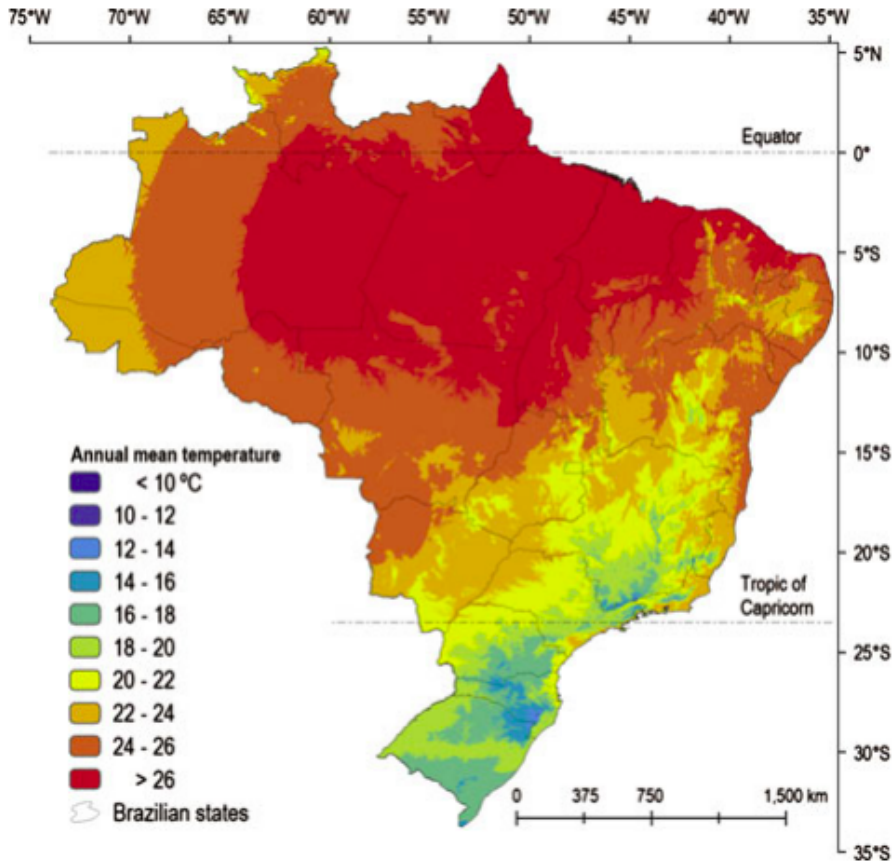

Figure 5 – Map of Brazilian mean temperature. Blue stands for temperature bellow 10 C° and green stands for temperatures above 26 C°. Source: (ALVARES et al., 2013)

perature is a major regulator of mosquito development, viral replication within infected mosquitoes, its survival and reproductive behavior.

Furthermore, there are key points in the dengue transmission cycle, that need to be understood in order to know how environmental factors determine the disease dynamic, which will be addressed in the following.

4.5.1 *Ae. aegypti* oviposition behavior and fecundity

Most studies evaluated where the eggs are laid or specific conditions like different water treatments (CHADEE; CORBET; TALBOT, 1995; FAY; PERRY et al., 1965).

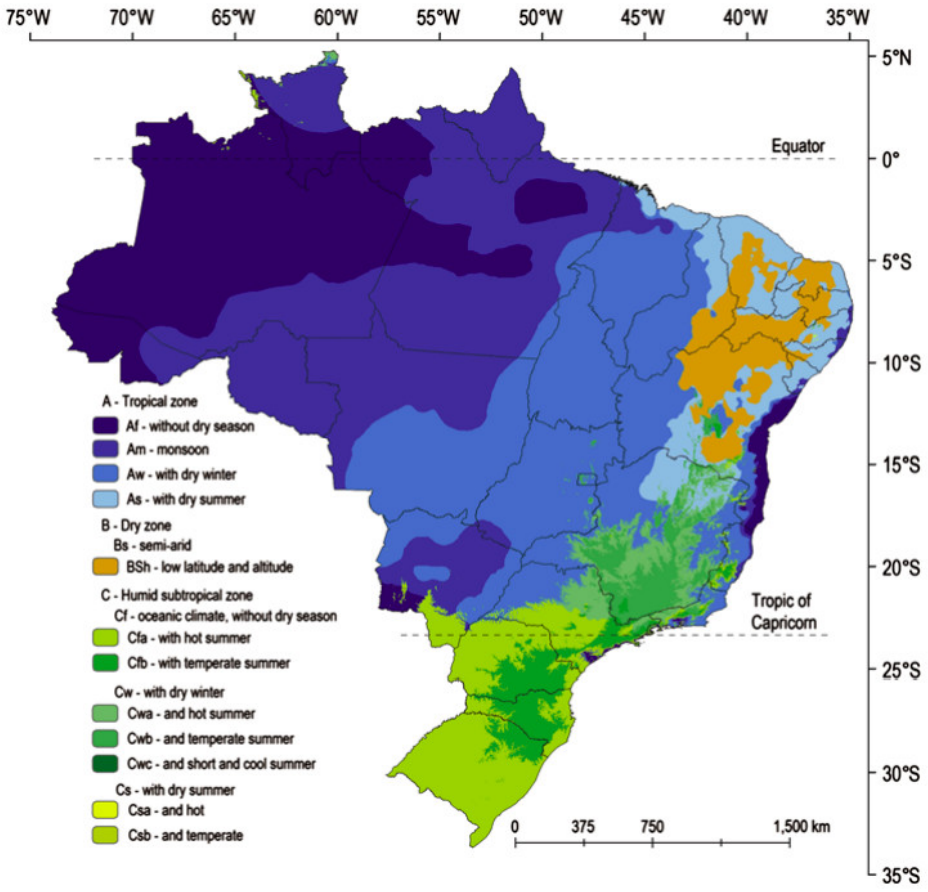

Figure 6 – Map of Brazilian climate using Köppen-Geiger classification. Blue stands for tropical weather and green stands for subtropical weather which have more probability of dengue cases. Source: (ALVARES et al., 2013)

Chadee, Corbet e Talbot (1995) showed that mosquitoes prefer laying eggs in dark corners of the container and most of them are laid during the day.

The average number of eggs laid by female *Ae. aegypti* mosquito has also been investigated. In an laboratory experiment, each colony with 54 females provided from 200 to 3,000 eggs per day, which means 3-55 eggs laid by female per day (FAY; PERRY et al., 1965). This number can change according to the weight of the female and other factors (FOCKS et al., 1993). Furthermore, the gonotrophic cycle, i.e. the period between the blood meal and oviposition, is regulated by the temperature and takes longer for the first oviposition than for the subsequent ones (FOCKS et al., 1993).

Oviposition is directly linked to environmental factors such as temperature and

precipitation. Chadee, Corbet e Talbot (1995) showed that most of the eggs laid in their study in Trinidad, West Indies, were obtained during the wet season: 86.4% of the 3,556 eggs of *Ae. aegypti*, whereas the remaining, proportionally very few eggs, were deposited during the dry season. A similar study in Brazil showed a positive correlation between precipitation (mm) with the number of eggs: 0.91 more eggs were found for each 1 mm of precipitation in ovitraps in the field, which fits a linear regression with 0 as intercept (ZEIDLER et al., 2008). Laboratory experiments also showed this correlation; low humidity (32%) more than halved the mean number of eggs laid per mosquito compared to high humidity level (84%) (CANYON; HII; MÜLLER, 1999).

Mathematical models have already been used to model oviposition as a function of temperature. Yang et al. (2009) fitted oviposition rate as a function of temperature in a quasi-linearly manner. Mordecai et al. (2017) gathered data from literature and modelled oviposition in response to temperature using a Brière function ($cT(T-T_{min})(T_{max}-T)^{-\frac{1}{2}}$), assuming that fecundity has its peak between 23 C° and 34 C°.

4.5.2 *Ae. aegypti* vertical transmission of DENV

Vertical transmission (VT) of DENV in mosquitoes has been demonstrated previously under laboratory conditions (LIMA; LIMA-CAMARA, 2018). Three consecutive generations of *Ae. aegypti* and *Ae. albopictus* transmitted the virus to their eggs (JOSHI; MOURYA; SHARMA, 2002). A number of studies further demonstraded the natural vertical transmission of DENV in *Ae. aegypti* and *Ae. albopictus* (MITCHELL; MILLER, 1990; SERUFO et al., 1993; COSTA et al., 2017).

In Brazil, the vertical transmission was observed in laboratory in 1990 (MITCHELL; MILLER, 1990). Natural vertical transmission was also demonstrated in 1993 (SERUFO et al., 1993), in three confirmed cases of DENV-1 in Campos Altos, Minas Gerais State. A recent study in the Amazon rainforest showed that all dengue serotypes were circulating at the same time, and were identified in larval samples (COSTA et al., 2017).

Vertical transmission is not a well-established parameter and studies do not converge about it. A study from 1992 assessing VT in *Aedes aegypti* in the United States reported 13% of vertical transmission rate (BOSIO et al., 1992). (BUCKNER; ALTO;

LOUNIBOS, 2013) studied mosquitoes in Florida and vertical transmission of DENV-1 was documented with rates of 11.11% (2 out of 18) for *Ae. albopictus* and 8.33% (3 out of 36) for *Ae. aegypti*. VT of DENV-4 showed 10.5% of Ae. aegypti naturally infected by this route in Brazil (CRUZ et al., 2015). On the other hand, Thailand researchers found considerably lower and different rates of VT over a year, varying from 0 to 2.4%; the peak of vertical transmission occurred four months before a large dengue outbreak in this case (CHOW et al., 1998). Finally, a study did not find any VT evidence (CHOW et al., 1998). In this case, it is noteworthy that several factors can contribute to the non-detection of VT, including low sensitivity of the tests, inappropriate methodology, and mosquito sample maintenance issues.

Bosio et al. (1992) claims that vertical transmission rates may be higher in epidemic areas, which may contribute to the maintenance of DENV circulation and the amplification of the cases since the adult insects are born naturally infected.

4.5.3 *Ae. aegypti* egg stage

Ae. aegypti eggs are laid in situations where conditions of transient water occur. However, they can be viable out of water for up to a year or longer (HARDWOOD; HORSFALL, 1959), in what is known as diapause or latency condition or quiescence (YANG et al., 2014). Diapause is a crucial adaptation to seasonal environmental variation in a wide range of arthropods. During diapause, desiccation resistance in eggs increases and they can survive in an extreme weather conditions (URBANSKI et al., 2010).

Sota e Mogi (1992) recorded different values for their *Ae. aegypti* eggs, in a study conducted in Japan, with the mean survival time varying between 101-128 days. On the other hand, Faull and Williams observed more than 7,000 eggs laid in Australia and concluded their mean survival time was 180-220 days (FAULL; WILLIAMS, 2015).

4.5.4 *Ae. aegypti* eggs hatching behavior

When the surroundings become favorable to larval development due to the water availability, the egg's latency is interrupted and the larva hatches (CLEMENTS

et al., 1992). Eggs hatching at the beginning of a favorable period is a critical event to ensure the larvae survival (BYTTEBIER; MAJO; FISCHER, 2014). Factors such as the water temperature and the physiological condition of eggs may determine the hatching response of *Ae. aegypti* eggs (BYTTEBIER; MAJO; FISCHER, 2014). Eggs of *Ae. aegypti* exhibit increased viability under conditions of high humidity (80%), as they hatched readily when kept under such conditions (SAIFUR et al., 2010).

Two types of eggs are described on the literature, one being "active" eggs, which hatched readily after oviposition, and the other being "subactive" eggs that hatched only after a long period of flooding (SAIFUR et al., 2010). Eggs of *Aedes aegypti* hatch more readily in the laboratory when moistened for several hours before submergence in water (SAIFUR et al., 2010). Focks et al. (1993) noticed that 19.7% of all newly eggs hatched spontaneously without flooding and 59.6% were "subactive" eggs.

Moura et al. (2020) showed that *Ae. aegypti* hatching rates for 3-day-old eggs was 85.4%, and hatching rates of batches of eggs stored for 12–61 days ranged between 84% and 90%; 339.037 eggs were arranged to hatch. Therefore, egg latency did not affect its survival, as the hatch rate did not present a significant change after storage for 12-61 days.

Alto e Juliano (2001) showed daily eclosion rates of 5-6% per day in their case study. They also noticed how precipitation and temperature affected the hatching. Precipitation had a quadratic effect, and there were more hatchings when the weather was neither too dry nor too wet. The temperature had a linear effect between 22 C° to 30 C°, with a higher hatching rate when temperature was near 30 C°. Focks et al. (1993) found a similar relation, observing the development rate of 1-2% in low temperatures (20-25 C°) which increased to 2-3% in high temperature (35 C°).

4.5.5 *Ae. aegypti* larvae stage

There are four larval instars (SCHAPER; HERNÁNDEZ-CHAVARRÍA, 2006). The larvae change considerably in size and structure during their development; the first instar is about 1 mm long, whereas the fourth instar grows to be eight times larger (SCHAPER; HERNÁNDEZ-CHAVARRÍA, 2006).

The environment, food supply, container, and temperature can affect the development time from the larvae stage to the pupae. Bar-zeev et al. (1957) reported a mean of 14.9 days for this period between different containers. In stressful situations, such as low food supply, the development stage becomes a function of food weight density, and they are negatively correlated and can go up to 20 days (FOCKS et al., 1993). When the food supply is not limited, development rates are limited by temperature rather than by food (FOCKS et al., 1993).

In experiments with *Aedes albopictus*, different rates were found for different average development times depending on the container: development times were 19.6, 27.3, and 37.5 days for a tree hole, a bamboo stump and an auto tire, respectively, the latter having the lowest food supply (GOMES et al., 1995). These development times are more realistic considering field conditions, as they are similar to Wijeyaratne et al. (1974)'s work, which observed a development time for larvae of 24 days and overall of 39 days in the city of Gainesville/USA, at the summer season.

Alto e Juliano (2001) showed a correlation between development time of the larval and temperature. At 22 C°, which is a harsh temperature for *Ae. aegypti*, the controlled sample in the laboratory took 14-16 days to develop, but this time decreased drastically at 30 C° temperature, reaching 10-11 days. Yang et al. (2011) also found correlation between temperature and larvae development time. Mordecai et al. (2017) modeled the development rate of the larvae using temperature, but with a quadratic function that has 40 C° as the limit.

Regarding mortality rates, larvae survival is very susceptible to food density. In experiments, 80% of larvae died in low food density, whereas only 15-30% died with enough food density, which corresponds to a 1% mortality rate per day (FOCKS et al., 1993).

4.5.6 *Ae. aegypti* pupae stage

Pupae belong to the aquatic phase of the mosquito life cycle. They stay dormant, metamorphosing, but can be activated through external stimuli such as vibrations swinging around the container (NELSON et al., 1986). In experiments, the pupae stage

hardly had any mortality rate in different kinds of stress conditions (FOCKS et al., 1993), primarily because pupae do not feed. Experiments made by Bar-zeev et al. (1957) showed pupal development time ranging between 1-8 days, once again correlated to temperature. Literature defines an average of 2 days for pupae development time (NELSON et al., 1986; FOCKS et al., 1995).

4.5.7 *Ae. aegypti* adult stage

This stage in mosquitoes is generally marked by reproduction and dispersion of the species; however, in opposition to other species, the *Ae. aegypti* has a more passive dispersion that comes from the transport of the eggs container more than the adult flight capacity (NELSON et al., 1986). The female often remains in the same household where it emerged, not flying more than 50 meters. Generally, the adult behavior includes: copulating, feeding, and sometimes migrating and resting (NELSON et al., 1986).

Brady et al. (2013) modeled the adult survival rate using a sample of 410 mosquitoes. Mosquitoes on field showed lower survival time compared to mosquitoes in laboratory, 10-20 days compared with 60-100 days, respectively. This gives a daily mortality rate between 0.05 and 0.082 (average 0.064) in laboratory compared to an observed in field mortality rate, 0.033 and 0.595 (average 0.288). These numbers are still far from the value used by Focks et al. (1995), of 8.6 days expected survival time or 0.118 daily mortality rate.

4.5.8 *Ae. aegypti* sex ratio

Only female mosquitoes need humans for blood meal (ORGANIZATION et al., 2015) and therefore can transmit the virus. As a result, the sex ratio, proportion between males and females inside the population, is an essential factor in determining dengue transmission. Focks et al. (2000) noticed a correlation between sex ratio and temperature: the higher the temperature, the higher the ratio of females. In these studies, ratios ranged from 1-0.88 (1 male to 0.88 females or 46% females) at 22 C° to 1-3.88 (1 male to 3.88 females or 80% females) at 32 C°. Most models prefer to use a 1-1 female-to-male sex ratio, although the reasons for this choice remain unclear (HUBER

et al., 2018; MAGORI et al., 2009).

4.5.9 *Ae. aegypti* environmental carrying capacity

Mosquito population is regulated by several factors such as quantity of hosts, breeding sites availability, water breeding sites temperature, food availability, and others. All of those factors are dependent of economic, demographic and climate factors (PALAMARA et al., 2014).

Some authors use the carrying capacity in the adult mosquito stage as function of temperature, prioritizing the climate factors (HUBER et al., 2018; PALAMARA et al., 2014). Other authors use the maximum number of mosquitoes per kilometer square (MAIDANA; YANG, 2007). One study has showed the correlation between the carrying capacity and area size (LANA et al., 2018).

In a complex approach, Erguler et al. (2016) modelled carrying capacity using a rainfall-human density-dependent function. Mosquito population can not evolve without rainfall or humans and differences in demographic could affect the relationship between humans and mosquitoes. Field studies showed an average of 0.7 rate between females mosquitoes per person in Panama (NEIRA et al., 2014) while in Amazon, the reported rates were of 1.2 females mosquitoes per person in the high-temperature season and 0.06 in the low-temperature season (ABAD-FRANCH; ZAMORA-PEREA; LUZ, 2017).

Finally, many authors prefer to limit the larvae or pupae population, but not in the adult mosquito (TRAN et al., 2013). Others prefer to link the adult mosquito population to studying the pupae since the mortality rate of pupae is insignificant. Focks et al. (2000) estimated a range between about 0.5 and 1.5 *Ae. aegypti* pupae per person with an average of 0.71.

4.5.10 *Ae. aegypti* biting behavior

Within 24 hours after hatching, female mosquitoes can take a blood meal (NELSON et al., 1986). They prefer to feed on humans during the daytime and have two peaks of biting activity: early morning, from 2 to 3 h after daybreak, and afternoon

right before dark (GUBLER, 1998).

Canyon, Hii e Muller (1999) estimated the number of bites per day using three intervals of host availability experiments, 6, 12, and 24 h intervals. Host-biting frequencies were 0.7 bites per female mosquito in the 24 h feeding interval, 0.54 bites per female in the 12 h, and 0.47 bites per female in the 6 h; thus, when hosts are more available, they trend to bite more (CANYON; HII; MULLER, 1999). However, laboratory experiment results can differ from field results. Mordecai et al. (2017) modeled biting behavior using temperature so that females do not bite more than 0.4 times per day and limited the biting behavior from 13.35 C° to 40.08 C° using a Brière function.

4.5.11 Probability of DENV transmission from mosquito to human

After an infected mosquito bite, humans can become exposed to the dengue virus. Watts et al. (1987) tested the transmission efficiency of *Ae. aegypti* using monkeys. In this study, the correlation between transmission and temperature was evident, since DENV-2 was only transmitted to monkeys in temperatures equal or higher than 30 C°. Using the Watts et al. (1987) experiment, Mordecai et al. (2017) modeled the probability of mosquito infectiousness with a Briére function with a maximum point of 80% in temperatures near 30 C°. Yang et al. (2016) used a constant rate of 6% while Polwiang (2015) used constant rate of 36%. and Abad-Franch, Zamora-Perea e Luz (2017) ranged from 50% to 90% rate of infection, considering 50% optimistic and 90% gloomy.

4.5.12 DENV intrinsic incubation period

Literature defines the intrinsic incubation period as the time that an exposed host takes to become fully infected (infectious), enough to transmit the virus to another vector. This period is estimated to be between 4 and 10 days for DENV (ORGANIZATION et al., 2015). McLean et al. (1975) studied this phenomenon using infected *Ae. aegypti* and mices. Mosquitoes transmitted the DENV-2 virus after six days incubation at 32 C°, 6-27 days at 24 C°, and 13-20 days at 13 C°, showing a correlation with temperature.

When studying Zika virus, Lessler et al. (2016) estimated 5.9 (95% CI: 4.4-7.6)

days of average intrinsic incubation period. Although this is specific to Zika, Huber et al. (2018) work use this estimation for dengue as well.

Focks et al. (1995) used four days as time default for the intrinsic incubation period for all dengue serotypes. However, they recognized this period can be longer, especially if they compare the period of infective viremia and detectable viremia. Newton e Reiter (1992), Chowell et al. (2007), Nishiura e Halstead (2007) uses, respectively, 5, 5.5 and 4 days as their intrinsic incubation period.

4.5.13 Human infectious period

After the incubation period, humans infected by DENV can transmit the virus to vectors. In this stage, the host can display a broad spectrum of illness or, in most cases, stay asymptomatic (ORGANIZATION et al., 2015). The febrile phase of dengue usually last 2-7 days (ORGANIZATION et al., 2015), but Nishiura e Halstead (2007) showed that some human hosts could transmit DENV two days before the onset of fever and even two days after the fever has passed. Huber et al. (2018) used an average of five days for the infectious period in their model, inspired by Gubler (1998) observations but Otero e Solari (2010) diverged, using three days instead.

Humans infected with dengue are protected from other dengue serotypes for 2-3 months after the primary infection, but with no long-term (cross-protective immunity) (ORGANIZATION et al., 2015).

4.5.14 Probability of DENV transmission from human to mosquito

Xiao et al. (2014) studied in the laboratory the probability of DENV transmission from a host to *Ae. albopcitus* after each mosquito takes a blood meal biting guinea pig fresh blood infected by DENV-2. In the experiments, mosquito infection rates correlated with temperature. For mosquitoes held at 18 C°, no infection was detected in the head and salivary glands after 25 days of incubation. Over the temperature range of 18–31 C°, the infection rate displayed a tendency to increase. The maximum infection rate was attained at 31 C°, at which the infection rates were 70.59 % in the head and salivary

glands. However, the infection rate of mosquitoes at 36 C° was lower than at 31 C°. At 36 C°, the infection rates of the salivary glands were 47.06 %. These values were used by Mordecai et al. (2017), which modeled the probability of vector infection with temperatures from 12.22 C° to 37.46 C° using a Brière function. Yang et al. (2016) used a constant rate of 30% ; Polwiang (2015) used constant rate of 20%, and Abad-Franch, Zamora-Perea e Luz (2017) used a range from 50% to 90% rate of infection, considering 50% optimistic and 90% "gloomy" in their words.

4.5.15 DENV virus extrinsic incubation period

DENV virus extrinsic incubation period is defined as how long an exposed vector takes to become fully infected. The literature describes it in a range of 8-12 days (ORGANIZATION et al., 2015). In experiments in mice for Zika virus, extrinsic incubation period was modeled (BOORMAN; PORTERFIELD et al., 1956). In those experiments, mosquitoes were infected with Zika and it took at least ten days to rise the virus level. Huber et al. (2018) used this value for dengue modeling.

Focks et al. (1995) noticed how extrinsic incubation time is correlated with temperature in a nonlinear regression. They modeled it using an exponential function with temperature as input. Afterwards, Mordecai et al. (2017) modeled extrinsic incubation time as well, but using a Brière function with temperatures ranging from 10.68 C° to 45.90 C° and extrinsic incubation period varying from 5 to 20 days.

4.6 Mathematical models of dengue transmission dynamics

Kermack e McKendrick (1927) were the first researchers to introduce a mechanistic model for virus transmission dynamic. They divided the population into susceptible, infected, and recovered compartments (SIR). These compartments are able to control the force of infection, that is, the rate at which a susceptible person acquires an infection, because the more the disease spread, less susceptible humans are in the population and thus less likely they are to become ill. Patients that were previous infected become

recovered and can not be infected again. Later on, Kermack e McKendrick (1933) extended their work, adding birth, migration, death and imperfect immunity; with these additions, recovered patients could once again become susceptible.

In Kermack e McKendrick (1927) model, infected patients could infect other humans, however in this Thesis, where dengue is the concern, humans can infect only susceptible vectors, which may later spread the disease to other humans. In a systematic review about models applied to dengue transmission, Andraud et al. (2012) found, in addition to the traditional SIR compartments, the following: symptomatic / asymptomatic humans, vaccinated humans, susceptible and infected vector population, and that vector population could also be divided into egg, larva, pupa and adult stages. Age stratification models were also found.

Those models can account for one to four serotypes, with and without cross-protection (ANDRAUD et al., 2012). They can present many biological processes related to dengue transmission such as bite rate, oviposition, virus incubation period and other parameters (ANDRAUD et al., 2012). Robust models with many components have the advantage that they can represent reality with more trustworthiness, but at the same time, this come at a computational cost and make the model more complex to be optimized.

5 Methodology

In this work, two mathematical models were proposed and a typical pipeline with six steps was followed (FREGLY, 2021): data collection and transformation, model development, optimization, evaluation, and fitting. These sections' workflow are presented in Figure 7. The first model is a SIR model and the second, a SEIR model.

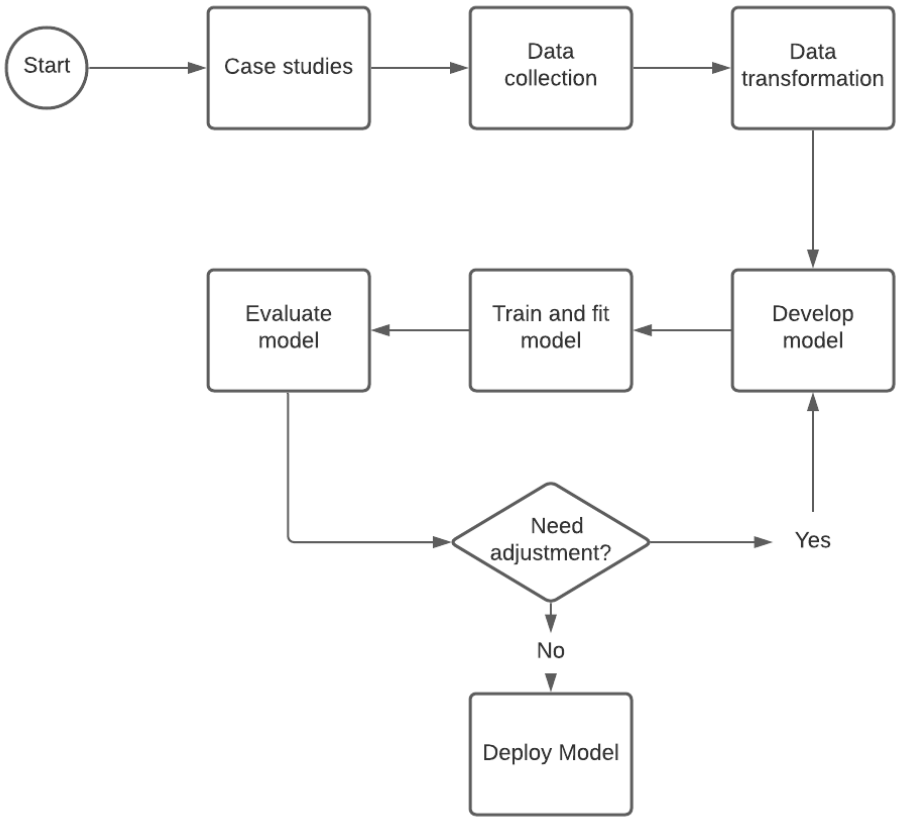

Figure 7 – Model analysis pipeline. Adapted by (FREGLY, 2021)

5.1 Case studies

To test the SIR model, it was chosen four Brazilian municipalities that have different DENV transmission dynamics and environmental patterns, namely Rio de Janeiro, Fortaleza, Foz do Iguaçu and Porto Alegre (Figure 8). All of them, except for

Porto Alegre, have suffered multiple severe dengue outbreaks between 2010 and 2019 (CODECO et al., 2018).

Fortaleza, the capital of the state of Ceará, is located on the northern coast of Northeastern Brazil, near the equator line. It exhibits a high demographic density of 8,390.76 people/km^2, with a population size of 2,452,185 inhabitants according to the 2010 Census (BRASIL, 2010). Fortaleza displays a warm and sub-humid tropical climate (CAPRARA et al., 2015), with an average temperature of 29 $\pm$ 1.4 C° in the last decade (WAN; HOOK; HULLEY, 2015). Periods of intense droughts with occasional rains are common; with an average rainfall of 14 $\pm$ 21 mm for an 8-day cycle in the last decade, (FUNK et al.,), the lowest average rainfall levels of all municipalities considered in this assessment. Due to its tropical climate and high population density, it is highly receptive to infestation by *Ae. aegypti*. Although it is a coastal area, Fortaleza does not receive the same influx of tourists as Rio de Janeiro or São Paulo municipalities in Brazil (BRASIL, 2020a).

The municipality of Rio de Janeiro, the capital of the state of Rio de Janeiro, also exhibits a high demographic density, of 5,556 people/Km^2, and a population size of 6,320,446 inhabitants (BRASIL, 2010). It shares some weather characteristics with Fortaleza, with a tropical humid and warm climate weather (CÂMARA et al., 2009), with an average temperature of 26 $\pm$ 3 C° in the last decade (WAN; HOOK; HULLEY, 2015). Occasionally, winters can comprise warm weeks with an average temperature of 30 C° (CÂMARA et al., 2009). Average rainfall values from last decade indicate 18 $\pm$ 19 mm per an 8-day cycle (FUNK et al.,), characterizing dry weather, although with heavy rains, especially in the fall.

Foz do Iguaçu is located in western part of the state of Paraná, in southern Brazil. It is set at an altitude of 164 m, with a demographic density of 418.5 people/km^2, and a population size of 256,088 inhabitants (BRASIL, 2010). The climate is subtropical humid mesothermal, with an average temperature of 24 $\pm$ 4 C° (WAN; HOOK; HULLEY, 2015) and average rainfall of 26 $\pm$ 25 mm (FUNK et al.,) in the last decade. The municipality shares borders with two countries, Paraguay and Argentina, and represent a well-known trade route stop between these countries (CONTE, 2013). At the same time, it is known

by its tourist activities (PERIS; LUGNANI, 2011). Therefore, in spite of the fact that it has a relatively small resident population and is located far from the coast, Foz do Iguaçu receives thousands of tourists every day (BRASIL, 2020a).

Porto Alegre, the capital of the state of Rio Grande do Sul, is the southernmost municipality among those analyzed in this study. It displays a humid subtropical climate (HASENACK; FLORES, 1994), and is located on the state coast, similarly to Rio de Janeiro and Fortaleza. Porto Alegre has a demographic density of 2,837.52 people/km^2 and a population size of 1,409,351 inhabitants (BRASIL, 2010). It receives thousands of tourists from Argentina and Uruguay, that border Rio Grande do Sul (BRASIL, 2020a). Porto Alegre is the coldest municipality considered herein, averaging 21 $\pm$ 4 C° in the last decade (WAN; HOOK; HULLEY, 2015). The average rainfall per 8 days is 22 $\pm$ 20 mm(FUNK et al.,) during the same period.

For the SEIR model proposed in this Thesis, in addition to three (Rio de Janeiro, Fortaleza and Porto Alegre) of the four municipalities previously studied for the SIR model, other nine were also added as case studies. The criteria for selecting municipalities was to choose the two most populous municipalities of each state of Brazil that has a partnership with InfoDengue research group (CODECO et al., 2018). Foz do Iguaçu was removed from the SEIR model analysis since it is not the first or second most populous municipality in Paraná State. Therefore, the municipalities studied in the SEIR model were:

Rio de Janeiro State: the two biggest municipalities in population size of Rio de Janeiro State are Rio de Janeiro and São Gonçalo. With 6,320,446 and 999,728 inhabitants, respectively, in 2010 (BRASIL, 2010) and projections of 6,747,815 and 1,091,737, respectively, in 2020 (BRASIL, 2020c), they share similar environments in respect to temperature and rainfall, but different economies. São Gonçalo per capita income (R$ 724,92) is less than half of the per capita income of Rio de Janeiro (R$ 1,784.44) (BRASIL, 2020b).

Ceará State: Fortaleza and Caucaia are the biggest cities of this State. They had a population size of 2,452,185 and 325,441, respectively, in 2010 (BRASIL, 2010) and projections of 2,686,612 and 365,212, respectively, in 2020 (BRASIL, 2020c). These

cities share the same economic disparity of Rio de Janeiro and São Gonçalo: Caucaia´s income per capita is R$ 405.51 whereas the income per capita of Fortaleza, the capital of the state, is more than the double, R$ 994.29. (BRASIL, 2020b).

Minas Gerais State: Belo Horizonte, the capital of the state, and Contagem represented the State of Minas Gerais. They had a population size of 2,375,151 and 603,442, respectively, in 2010 (BRASIL, 2010) and projections of 2,521,564 and 668,949, respectively, in 2020 (BRASIL, 2020c). In relation to per capita income, the difference between municipalities is not as big as in the municipalities previously mentioned above although still significant: Contagem has R$ 908.23 per capita income and the capital has less than the double of this value, R$ 1,766.47 (BRASIL, 2020b).

Paraná State: Curitiba and Londrina are the biggest municipalities from this State. They had a population size of 1,751,907 and 506,701, respectively, in 2010 (BRASIL, 2010) and projections of 1,948,626 and 575,377, respectively, in 2020 (BRASIL, 2020c). Curitiba is located in the south of Brazil, so it has a low mean temperature along the year compared to the rest of the country, 19 C° average with 3.17 C° deviation (WAN; HOOK; HULLEY, 2015). Londrina is in almost the same latitude of Rio de Janeiro, which causes a warmer weather, 24.31 C° average with 3.66 C° deviation along the year (WAN; HOOK; HULLEY, 2015). Both municipalities appear in the list of one hundred municipalities with the highest income per capita in Brazil. Curitiba´s per capita income is R$ 1802.45 and Londrina´s, R$ 1,217.45 (BRASIL, 2020b).

Santa Catarina State: Joinville is the biggest city of this State, and Florianópolis is the capital. They had a population size of 515,288 and 421,240, respectively, in 2010 (BRASIL, 2010) and projections of 597,658 and 508,826, respectively, in 2020 (BRASIL, 2020c). Florianópolis has the sixth per capita income from Brazil: R$ 2,096.56. Joinville is an industrial city with R$ 1,310.36 of per capita income (BRASIL, 2020b).

Espírito Santo State: the biggest municipalities in Espírito Santo are Serra and Vila Velha, none of them are the capital city. They had a population size of 409,267 and 414,586, respectively, in 2010 (BRASIL, 2010) and projections of 527,240 and 501,325, respectively, in 2020 (BRASIL, 2020c). They represent the biggest relative population

growth from municipalities inside this study case. Espírito Santo is located next to Rio de Janeiro State, with similar environment (WAN; HOOK; HULLEY, 2015). However, unlike Rio de Janeiro, which received almost 1,000,000 tourists in one year (in 2010), Espírito Santo´s tourism activity is small, having received near to 5,000 tourist per year (BRASIL, 2020a). Their per capita income are small compared to others municipalities from Brazil, reaching R$ 1,384.33 for Vila Velha and R$ 787.83 for Serra (BRASIL, 2020b).

5.2 Data

5.2.1 Demographic and geographic data

The centroid of the municipalities (latitude, longitude), their size and population growth were obtained from *Instituto Brasileiro de Geografia e Estatística* (IBGE) (BRASIL, 2010; BRASIL, 2020c). In the SIR model, birth and mortality human rates were based on 2010 data (Rio de Janeiro, 2020) from Rio de Janeiro city and were also used for all the other cities in the model. In the SEIR model, each city had its own population daily growth based on the difference between 2010 data and 2020 populations (BRASIL, 2010; BRASIL, 2020c). The average Brazilian mortality rate in 2010 ($0,603\%$) was also obtained from IBGE (BRASIL, 2010).

The number of tourists was provided by the Tourism Ministry (BRASIL, 2020a). It provided yearly data aggregated by State.

5.2.2 Epidemiological data

Dengue notification is mandatory in Brazil and the data from 2010 to 2020 was obtained from InfoDengue *Application Programming Interface* (API) that gather data from *Sistema de Informação de Agravos de Notificação* (SINAN) (BRASIL., 2007). InfoDengue provides reported cases aggregated per municipality per week. The patient's residence was used as the reference for dengue occurrence (CODECO et al., 2018).

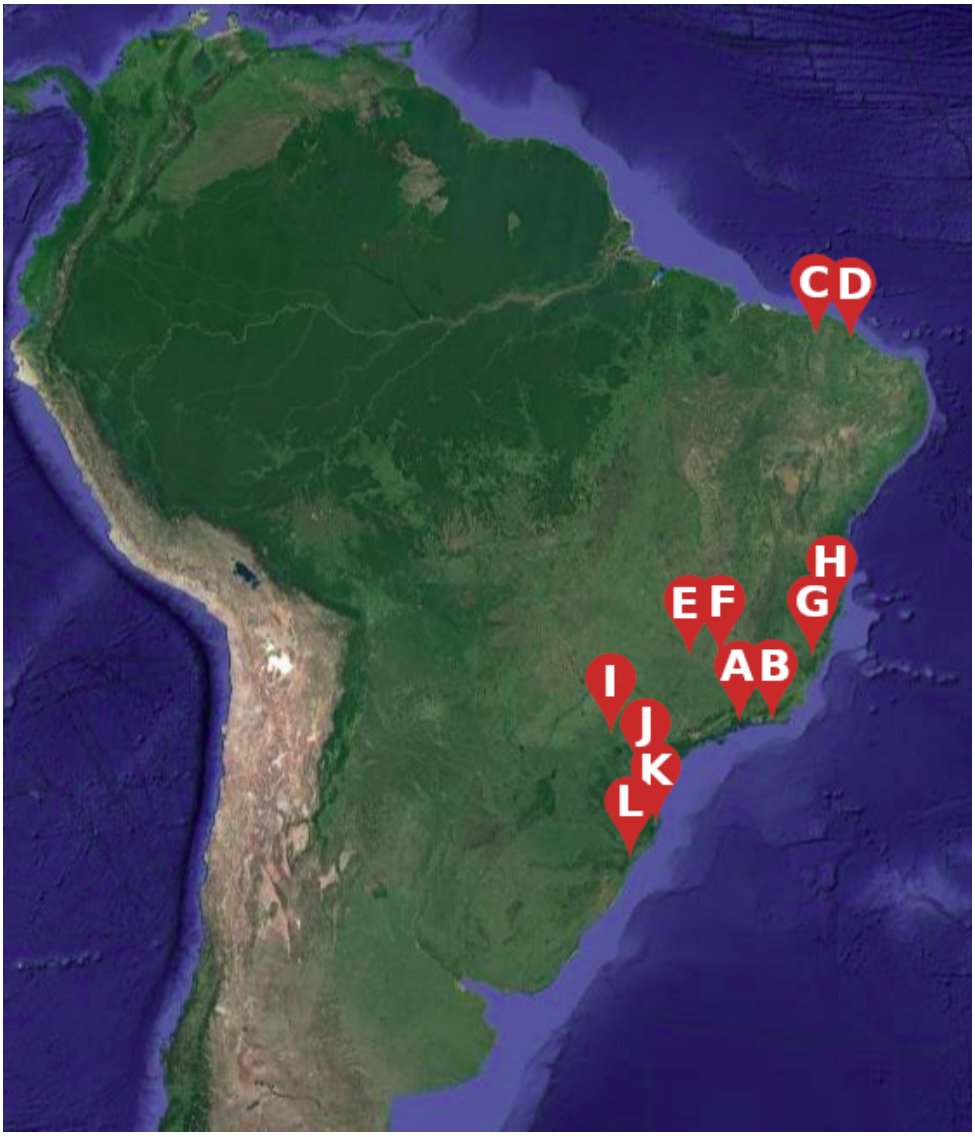

Figure 8 – Brazilians municipalities used in this Thesis as case studies, pointed in South America satellite view: (a) Rio Janeiro; (b) São Gonçalo; (c) Caucaia; (d) Fortaleza; (e) Contagem; (f) Belo Horizonte; (g) Vila Velha; (h) Serra; (i) Londrina; (j) Curitiba; (k) Joinville; and (l) Florianópolis (MAPS, 2021)

5.2.3 Climate data

The Earth Surface Temperature (LST) data came from the MODerate Resolution Imaging Spectroradiometer (MODIS / MOD11A2) sensor on the Terra satellite (WAN; HOOK; HULLEY, 2015). It has 8 days of Emissivity, with a resolution of 1 square km of Sine Grid. The data emitted by the satellite refer to the average daily temperature (LST Day) and night (LST Night) every 8 days. The average between day and night temperature was chosen to represent the average overall temperature. Many parameters are bounded by maximum and minimal values, which makes raw temperature data (either day or night) not a good fit to those parameters.

Rainfall data was obtained from the Climate Hazards Group InfraRed Precipitation with Station Data (CHIRPS) database at the Climate Hazard Center at the University of California, Santa Barbara (UCSB-CHG) (FUNK et al.,). CHIRPS has more than 30 years of operation and continues to operate to this day, with a daily resolution of 5 km. The sum of all rainfall in the 8-day period was used to represent that period. Rainfall data was aggregated by municipality with the same method used for temperature.

5.3 Data transformation

Population size from 2010 was used to represent total population size. The 8-day birth and death rates were the same for the SIR model and were measured from the number of births in the Rio de Janeiro State in 2010 divided by $\frac{365}{8}$ (Rio de Janeiro, 2020), which means the population size maintained in the same number between time. In the SEIR model, birth and death rates were considered different; it was used the Brazilian average mortality rate as the death rate in all municipalities, but the birth rate was the sum of the average mortality rate in 2010 Brazil ($6.03 * 10^{-3}$ yearly rate or $1.64 * 10^{-5}$ daily rate) and the daily growth of each municipality, in the end, all municipalities ended with a bigger population comparing 2010 to 2020. The daily growth was a function between 2010 population and 2020 population, as given by:

$$\text{daily growth of municipality} = \left(\frac{\text{2020 population size}}{\text{2010 population size}}\right)^{\frac{1}{3650}} - 1$$

The centroid of each municipality was used to extract the climate data. From

Table 1 – Population size and growth in 2010 for each studied municipality (BRASIL, 2010), mean and standard deviation of the temperature (C°), and mean and standard deviation yearly rainfall (mm).

Municipality	Population	Daily Growth	$\mu_{temperature}$	$\sigma_{temperature}$	$\mu_{rainfall}$	$\sigma_{rainfall}$
Rio de Janeiro	6,320,446	$1.79 * 10^{-5}$	26,35	3,06	748,41	102,75
Fortaleza	2,452,185	$2.50 * 10^{-5}$	28,332	2,01	512,81	101,89
Belo Horizonte	2,375,151	$1.64 * 10^{-5}$	23,64	2,30	701,47	139,03
Curitiba	1,751,907	$2.92 * 10^{-5}$	19,20	3,17	1040,44	114,43
São Gonçalo	999,728	$2.41 * 10^{-5}$	25,82	2,99	756,86	101,37
Contagem	603,442	$2.82 * 10^{-5}$	23,53	2,33	732,10	143,99
Joinville	515,288	$4.06 * 10^{-5}$	19,92	3,14	1341,74	141,50
Londrina	506,701	$3.48 * 10^{-5}$	24,31	3,66	1010,49	132,07
Serra	409,267	$6.94 * 10^{-5}$	24,29	2,41	690,40	116,36
Florianópolis	421,240	$5.18 * 10^{-5}$	19,97	3,28	1090,27	125,30
Vila Velha	414,586	$5.2 * 10^{-5}$	24,44	2,45	690,88	116,82
Caucaia	325,441	$3.16 * 10^{-5}$	28,59	2,14	481,14	93,74

each one, it was subtracted and added 0.2° (almost 23 km), thus creating, in the end, four coordinates points representing enough square to contemplate the municipality. After that, all pixels within the square of the municipality were extracted from the temperature and rainfall maps. The average pixels were used to represent the climate data.

The SIR model used an 8-day period time-frame to match the periodicity of satellite-based weather data, while the SEIR model used a daily time-frame to match with works done in literature such as Huber et al. (2018). Since temperature had an eight day emissivity, to standardize, the accumulated rainfall were collected at the same 8 day period.

Although the analysis used either eight-day periods or daily periods, the number of dengue cases has a weekly periodicity (CODECO et al., 2018). Thus, this weekly period was transformed to daily by dividing by seven. For the analysis using eight-day period, after transforming in daily period, it was summed every eight-day to transform it into an eight-day period in such a way that the eight-day period has some part of cases of two different weekly reports.

The number of tourists was obtained aggregated by year and by state (BRASIL, 2020a). Since in this analysis the most influential (in terms of population size) municipalities of each State were used, the number of the State was used to represent

the municipality. The yearly aggregation was divided by $\frac{365}{8}$ to become an eight-day time-frame and by 365 to become a daily time-frame.

In addition to these transformations, temperature and rainfall data were stored in linear interpolation functions. The interpolation was necessary since the models had a continuous time frame. The functions received as input the time, that could be a decimal, and returned the temperature or rainfall related to that time, which was calculated by weight average between the two nearest values extracted from maps.

5.4 Models developed

5.4.1 SI-SI-SIR model

The model used a SI-SI-SIR structure to describe the DENV transmission dynamics. The model has susceptible (S), infected (I) and recovered (R) compartments for human population and S and I compartments for *Ae. aegypti* egg and adult populations, because mosquitoes stay infected for their entire life. Figure 9 presents the model diagram.

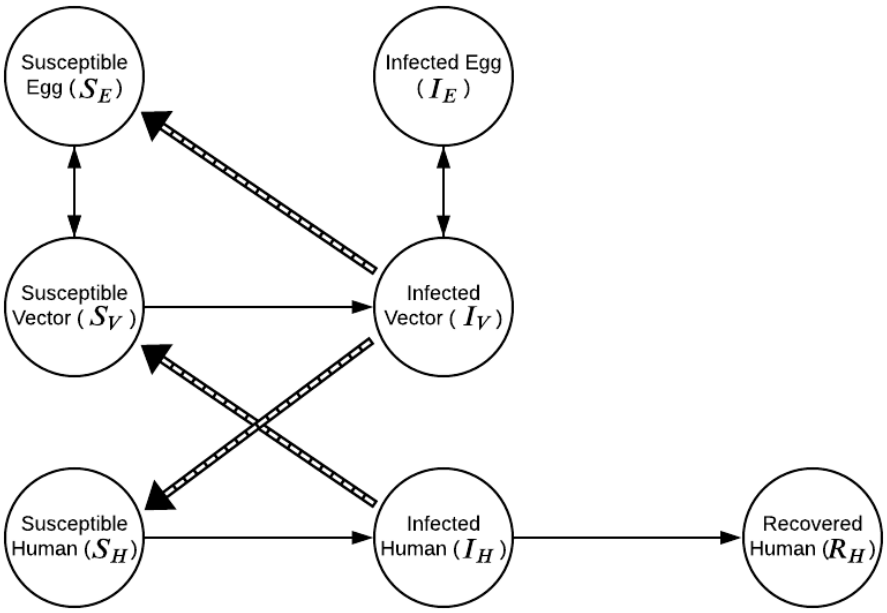

Figure 9 – SI-SI-SIR model diagram. S_E and I_E represent the non-infected and infected egg of the vector population; S_V and I_V, the susceptible and infectious compartments of the adult mosquito population; and S_H, I_H and R_H the susceptible, infectious and recovered portions of the human population, respectively. Solid arrows indicates the direction of transmission.

The equations bellow represent the interactions between each population compartment. The first equations (5.1a and 5.1b) represent the egg population, where S_E is the susceptible eggs compartment and I_E, the infected eggs. The temperature-dependent function $o(T)$ is the number of eggs laid by female mosquito. The rainfall-dependent function $d(R)$ represents the eggs development rate. f_v is the female proportion in the mosquito population, v_t is the vertical transmission rate and μ_e is the egg mortality rate. Temperature and rainfall time series are denoted respectively by T and R.

$$\frac{dS_E}{dt} = o(T)S_V + (1 - v_t)o(T)I_V - (\mu_e + d(R))S_E \tag{5.1a}$$

$$\frac{dI_E}{dt} = v_t o(T)I_V - (\mu_e + d(R))I_E \tag{5.1b}$$

$$\frac{dS_V}{dt} = d(R)f_v s_a(T)S_E\left(1 - \frac{N_V}{KN_H}\right) - \left(a(T)p_{hm}(T)\frac{(I_H + I_m)}{N_H} + \mu_v\right)S_V \tag{5.1c}$$

$$\frac{dI_V}{dt} = d(R)f_v s_a(T)I_E\left(1 - \frac{N_V}{KN_H}\right) + \left(a(T)p_{hm}(T)\frac{(I_H + I_m)}{N_H}\right)S_V - \mu_v I_V \tag{5.1d}$$

$$\frac{dS_H}{dt} = \mu_h N_H - a(T)p_{mh}(T)I_V\frac{S_H}{N_H} - \mu_h S_H \tag{5.1e}$$

$$\frac{dI_H}{dt} = a(T)p_{mh}(T)I_V\frac{S_H}{N_H} - (\gamma + \mu_h)I_H \tag{5.1f}$$

$$\frac{dR_H}{dt} = \gamma I_H - \mu_h R_H \tag{5.1g}$$

Equations 5.1c and 5.1d represent adult mosquitoes, with S_V standing for susceptible and I_V for infected adult mosquitoes. $s_a(T)$ is the egg-to-adult survival rate and μ_v the adult mortality rate. The aquatic phase (larvae and pupae) is not explicitly represented in the model and thus the survival and mortality rates are absorbed into the egg-to-adult rates described above. N_V is the total number of the vector population ($S_v + I_v$). K is the environmental carrying capacity, which constrains the growth of the mosquito population. $a(T)$ is the mosquito biting rate, p_{hm} is the probability of a human infecting a mosquito per bite, I_m is the rate of pendular immigration of infected humans and N_H is the total number of humans in the model ($S_H + I_H + R_H$).

The SIR sub-model (equations 5.1e, 5.1f and 5.1g) represents human population with S_H, I_H and R_H compartments governed by equations 5.1e, 5.1f and 5.1g, respectively. Human population was assumed as constant with same birth and death rates (μ_h) plus a small pendular migration rate. The pendular migration represents residents that live in one municipality and work or study in another (ZASLAVSKY; GOULART, 2017). Pendular migration does not affect the population size in the model, but affects the force of infection since mosquitoes can bite infected humans coming from others places. γ represents the recovery rate of humans after infection. Lastly, $p_{mh}(T)$ is the probability of a mosquito to infect a human.

5.4.1.1 SI-SI-SIR initial conditions

Initial conditions of the model for each municipality were defined in Table 2. $S_H(0)$ were determined empirically, by fitting the model to data. $I_H(0)$ was set to the DENV incidence in the first week of January 2010, the beginning of the analysis. $R_H(0)$ was set to $N_H(0) - S_H(0) - I_H(0)$.

Table 2 – Municipality-specific initial conditions for simulations

Municipality	N_H	$S_H(0)$	$I_H(0)$	Tourists (8 day)$^{-1}$
Rio de Janeiro	6.320.446	327.259	40	21.535
Fortaleza	2.452.185	87.734	70	2.099
Porto Alegre	1.409.351	171.628	2	14.325
Foz do Iguaçu	256.088	37.332	35	15.892

For the initial conditions of adult mosquito population ($S_V(0) + I_V(0)$), 0.7 female mosquitoes per person was used, as reported by Neira et al. (NEIRA et al., 2014), thus $S_V(0)$ and $I_V(0)$ were directly proportional to $S_H(0) + R_H(0)$ and $I_H(0)$, respectively, multiplying it by 0.7. This ratio was used for the egg compartment as well: $S_E(0)$, the initial state of susceptible eggs, was equal to $0.7(S_H(0) + R_H(0))$, while $I_E(0)$, the initial state of infected eggs, was equal to $0.7I_H(0)$.

Most of the vector parameters were reported in a daily time frame; for these, the parameters were multiplied by 8 to transform to an eight-day time frame. Egg and adult mortality rates were the only ones different, as they were calculated using the following formula: $1 - (1 - x)^8$, assuming the daily values are x, since $(1 - x)^8$ represent the probability of surviving in eight day period. Rates that did not depend on time were maintained the same.

The eight-day time frame parameters are presented in Table 3 for constants values and Table 4 for values defined by a function.

Table 3 – Constant eight-days time-frame parameters for dengue transmission dynamic model SI-SI-SIR. †these values were found in the literature with daily rates and were converted to 8 day rate. ‡converted from annual rates.

Parameter	Definition	Value	Source
f_v	Mosquito sex ratio	0.5	(MAGORI et al., 2009)
μ_e	Egg mortality rate (8 day)$^{-1}$	0.077255†	(BAR-ZEEV et al., 1957)
v_t	Vertical transmission rate	0.1	(ADAMS; BOOTS, 2010)
γ	DENV recovery rate (8 day)$^{-1}$	1	(ORGANIZATION, 2009)
I_m	Infected immigrants	0.001	
μ_h	Human mortality and birth rate (8 day)$^{-1}$	0.0003656 ‡	(Rio de Janeiro, 2020)
k	Carrying Capacity	0.7	(NEIRA et al., 2014)

Table 4 – Temperature and rainfall dependent rates for dengue transmission dynamic model SI-SEI-SEIR (eight-days). The Brière function is given by $[aT(T-b)(c-T)^{\frac{1}{2}}]$. The quadratic is $[a(T-b)(T-c)]$ and the linear function is aR function. T represents temperature and R represents rainfall.

Variable	Definition	Function	a	b	c	Source
$a(T)$	Biting rate (8 day)$^{-1}$	Brière	0.00161	13.35	40.08	(MORDECAI et al., 2017)
$o(T)$	Oviposition rate per 8 days	Brière	0.06848	14.58	34.61	(MORDECAI et al., 2017)
$s_a(T)$	Aquatic survival rate	Quadratic	-0.00599	13.56	38.29	(MORDECAI et al., 2017)
$p_{hm}(T)$	human to mosquito infection rate per bite	Brière	0.000491	12.22	37.46	(MORDECAI et al., 2017)
$p_{mh}(T)$	mosquito to human infection rate per bite	Brière	0.000849	17.05	35.83	(MORDECAI et al., 2017)
$\mu_v(T)$	Adult mosquito mortality rate (8 day)$^{-1}$	Quadratic	-0.0185	9.16	37.73	(MORDECAI et al., 2017)
$d(R)$	Development rate	Quadratic	-2.29574	-1.18161		(ALTO; JULIANO, 2001)

5.4.2 SI-SEI-SEIR model

The SEIR model was adapted to a daily time frame and introduced the exposed compartment to the vector and to the human population. The SI-SEI-SEIR model was used to describe the DENV transmission dynamics. The new compartment, the exposed (E) compartment, represents the intrinsic and extrinsic incubation period. They represent individuals that are passing by their incubation period, extrinsic for vector and intrinsic

for humans, and will become infectious right after this period. The daily time frame model was evaluated with and without the exposed compartment to understand the impact of this change. Figure 10 presents the model diagram.

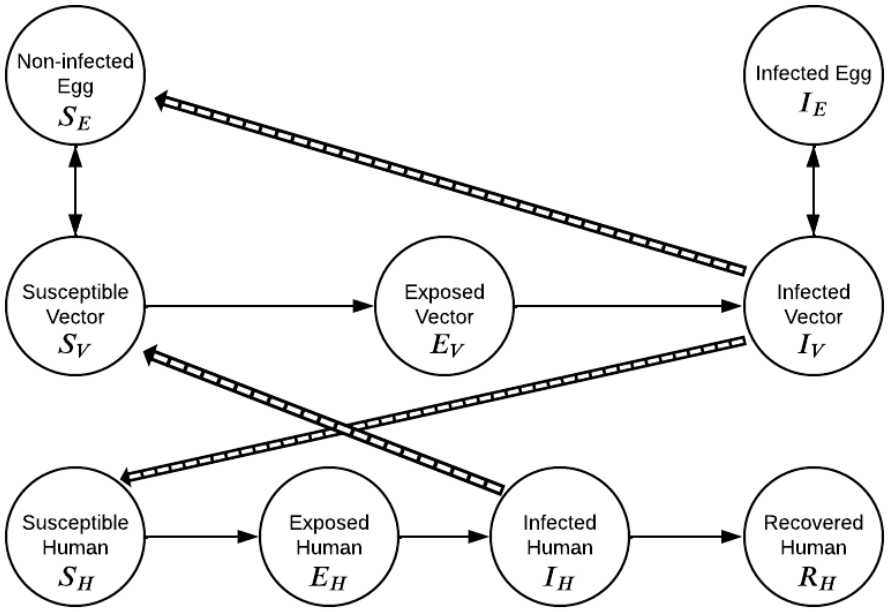

Figure 10 – SI-SEI-SEIR model diagram. S_E and I_E represent the non-infected and infected egg of the vector population; S_V, E_V and I_V, the susceptible, exposed and infectious compartments of the adult mosquito population; and S_H, E_H, I_H and R_H the susceptible, infectious, exposed and recovered portions of the human population, respectively. Solid arrows indicate the direction of transmission.

The equations below constitute the SEIR model. Since two new exposed compartment were introduced, it also added two new parameters: the intrinsic incubation rate (γ) and extrinsic incubation rate ($e(T)$); which reflect the velocity an individual change from exposed to infected in humans and mosquitoes, respectively.

$$\frac{dS_E}{dt} = o(T)S_V + (1 - v_t)o(R)I_V - (\mu_e + h)S_E \tag{5.2a}$$

$$\frac{dI_E}{dt} = v_t o(T)I_V - (\mu_e + h)I_E \tag{5.2b}$$

$$\frac{dS_V}{dt} = d(R)f_v s_a(T)S_E\left(1 - \frac{N_V}{KN_H}\right) - \left(a(T)p_{hm}(T)\frac{(I_H + I_m)}{N_H} + \mu_v\right)S_V \tag{5.2c}$$

$$\frac{dE_V}{dt} = a(T)p_{hm}(T)\frac{(I_H + I_m)}{N_H}S_V - (e(T) + \mu_v)E_V \tag{5.2d}$$

$$\frac{dI_V}{dt} = d(R)f_v s_a(T)I_E\left(1 - \frac{N_V}{KN_H}\right) + e(T)E_V - \mu_v I_V \tag{5.2e}$$

$$\frac{dS_H}{dt} = \mu_h N_H - a(T)p_{mh}(T)I_V\frac{S_H}{N_H} - \mu_h S_H \tag{5.2f}$$

$$\frac{dE_H}{dt} = a(T)p_{mh}(T)I_V\frac{S_H}{N_H} - (\delta + \mu_h)E_H \tag{5.2g}$$

$$\frac{dI_H}{dt} = \delta E_H - (\gamma + \mu_h)I_H \tag{5.2h}$$

$$\frac{dR_H}{dt} = \gamma I_H - \mu_h R_H \tag{5.2i}$$

5.4.2.1 SI-SEI-SEIR initial conditions

Twelve municipalities were used as case studies. Table 5 shows the initial values for compartments used in the model and parameters that differ from municipality to municipality (Table 1). The dengue incidence in the municipality in the first week of 2010 was used as the initial condition for $E_H(0)$ and $I_H(0)$. The proportion of infectious in the vector population followed that of the human population. $S_H(0)$ was set by optimization in the first simulation, which will further be discussed, and $R_H(0) = 1 - S_H(0) - E_H(0) - I_H(0)$.

The constant daily rates are in Table 6 and the rates defined by a function are in Table 7.

5.5 Model fitting

5.5.1 Sensitivity analysis

A Sobol sensitivity analysis was conducted to determine the leverage of each parameter concerning the fit between the simulated and observed data (MARTINEZ-

Table 5 – Municipality-specific initial conditions and parameters

Municipality	$I_H(0)$ and $E_H(0)$ values	**Tourists per day**
Rio de Janeiro	40	2,691
Fortaleza	70	262
Belo Horizonte	70	154
Curitiba	70	1,986
São Gonçalo	35	2,691
Contagem	28	154
Joinville	10	351
Londrina	23	1,986
Serra	26	14
Florianópolis	27	351
Vila Velha	22	14
Caucaia	10	262

Table 6 – Initial values for constant daily time-frame parameters for dengue transmission dynamic model SI-SEI-SEIR

Parameter	**Definition**	**Value**	**Source**
f_v	Mosquito sex ratio	0.5	(MAGORI et al., 2009)
μ_e	Egg mortality rate (1 day)$^{-1}$	0.01	(BAR-ZEEV et al., 1957)
δ	Intrinsic incubation rate	5.9^{-1}	(LESSLER et al., 2016)
v_t	Vertical transmission rate	0.1	(ADAMS; BOOTS, 2010)
γ	DENV recovery rate (1 day)$^{-1}$	5^{-1}	(ORGANIZATION, 2009)
I_m	Infected immigrants	0.001	
k	Carrying Capacity	0.7	(NEIRA et al., 2014)

ROMERO et al., 2002). The sensitivity analysis identified the parameters that more substantially affect model adherence to the observed data. The Python Sensitivity Analysis Library (SALib) was used (HERMAN; USHER, 2017). The sum of squared errors (SSE) between the simulated and observed time series was applied as the model output.

The following parameters and respective ranges were scanned in this analysis for SI-SI-SIR model: $o(T)$ (0.25-4), v_t (0.25-4), K (0.25, 4), $a(T)$ (0.25-4), i_m (0.25-4), p_{mh} (0.25-1), p_{hm} (0.25-1), f_v (0.5-1.5), u_e (0.25-4), u_v (0.25-4), γ (0.25-2), u_h (0.25-4), $s_a(T)$ (0.25-2). For constant parameters, the range represents the exact variable value; for dependent parameters, the range represents a multiplier applied to the constant a in the Brière [aT(Tb)(cT)12] and quadratic [a(Tb)(Tc)], [a(R2+bR)] functions. Others parameters were also scanned, such as minimal and maximum temperature in the

Table 7 – Initial values for temperature and rainfall dependent daily rates for dengue transmission dynamic model SI-SEI-SEIR. The Brière function is given by $[aT(T-b)(c-T)^{\frac{1}{2}}]$. The quadratic is $[a(T-b)(T-c)]$ and the linear function is aR function. T represents temperature and R represents rainfall.

Variable	Definition	Function	a	b	c	Source
$a(T)$	Biting rate (1 day)$^{-1}$	Brière	0.000202	13.35	40.08	(MORDECAI et al., 2017)
$s_a(T)$	Aquatic survival rate	Quadratic	-0.00599	13.56	38.29	(MORDECAI et al., 2017)
$p_{hm}(T)$	human to mosquito infection rate per bite	Brière	0.000491	12.22	37.46	(MORDECAI et al., 2017)
$p_{mh}(T)$	mosquito to human infection rate per bite	Brière	0.000849	17.05	35.83	(MORDECAI et al., 2017)
$e(T)$	virus extrinsic incubation rate (day^{-1})	Brière	0.0000665	10.68	45.90	(MORDECAI et al., 2017)
$\mu_v(T)$	Adult mosquito mortality rate (day^{-1})	Quadratic	-0.148	9.16	37.73	(MORDECAI et al., 2017)
$o(T)$	Oviposition rate per day	Brière	0.00856	14.58	34.61	(MORDECAI et al., 2017)
$d(R)$	Development rate	Quadratic	-2.29574	-1.18161		(ALTO; JULIANO, 2001)

environmental-dependent functions: t_{min} (-4-+4) and t_{max} (-4-+4); it was increased or subtracted from 0 to 4 C° to each. The initial values for the susceptible population for egg and adult vector population $SEV(0)$ (0-1 times the total human population), $SV(0)$ (0-1 the total human population) were also scanned ; and initial value for susceptible human population $S(0)$ (0.3-1 the total human population).

5.5.2 Calibration

Following the sensitivity analysis, constant and climate-dependent parameters obtained from the literature were adapted for each municipality, in order to better adapt to the climate context of each municipality. This process was performed empirically for the SIR model, observing the analysis result. We sought to alter the parameters as little as possible from those reported in the literature, and even with the employed adaptations, the same order of magnitude of the original values was always maintained, and they all remained biologically realistic. The adaptations were performed based on

the understanding that mosquitoes adapt differently to the climate of each municipality, and so slightly different biological parameters than those observed in the laboratory under controlled and fixed conditions are, therefore, possible and likely.

For the SEIR model, the values of each parameter were fitted using the Grid Search Algorithm, which searches over a given subset of the hyperparameters space of the training algorithm (FREEMAN; DOE; SIEMIGINOWSKA, 2001). The best parameters values were the ones that produced the smaller SSE between the grid.

5.6 Model evaluation

The Akaike information criterion (AIC) was used as the mean to assess the goodness-of-fit of different models version. The AIC penalizes models having a large dimension at the same time that measure lack of fit to the data (WAGENMAKERS; FARRELL, 2004). The AIC was calculated using equation 5.3.

$$AIC = -2Log(L_i) + 2V_i \tag{5.3a}$$

Where L_i is the maximum likelihood for the candidate model i and V_i the number of free parameters.

A set of visualizations was also used for comparing simulations and observed data. All models were tested using Python computer language (ROSSUM; JR, 1995) with the Python library numpy (HARRIS et al., 2020).

6 Results

6.1 SI-SI-SIR model

6.1.1 Sensitivity Analysis

The sensitivity analysis pointed to the most important parameters using the first order and the second order values (MARTINEZ-ROMERO et al., 2002). First order analyzes how much a parameter contributes to model sensitivity. High first order values mean that small changes in the parameter influence greatly the model. Second order indicates how much a parameter contributes to other parameters' sensitivity. High second order values mean two or more variables are correlated and, since they are correlated, changes in one variable are enough to change all correlated ones. When choosing variables, the most important ones are usually those that have high first order values and do not have high second order values between themselves. (MARTINEZ-ROMERO et al., 2002).

According to the sensitivity analysis, dengue recovery rate (γ), human birth and mortality rate (μ_h), and biting rate ($a(T)$) all affect the model behavior more strongly than the other evaluated parameters. When averaging the values for the four municipalities, the following parameters had first and total order sensitivity coefficients higher than 5%: γ, μ_h and $a(T)$ (Figure 11). The second order sensitivity coefficients revealed that mosquito-to-human infection probability per bite ($p_{mh}(T)$), human-to-mosquito infection probability per bite ($p_{hm}(T)$) and carrying capacity (K) exhibited dependent associations between each other and the other assessed parameters (Figures 26, 27, 28 and 29 from Annex D). The recovery rate (γ) was the only parameter that exhibited a negative correlation with SSE ($R^2 > 80\%$) for all municipalities (Figures 30, 31, 32 and 33 from Annex D). The other evaluated parameters exhibited weak correlations with SSE, less than 50% and greater than -50% for the Pearson Correlation Index. When comparing parameter sensitivities between municipalities, Rio de Janeiro was the only municipality

where $\mu_v(T)$ comprised over 0.5% of the total order sensitivity coefficient, while Fortaleza was the only municipality not sensitive to i_m, the rate of infectious immigrants.

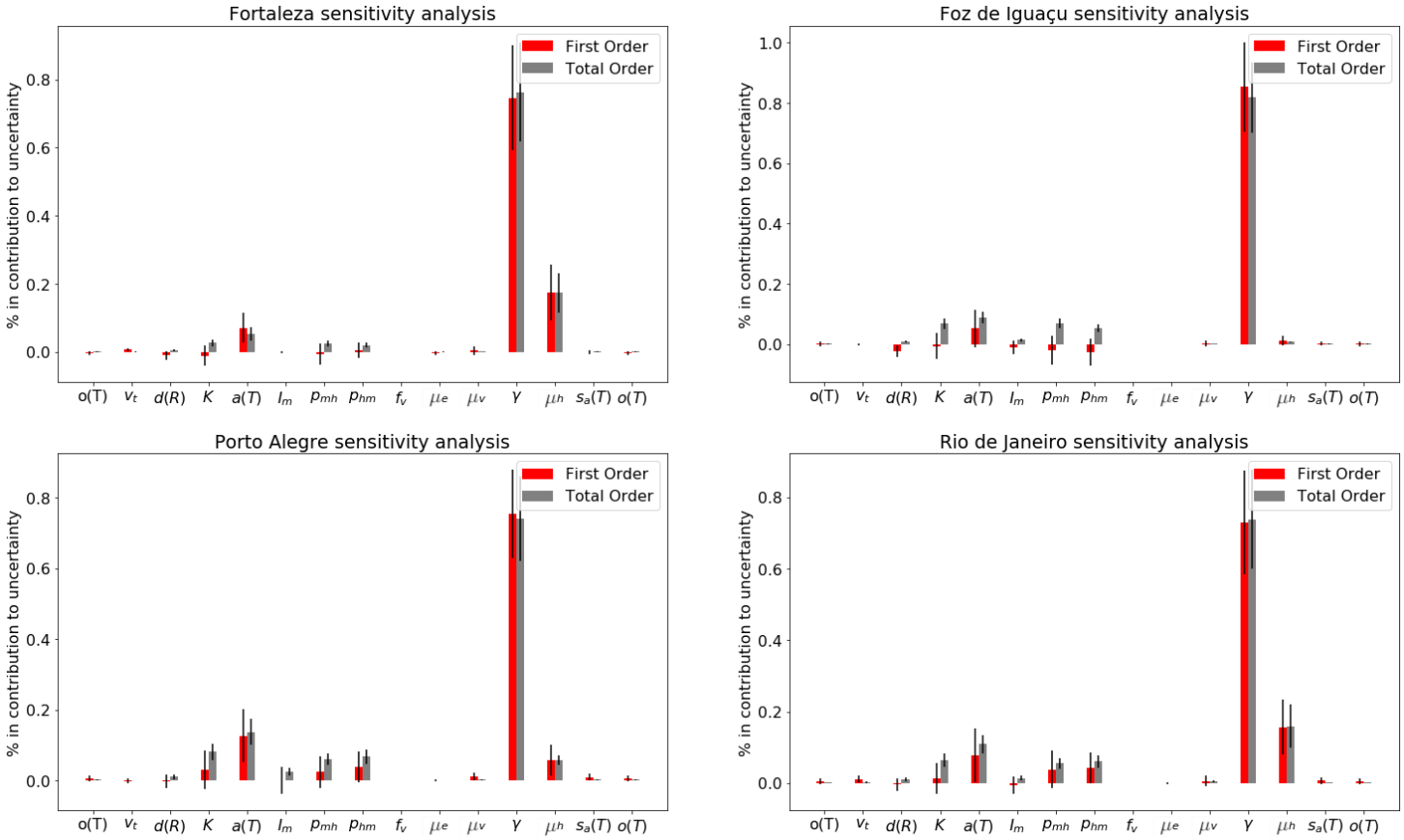

Figure 11 – Sensitivity analysis for each model parameter. From top to bottom, from left to right: Fortaleza, Foz do Iguaçu, Porto Alegre and Rio de Janeiro.

6.1.2 Calibration Process

The SI-SI-SIR model had a quality evaluation under four weather regimes across different Brazilian municipalities. Starting with parameter values from the literature (Tables 4 and 3), the vicinity of their values was explored to see how they would affect the model's fit to data. These changes aimed at bringing the parameters values closer to representing local mosquito population while keeping values in the same order of magnitude of original values (Table 8). The constant coefficients of carrying capacity (K), biting rate ($a(T)$), development rate ($d(R)$), and the probabilities of transmission between human and mosquito ($p_{mh}(T)$ and $p_{hm}(T)$) were adapted for each municipality.

The most significant changes in this qualitative process were observed in the

Table 8 – Adapted parameter values resulting from the exploratory analysis in four different geographical contexts. Concerning the temperature and rainfall dependent functions, the new value substitutes the a variable within their function.

Municipality	$p_{hm}(T)$	$p_{mh}(T)$	$a(T)$	K	$d(R)$
Rio de Janeiro	0.000491	0.0003396	0.00161	0.6	-0.1607018
Fortaleza	0.0001473	0.0003396	0.0012075	3	-0.229574
Porto Alegre	0.0002946	0.0002547	0.000966	0.6	-0.688722
Foz do Iguaçu	0.000491	0.0001698	0.00161	3	-0.0114787

municipality of Fortaleza, as, similarly to Foz do Iguaçu, the carrying capacity was 5-fold higher than that of Rio de Janeiro and Porto Alegre. Furthermore, $d(R)$ and $p_{hm}(T)$ were reduced to a third. Foz do Iguaçu's $p_{mh}(T)$ was also 50% lower, while $d(R)$ decreased to 5%. Porto Alegre variables displayed at least a half decrease, while Rio de Janeiro exhibited small changes to $d(R)$ and K.

Simulations obtained with the parameter values from Table 8 are displayed in Figure 12. Fortaleza and Rio de Janeiro most often presented simulated epidemic peaks resembling the observed peaks. This contrasts with Porto Alegre and Foz do Iguaçu, which exhibited less agreement between the simulated and observed peaks. From 2010 to 2016, simulations adhered to the observed series, both in terms of peak magnitudes and seasonality, while the simulated incidence began to stray away from the observations both in magnitude and in phase in all cities after 2016.

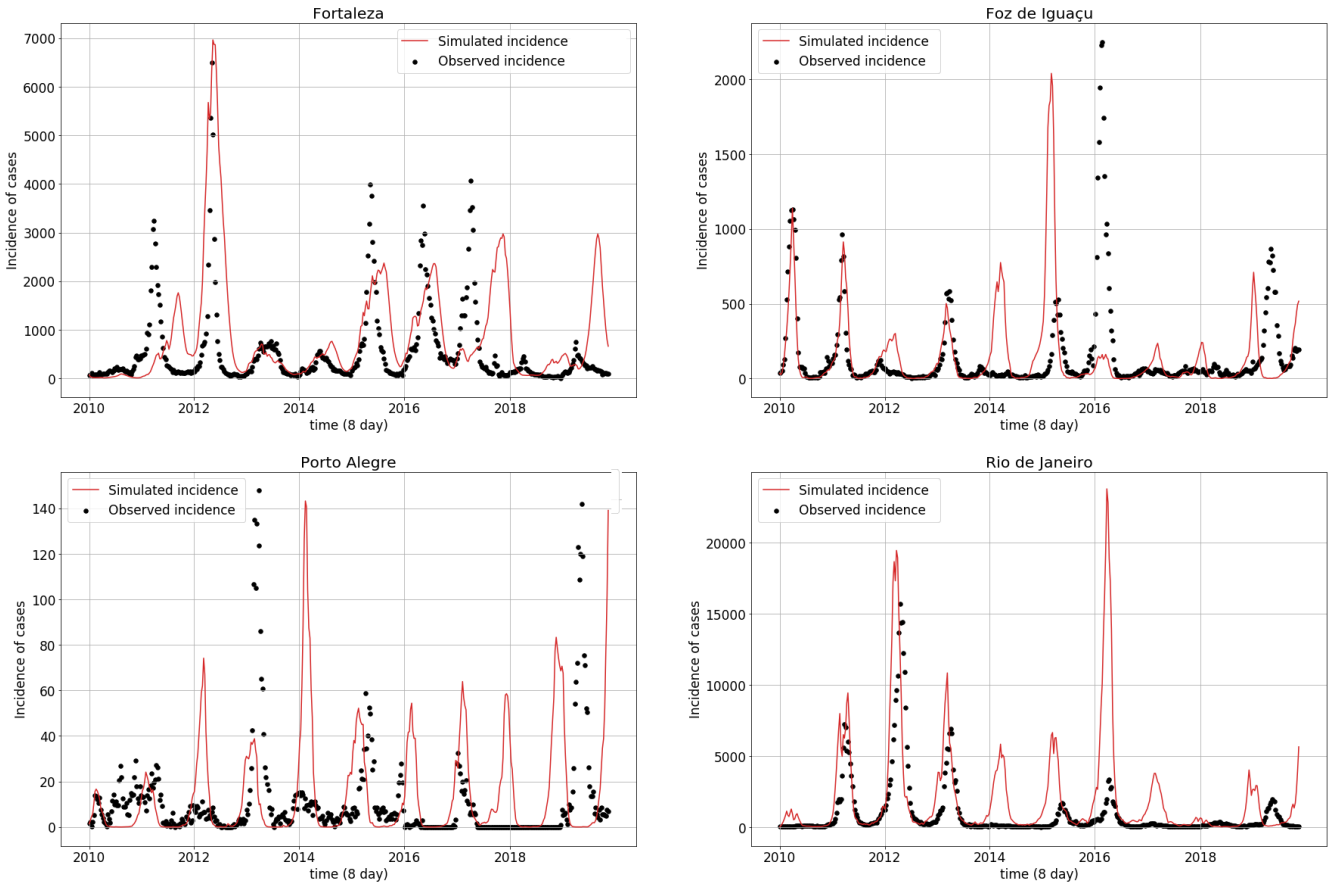

Figure 12 – Observed (black dots) and simulated (red line) dengue incidence time series for the four studied municipalities.

Table 9 indicates the attack rates for each municipality, i.e., the sum of all infected individuals during the period divided by the size of the population at risk. This differed between the simulated and observed time series. Foz do Iguaçu presents a lower simulated attack rate than the observed (9.64% difference), while overestimation in the attack rate of 8.05%, 6.02% and 0.09% were observed for Rio de Janeiro, Fortaleza and Porto Alegre respectively.

6.1.3 Vertical Transmission

Figure 13 compares simulations with and without vertical transmission. Removing vertical transmission influenced the epidemic peak size. Foz do Iguaçu and Rio de Janeiro, for example, exhibited a minor incidence peak in 2011, which has consistently increased from 2013 to 2020, and sometimes, as in 2015, presented higher differences.

Table 9 – **Adapted parameter values resulting from the exploratory analysis in four different geographical contexts.** Concerning the temperature and rainfall dependent functions, the new value substitutes the a variable within their function.

Municipality	Observed Attack Rate (%)	Simulated Attack Rate (%)
Rio de Janeiro	6.52	14.57
Fortaleza	10.34	16.36
Porto Alegre	0.37	0.46
Foz do Iguaçu	35.96	26.32

In Fortaleza, removing vertical transmission increased dengue incidence in certain epidemic peaks, especially in 2013. Porto Alegre did not exhibit significant epidemic size variations, although vertical transmission smoothed the epidemic peaks.

Figure 14 indicates the influence of vertical transmission on attack rates. Vertical transmission was positively correlated with attack rates for every municipality, indicating that with increasing vertical transmission there are also higher attack rates. In Rio de Janeiro, increasing the vertical transmission value from 3% to 13% (JOSHI; MOURYA; SHARMA, 2002; BOSIO et al., 1992; LEQUIME; PAUL; LAMBRECHTS, 2016) caused a 2% disparity in attack rates between the simulations, indicating an $126,408$ increase in dengue cases. Porto Alegre, on the other hand, requires a vertical transmission success rate of over 50% to begin displaying epidemic behavior.

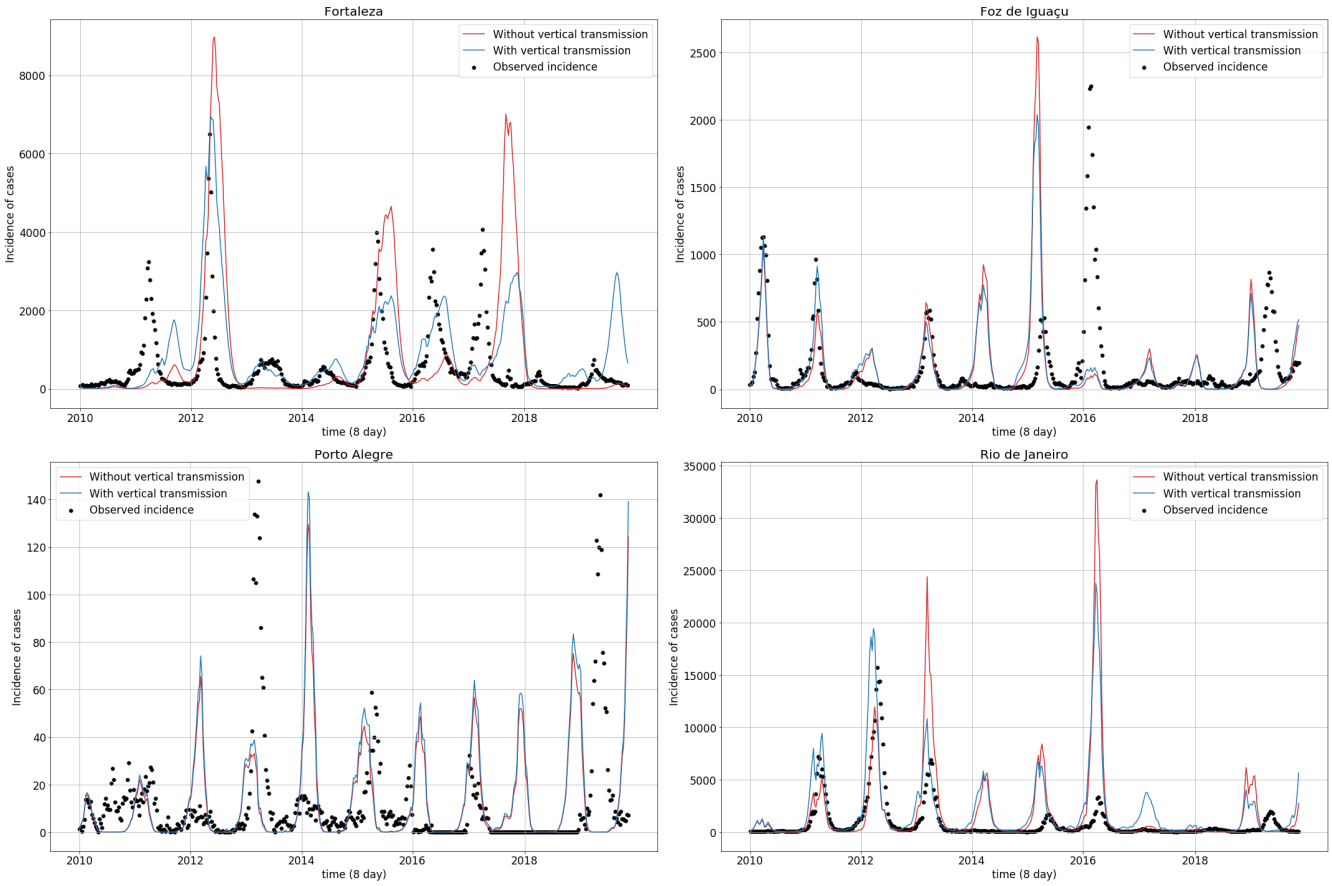

Figure 13 – Observed (dots) and simulated (solid line) dengue incidence time series, with (blue lines) and without (red lines) vertical transmission, for the four studied municipalities. Parameter values used in the simulations are shown in Table 8.

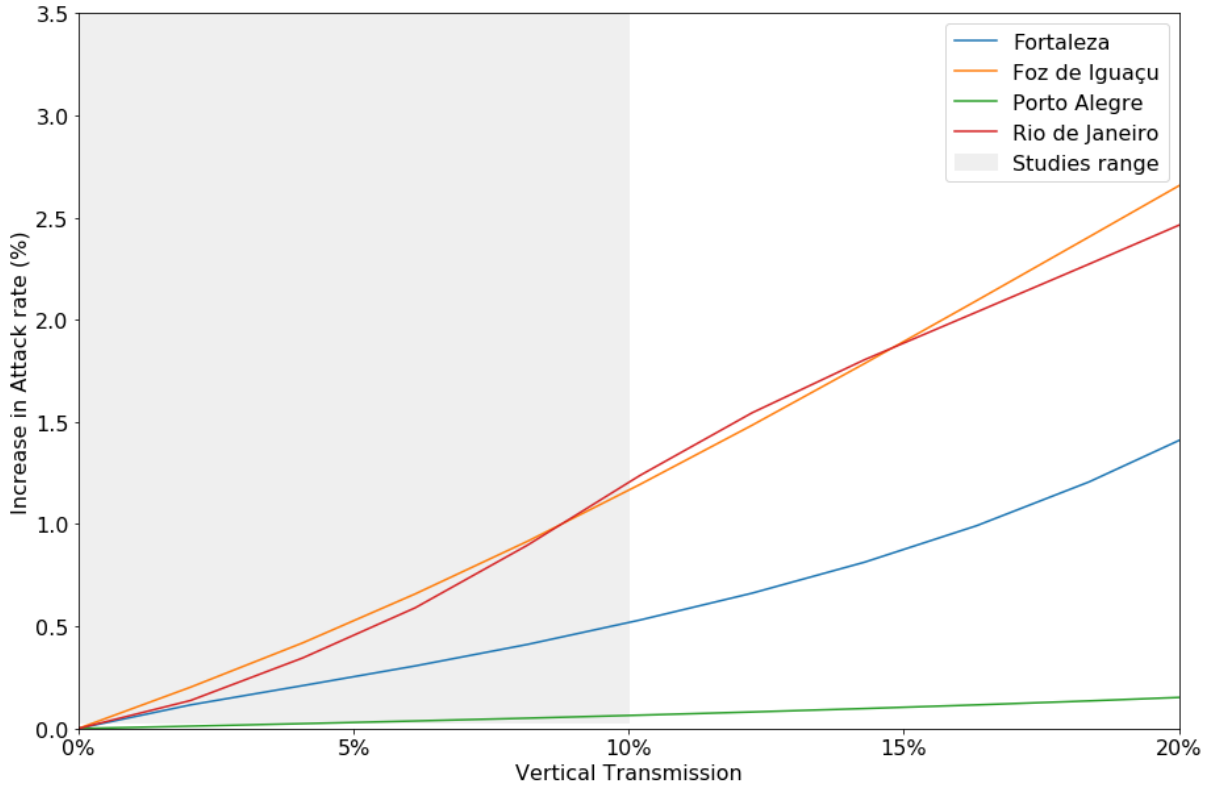

Figure 14 – Increased attack rates (%) with different vertical transmission levels. The gray area indicates the range of vertical transmission reported in the literature.

6.2 SI-SEI-SEIR model

The SEIR model expanded the SIR model of this Thesis, changing the timeframe from 8-day period to a daily period. This change enabled the addition of the exposed compartment (E) to the model. To fully understand these changes, the two versions of this model were evaluated with and without the exposed compartment.

6.2.1 Sensitivity Analysis

According to the sensitivity analysis, changes to the maximum temperature values inside the briére functions (t_{max}), human susceptible population ($S(0)$), and biting rate ($a(T)$) affect the model behavior more strongly than the other evaluated parameters, although they all share relatively small first order values, bellow 10%. The following parameters had first and total order sensitivity coefficients higher than 5%: biting rate

($a(T)$), mosquito-to-human infection probability per bite ($p_{hmh}(T)$), human-to-mosquito infection probability per bite ($p_{hm}(T)$), vector mortality rate ($\mu_v(T)$), carrying capacity (K), changes to maximum temperature (t_{max}) and initial value for susceptible humans ($S(0)$) (Figure 15).

The second order analysis showed strong links between most parameters (Figure 16). Human and egg mortality rates (u_e and u_h respectively), survival from aquatic phase ($s_a(T)$), vector female ratio (f_v), vertical transmission (v_t) and intrinsic incubation period rate (γ) showed no association to the other parameters (Annex E). The oviposition ($o(T)$) and egg development ($d(R)$) rates presented an important correlation to others parameters, which is the opposite of the SIR model.

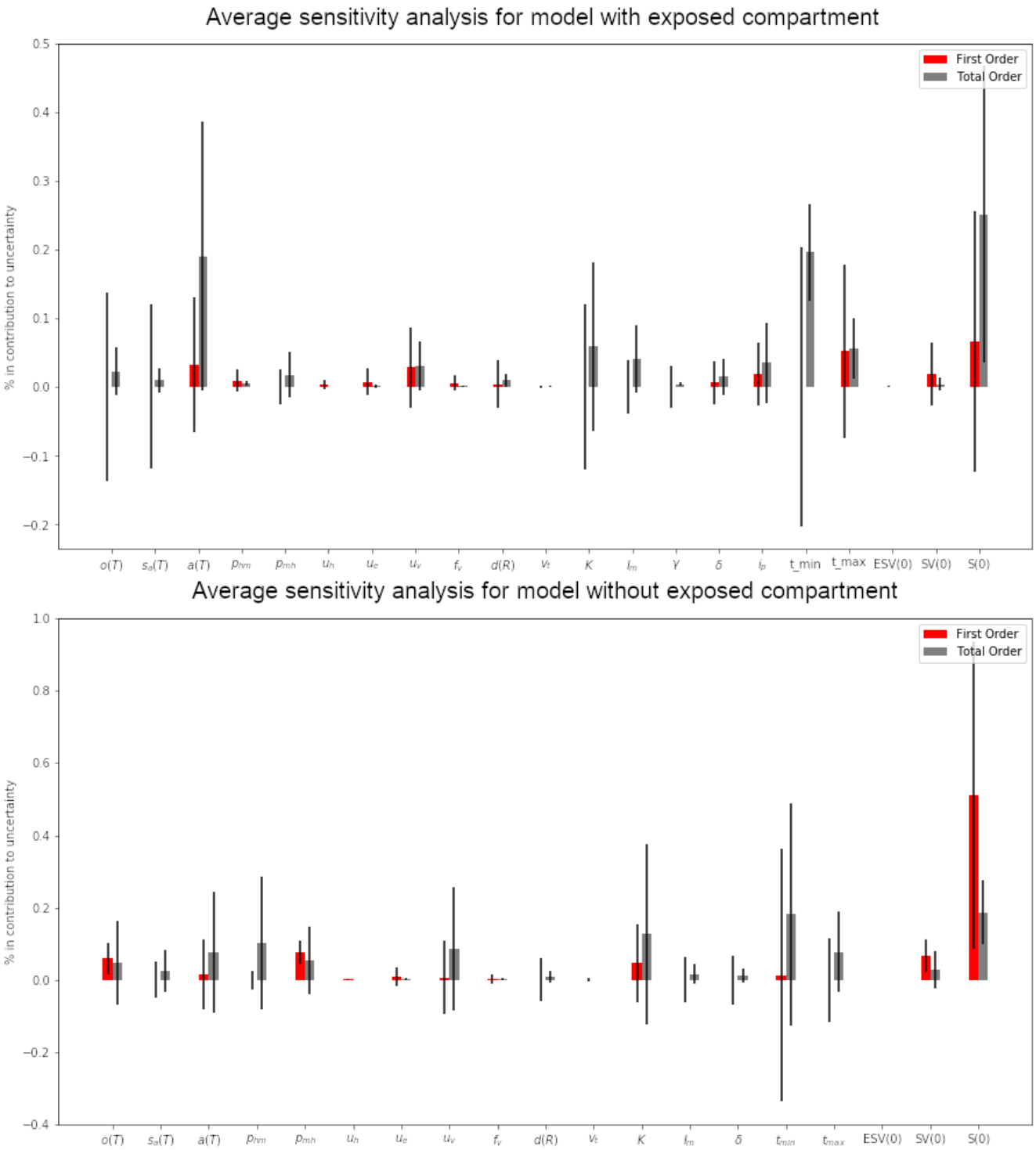

Figure 15 – Sensitivity analysis for SEIR model without and with exposed compartment. The values represent the average between all 12 municipalities.

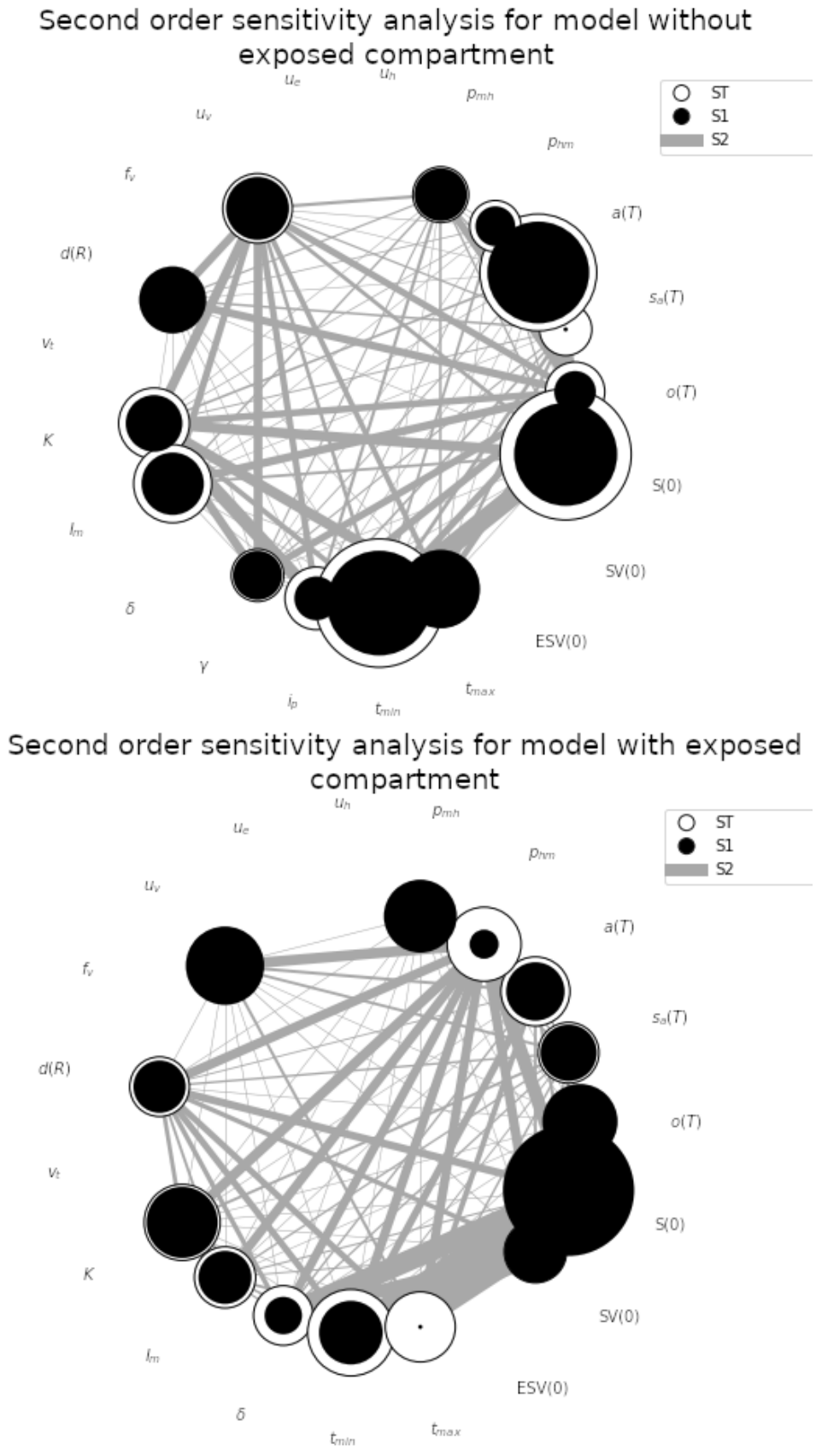

Figure 16 – Second order sensitivity analysis for SEIR model without and with exposed compartment. The values represent the average between all 12 municipalities.

Table 10 – Goodness-of-fit for the proposed model in twelve Brazilian municipalities

	Model without exposed		Model with exposed	
Municipality	**SSE**	**AIC**	**SSE**	**AIC**
Rio de Janeiro	14955	6468	13534	6985
São Gonçalo	919	4237	882	4583
Fortaleza	4624	5529	4646	6045
Caucaia	115	2581	89	2572
Belo Horizonte	2233	4947	1595	5104
Contagem	861	4185	761	4453
Curitiba	51	1924	45	1976
Londrina	1242	4478	1190	4846
Joinville	12	807	12	823
Florianópolis	11	753	10	722
Serra	521	3784	448	3987
Vila Velha	497	6520	423	4198

In respect to each parameter correlation with the SSE between observed and simulated incidence, the following parameters showed fitted R-squared value above 20%: oviposition rate ($o(T)$), biting rate ($a(T)$), human-to-mosquito infection probability per bite ($p_{hm}(T)$), vector mortality rate ($\mu_v(T)$), carrying capacity (K) (Figures 36, 37, 38, 39, 40, 41, 42, 43, 44, 45, 46, 47 from Annex E). Changes to maximum temperature (t_{max}) was the only parameter that exhibited a negative correlation with SSE, with $R^2 > 50\%$ for all municipalities. The other evaluated parameters exhibited weak correlations with SSE, less than 50% and greater than -50% for the Pearson Correlation Index, but those that showed at least 20% R-squared were: u_v, I_m, p_{mh} and p_{hm}.

6.2.2 Comparing models with and without exposed compartment

The SEIR model was implemented as a daily time frame while the SIR model, eight-day time frame. This was done to add the exposed compartment to the model. Table 10 shows the comparison between the two models' main results. The smaller the two parameters, the best is the goodness-of-fit in the model. AIC penalizes adding more variables, making the model with exposing compartment justify the inclusion of the parameters with the better fit.

The model with an exposed compartment consistently fits better to observed incidence. In all municipalities, the error was reduced on average 5-15% compared

with the model without the exposed compartment. Opposite to these findings, the model without exposed compartment presented smaller AIC in almost all municipalities, only Florianópolis, Vila Velha, and Caucaia do not present this trend. This shows that, although adding an exposed compartment reduces overall error of the model, it is still not a significant reduction because it increases the complexity of the model thus scoring a bigger AIC value.

Figures 17 shows the results of the simulations using the best parameters found in the grid search produced by the sensitivity analysis from 2010 to 2014. The two models produced similar curves to the observed data with seasonality expected to dengue incidence.

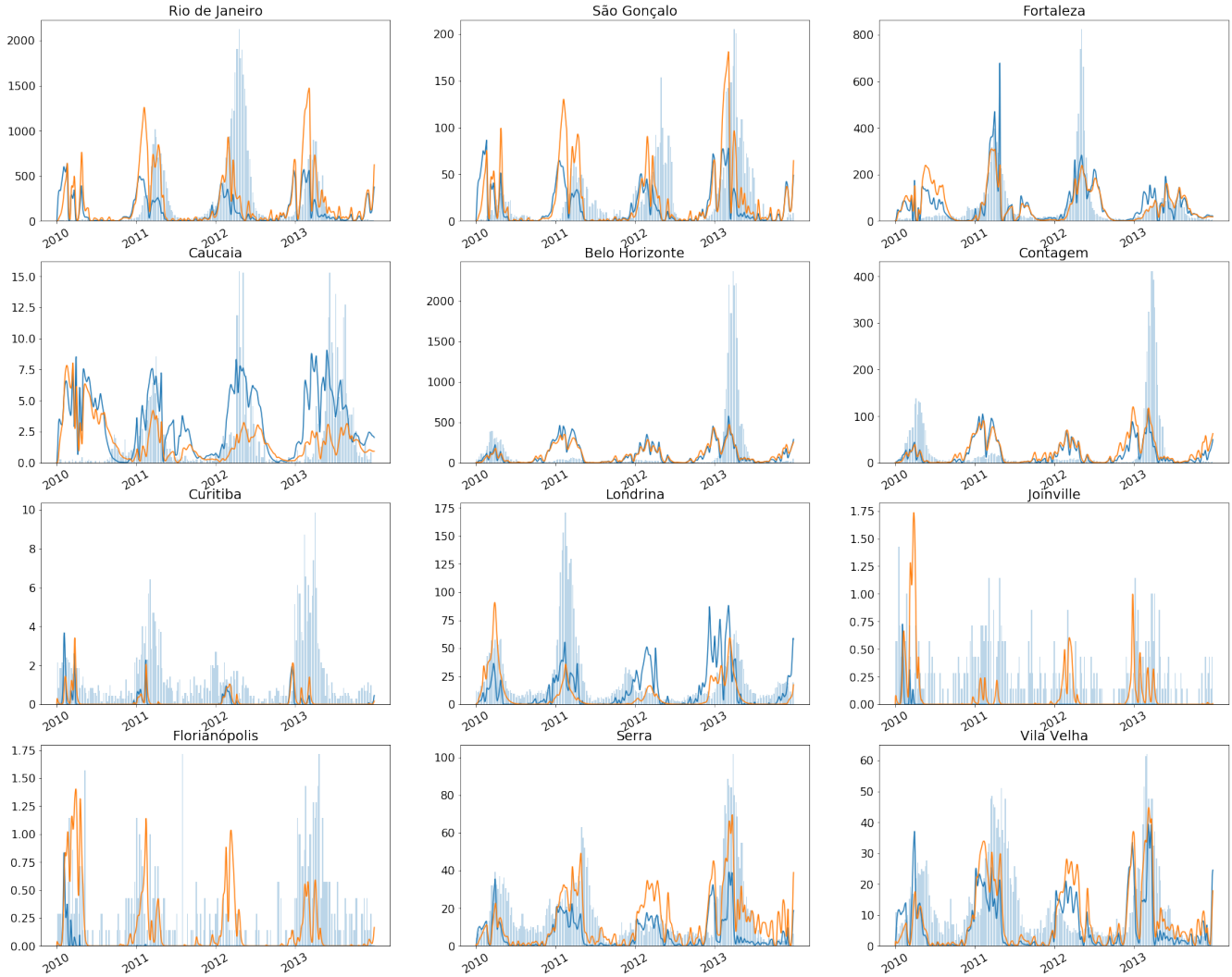

Figure 17 – Simulations from model with and without exposed compartment simulations from 2010 to 2014, from left to right from top to bottom: Rio de Janeiro, São Gonçalo, Fortaleza, Caucaia, Belo Horizonte, Contagem, Curitiba, Londrina, Joinville, Florianópolis, Serra and Vila Velha. Orange line represent the simulation with exposed compartment while blue line represent the simulation without exposed compartment. Blue bars represent the observed incidence.

Figures 18 shows the results of the simulations using the best parameters found in the grid search produced by the sensitivity analysis from 2010 to 2020. When there is a large timeframe, it becomes clear that the simulations could not reproduce when the disease occurs, since it always aims for the period where temperature and rainfall would likely cause an epidemic.

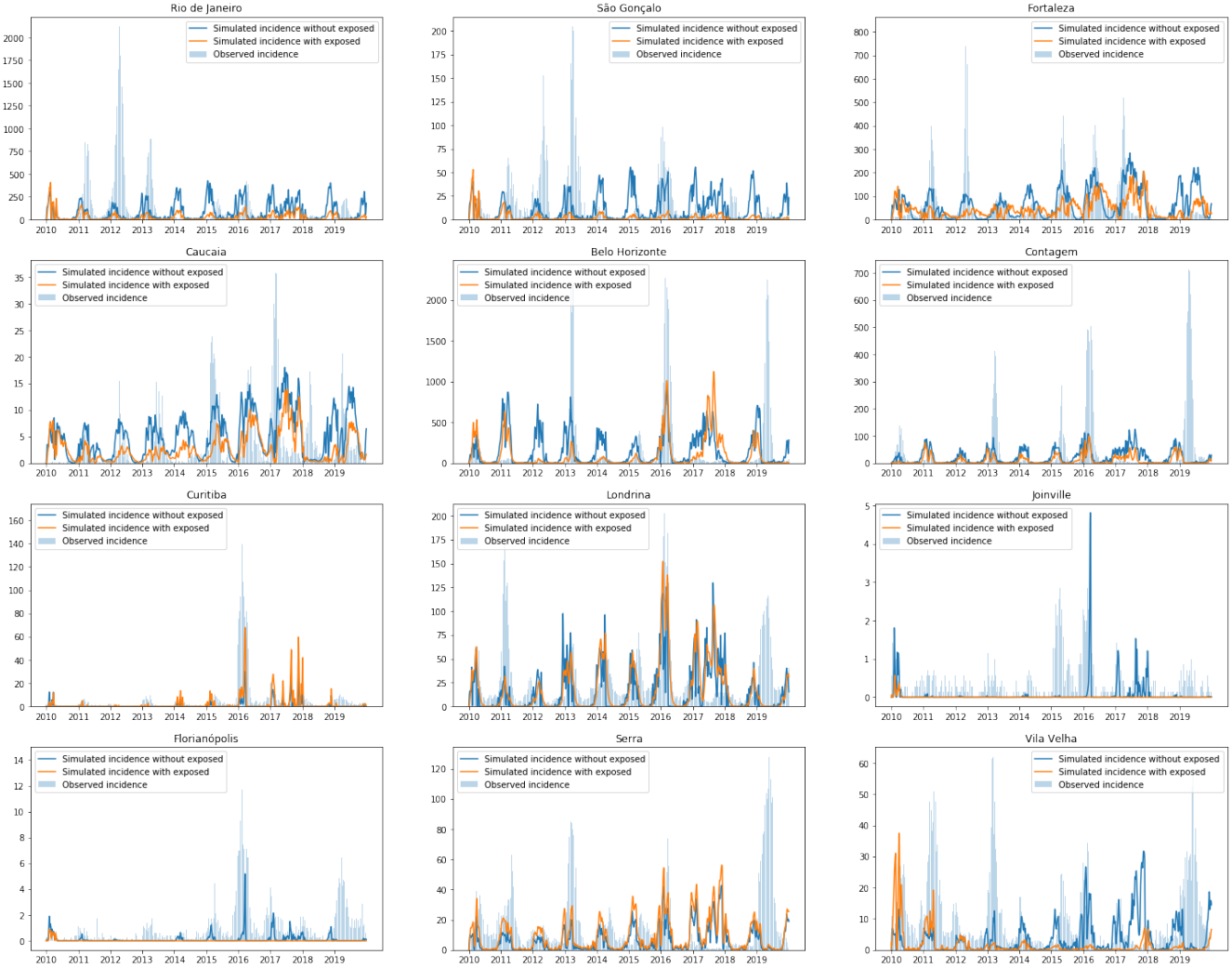

Figure 18 – Simulations from model with and without exposed compartment from 2010 to 2020, from left to right from top to bottom: Rio de Janeiro, São Gonçalo, Fortaleza, Caucaia, Belo Horizonte, Contagem, Curitiba, Londrina, Joinville, Florianópolis, Serra and Vila Velha. Orange line represent the simulation with exposed compartment while blue line represent the simulation without exposed compartment. Blue bars represent the observed incidence.

The two models do not converge to the municipalities of Minas Gerais state. Both had a small number of cases from 2010 to 2012 but had an epidemic year in 2013 which could not be reproduced by the models.

Table 11 presents the best fit based on SSE to each parameter for the model without exposed compartment. While, table 12 present the same, but for the model with exposed compartment.

The fitted parameters show a trend between municipalities belonging to the

Table 11 – Best fitted parameters values in the model without exposed compartment for the 12 municipalities. The new value substitutes the a variable within temperature and rainfall dependent functions; or substitutes directly the constant parameter.

Parameter	$o(T)$	$s_a(T)$	$a(T)$	$p_{hm}(T)$	$p_{mh}(T)$	u_h	u_e	u_v	f_v	$d(R)$	v_t	k	I_m	t_{min}	t_{max}	$ESV(0)$	$SV(0)$	$SH(0)$
Rio de Janeiro	0.0132	-0.003	0.0001	0.0002	0.0003	0.0002	0.0182	-0.050	0.53198	-0.132	0.3234	0.5159	0.0132	-1.851	-0.585	5339048	4548992	2410287
São Gonçalo	0.0132	-0.003	0.0001	0.0002	0.0003	0.0002	0.0182	-0.050	0.53198	-0.132	0.3234	0.5159	0.0132	-1.851	-0.585	844496	719530	381243
Fortaleza	0.0332	-0.003	0.0006	0.0004	0.0005	7.8e-5	0.0135	-0.119	0.43823	-0.153	0.2719	1.5003	0.0179	3.1484	-3.585	1151856	232287	1149701
Caucaia	0.0132	-0.003	0.0001	0.0002	0.0003	0.0002	0.0182	-0.050	0.53198	-0.132	0.3234	0.5159	0.0032	-1.851	1.9609	274908	234228	124106
Belo Horizonte	0.0093	-0.001	8.8e-5	0.0002	0.0002	0.0001	0.0177	-0.336	0.60961	-0.108	0.2743	1.8745	0.0267	-3.257	-1.585	642496	828055	1262958
Contagem	0.0093	-0.001	8.8e-5	0.0002	0.0002	5.2e-5	0.0229	-0.336	0.60961	-0.108	0.2743	1.8745	0.0267	-3.257	-1.585	163235	210379	320873
Curitiba	0.0132	-0.003	0.0001	0.0002	0.0003	0.0002	0.0037	-0.050	0.53198	-0.132	0.3234	0.5159	0.0132	-1.851	1.9609	1479882	1260894	668085
Londrina	0.0093	-0.001	6.5e-5	0.0002	0.0002	5.2e-5	0.0177	-0.336	0.60961	-0.108	0.2743	1.8745	0.0267	-3.257	-1.585	137066	176652	269432
Joinville	0.0041	-0.002	8.8e-5	0.0002	0.0006	0.0001	0.0382	-0.484	0.27416	-0.083	0.3332	0.7620	0.0190	1.3984	1.2109	322558	32708	433214
Florianópolis	0.0304	-0.002	8.8e-5	0.0002	0.0006	0.0001	0.0382	-0.484	0.27416	-0.083	0.3332	0.7620	0.0190	1.3984	1.2109	263686	26738	354146
Serra	0.0132	-0.003	0.0001	0.0002	0.0003	0.0002	0.0182	-0.050	0.53198	-0.132	0.3234	0.8902	0.0132	-1.851	1.9609	345718	294560	156073
Vila Velha	0.0132	-0.003	0.0001	0.0002	0.0003	0.0002	0.0182	-0.050	0.53198	-0.132	0.3234	0.8902	0.0132	-1.851	1.9609	350211	298388	158101

Table 12 – Best fitted parameters values in the model with exposed compartment for the 12 municipalities. The new value substitutes the a variable within temperature and rainfall dependent functions; or substitutes directly the constant parameter.

Parameter	$o(T)$	$s_a(T)$	$a(T)$	$p_{hm}(T)$	$p_{mh}(T)$	u_h	u_e	u_v	δ	f_v	$d(R)$	v_t	k	i_p	I_m	t_{min}	t_{max}	$ESV(0)$	$SV(0)$
Rio de Janeiro	0.0157	-0.005	0.0001	0.0001	0.0007	8.1e-5	0.0251	-0.278	0.4526	0.5868-0.015	0.1390	2.5923	7.2e-5	0.0038	2.6706	1.0886	5400771	1820831	2470775
São Gonçalo	0.0157	-0.005	0.0001	0.0001	0.0007	8.1e-5	0.0251	-0.278	0.4526	0.5868-0.015	0.1390	2.5923	7.2e-5	0.0038	2.6706	1.0886	854259	288007	390811
Fortaleza	0.0127	-0.005	0.0003	0.0004	0.0002	9.2e-5	0.0239	-0.052	0.5519	0.6228-0.140	0.1004	2.1822	4.9e-5	0.0048	3.2565	0.7370	1252434	1396117	1655943
Caucaia	0.0132	-0.003	0.0001	0.0002	0.0003	0.0002	0.0182	-0.139	0.2130	0.5319-0.132	0.3234	0.5159	0.00020	0.0132	1.2570	3.0441	37819	195455	245129
Belo Horizonte	0.0288	-0.003	8.8e-5	0.0002	0.0007	0.0002	0.0052	-0.330	0.2341	0.7978-0.053	0.3066	0.8697	0.00017	0.0235	1.3815	2.6120	25514	164683	772619
Contagem	0.0288	-0.003	8.8e-5	0.0002	0.0007	0.0002	0.0052	-0.330	0.2341	0.7978-0.053	0.3066	0.8697	0.00017	0.0235	1.3815	2.6120	6482	41840	196295
Curitiba	0.0252	-0.003	8.1e-5	0.0001	0.0004	0.0002	0.0204	-0.347	0.2143	0.6806-0.123	0.2937	2.2642	0.00010	0.0059	1.2644	1.5573	1715979	723688	1451311
Londrina	0.0051	-0.004	0.0007	0.0003	0.0004	0.0002	0.0064	-0.189	0.0541	0.3444-0.175	0.3203	1.1721	0.00014	0.0226	0.3195	2.1066	185559	177642	292985
Joinville	0.0037	-0.003	8.1e-5	0.0001	0.0004	0.0002	0.0204	-0.347	0.2143	0.6806-0.123	0.2937	2.2642	0.00010	0.0059	1.2644	1.5573	504720	212858	162688
Florianópolis	0.0037	-0.003	8.1e-5	0.0001	0.0004	0.0002	0.0204	-0.347	0.2143	0.6806-0.123	0.2937	2.2642	0.00010	0.0059	1.2644	1.5573	412601	174008	132995
Serra	0.0037	-0.004	6.5e-5	0.0001	0.0007	0.0001	0.0229	-0.258	0.4514	0.2507-0.110	0.2687	2.1565	0.00023	0.0272	2.6633	3.5129	201036	92324	129214
Vila Velha	0.0037	-0.003	8.1e-5	0.0001	0.0004	0.0002	0.0204	-0.258	0.2143	0.6806-0.123	0.2937	2.2642	0.00010	0.0059	1.2644	1.5573	406083	171259	343450

same state. Most of them presented the same value for each parameter, except the municipalities of Paraná (Curitiba and Londrina) and Ceará (Fortaleza and Caucaia).

From Tables 11 and 12 is also possible to notice that parameters values vary between municipalities. Vertical transmission (v_t) and egg mortality (u_e) were overestimated in the two models compared to Bar-zeev et al. (1957) and Adams e Boots (2010). Parameters related directly to infection rate such as vector female ratio (f_v), biting rate ($a(T)$), probability of human-to-mosquito infection ($p_{hm}(T)$) and probability of mosquito-to-human infection ($p_{mh}(T)$ were always underestimated in the models compared to Mordecai et al. (2017) values. The primarily difference between the model with exposed and without exposed compartment resides in the $o(T)$, K, $ESV(0)$, $SV(0)$ and $S(0)$ values. The carrying capacity (K) has larger values with the exposed compartment; while oviposition ($o(T)$) values fluctuates around Mordecai et al. (2017) value, sometimes overstimating, sometimes understimating.

7 Discussion

7.1 SI-SI-SIR model

The SIR model (5.1) was validated with data from 2010 to 2019 in four Brazilian municipalities. The model provides a framework for understanding weather-driven dengue transmission considering rainfall dependency, one of the challenges for these type of models (CHÁVEZ et al., 2017; GÖTZ et al., 2017). The addition of susceptible and infected egg states allowed for the inclusion of rainfall dependency and vertical transmission in the studied model.

This work was inspired by the model developed by Huber et al. (2018), whose performance was tested using different sinusoidal functions to represent temperature. Here, we used temperature and rainfall time series derived from weather satellite data. Other works in the literature usually employ sinusoidal functions to represent temperature variations (CHÁVEZ et al., 2017; HUBER et al., 2018; RASHKOV et al., 2019; OSORIO et al., 2015) or constant temperature (DEFTERLI, 2020; PHAIJOO; GURUNG, 2017; ESTEVA; YANG, 2015). Our model was capable of producing similar patterns to those observed for dengue incidence, presenting both seasonality and similar epidemic sizes. In contrast to Huber et al. (2018), our simulations displayed sharper epidemic peaks, more similar to observed peaks, due to the use of observed temperature data and the addition of the egg compartment, which drove the force of infection even higher, as adult mosquitoes are almost always at the carrying capacity level when the temperature permits.

Environmental variables affected the dynamics, as expected: in Fortaleza, Rio de Janeiro and Foz do Iguaçu, which display warmer climates where transmission is facilitated, both the simulated and observed time series exhibited higher dengue incidence and the same epidemic pattern. In Porto Alegre, a municipality that has a colder climate, a lower dengue incidence was observed, not enough to generate epidemic cycles, instead producing only sporadic outbreaks. Nonetheless, the qualitative

calibration process mostly affected parameters which, in the literature, are highly variable. The colder weather of Porto Alegre represents unfavorable conditions for the vector, which explains the fact that most parameter values are smaller than in other cities. Fortaleza and Foz do Iguaçu present favorable climates, allowing for higher carrying capacity, leading to a better fit to data. Lastly, the sensitivity analysis clarified how each parameter affected the model's ability to match the observed dynamics. It further demonstrated that the parameters, especially dengue recovery rate (γ), can be better adapted to the Brazilian environment, since a higher γ reduced the SSE.

With respect to the discordance between the simulated and observed time series, most of the inaccuracies concerning epidemic size and peak dates were noted after 2016, which can be explained by the following factors: (a) the model conflates all dengue serotypes into only one, and though this simplification is common in conceptual framework articles, it does not adequately represent the susceptible population, which can accumulate errors over time; (b) after 2016, Zika and chikungunya were introduced in the studied municipalities (Figures 21 and 22 in Annex B), and the co-circulation of this disease can lead to their misdiagnosis, as they result in similar clinical conditions (BELTRÁN-SILVA et al., 2018); (c) in 2015–2016, extreme weather changes due to the El Niño phenomenon were observed (JIMÉNEZ-MUÑOZ et al., 2016), which may cause changes in epidemiology scenarios (GAGNON; BUSH; SMOYER-TOMIC, 2001; TIPAYAMONGKHOLGUL et al., 2009; PETROVA et al., 2020); (d) not all developmental *Ae. aegypti* stages were accounted for in the model, with the aquatic phase not explicitly represented.

The sensitivity analysis demonstrates that parameters related to egg compartment (such as $o(T)$, v_t, $s_a(T)$ and μ_e) did not play a strong role in model sensitivity. When tracking the egg population (Figure 25 in Annex D), it is clear that an abrupt growth occurs, forcing the adult population quickly towards its carrying capacity, even when its parameters are underestimated. It is noteworthy, however, that this growth behavior demonstrates the relevance of an explicit egg compartment in the model.

Rainfall influence on epidemic peaks is related to the timing of egg hatching. Low rainfall rates can bring the mosquito adult population size to its carrying capacity,

but cannot alter the general dengue impact. Other aspects of mosquito biology such as eggs, larvae and pupae mortality and oviposition rates, are also influenced by rainfall rates (DIENG et al., 2012). Although the presented model did not assess this impact, this should be a concern in future studies for the improvement of this model.

The last investigated parameter was vertical transmission. Most dengue transmission models do not include vertical transmission (MORDECAI et al., 2017; ANDRAUD et al., 2012), as it complicates the model too much and it is assumed it would not bring significant changes in the model output. However, in this study, vertical transmission played an important role. When removed, it altered the transmission dynamics, modifying the timing of the dengue epidemic peaks and the overall burden. The effect of different transmission values was assessed as indicated in Figure 14, and the higher the vertical transmission, the higher the overall burden calculated by the attack rate in the simulations.

To further investigate vertical transmission, would be necessary a study that tracks infected eggs over the years. A positive correlation between the infected egg population and dengue cases could be indicative of how important vertical transmission can be to sustain epidemics. Also, It could help to understand which variable is more important to start a new epidemic: the importation of infected humans to a susceptible population or a pool of already infected eggs.

7.2 SI-SEI-SEIR model

The SEIR model (5.2) proposed in this Thesis expanded the SIR model, changing the time-frame to daily periods which allowed more compartments in the models such as the exposed vector and exposed humans.

This time-frame modification brought changes to the results even to the model without an exposed compartment. The egg compartment increased in importance when compared to the SI-SI-SIR model. This was probably due to the more localized effects of rainfall, which before affected uniformly the 8-day period in which it happened, but with the daily time-frame, its effects can be considered on a scale of a single day.

While the SI-SI-SIR model presented a qualitative calibration, SEI-SEI-SEIR model was calibrated by optimization with a grid-search. In municipalities such as Belo Horizonte and Contagem, the model could not find a suitable simulation based on this criterion only. The best fit parameters between municipalities in the same state are similar, probably because of the homogeneity in the environmental, demography, and dengue incidence patterns. However, municipalities in the same state, such as Curitiba and Londrina, that have more than 5 C° of difference in the average temperature, presented variations between parameters (Table 1).

The model presented a reasonable goodness-of-fit for most municipalities, except for Minas Gerais State. Those municipalities had similar dengue profiles since they had a small number of cases until the 2013 epidemic happened. This epidemic was caused by the invasion of DENV-4 serotype in those municipalities (RABELO et al., 2020). Although DENV-4 was abundant in the year 2013, which constitute more than 50% of the dengue cases, it rapidly vanished from the region having less than 3% in 2014. Since a single serotype model could hardly recreate this kind of behavior, this shows the importance of expanding the current model to manage all dengue serotypes.

Data from simulations for all 2010 decade showed that the model captures the epidemic peaks based on rainfall and temperature. In this model, rainfall presented a bigger impact, which could make possible predictions for municipalities such as Fortaleza, where the temperature is stable during the year, but rainfall is scarce, making dengue cases mostly happen in rainfall season. The overestimation of egg mortality (u_e) and the underestimation of the oviposition rate ($o(T)$), when compared to Bar-zeev et al. (1957) and Mordecai et al. (2017), shows that the egg population in simulations maybe be growing more than it should, which could be caused by a wrong approach in the present model or by a biological difference, since these values were taken from mosquitoes from the Northern Hemisphere and not from Brazil.

The underestimation of all parameters directly linked to dengue infection, making the force of infection smaller, and the fact that the simulations presented an epidemic every year of the decade simulation showed a need to still improve the model. In the long term, this single-serotype model could not reproduce a recurrent phenomenon

in dengue dynamics: when no incidence happens in a year. This kind of behavior in a long term study probably can only be achieved in a multi-serotype model, having a high enough force of infection to continue bringing the susceptible population of a given serotype to low enough levels for blocking transmission in the following years if the dominant available serotype is the same.

The SEIR model can be used in an effective way to know when dengue cases will not happen, since the vector will need the temperature and rainfall conditions to reproduce and infect. At the same time, it can also be a valuable asset to predict the dengue epidemic in the short term, since the model had a good fit for 10 of the 12 tested municipalities in a 4-year range.

8 Conclusions and Recommendations

Every specific objective in this Thesis was completed. The climatic, epidemiological and demographic database was built and put to open access in InfoDengue website (CODECO et al., 2018). The two models highlighted the importance of tracking the egg compartment of the mosquito population, including vertical transmission and rainfall dependence. The SIR model showed how vertical transmission can change dengue transmission dynamics and should be better analyzed. Overall, the simulations indicate similar patterns to observed data, showing that the models had a good fit.

The findings of the first SIR model suggests the need to further investigate the contribution of vertical transmission to dengue transmission dynamics. But more studies are required concerning the biology of the vector and its interaction with the virus to improve future models. The 8-day time frame made it more easy to study long term effects but, as showed by the SEIR model, it probably caused an underestimation of the egg compartment a a reservoir for the long-term persistence of the virus.

The SEIR model produced an effective way to predict the number of dengue cases. It highlighted the importance of considering temperature and rainfall in order to achieve a better fit to observational data. But at the same time, it showed the importance to extend the current model to a multi-serotype model. Also, some authors correlated oviposition to rainfall and not temperature (CHADEE; CORBET; TALBOT, 1995; ZEIDLER et al., 2008; CANYON; HII; MÜLLER, 1999), and since oviposition values were underestimated in the SEIR model, it would be reasonable to test this approach in further studies.

Future studies should be conducted to further improve these two models, for example, by including the four dengue serotypes and simplifying the model by removing parameters that did not affect the model results, as revealed by the sensitivity analysis of this Thesis. Notwithstanding, many issues remain in regards to dengue biology that also need to be addressed in parallel to improve models: parameters values are often not well contextualized in literature, and their importance is seldom discussed. In this

sense, some improvement opportunities include an evaluation of how parameters could influence the competition between serotypes, which this Thesis did not study, and how some parameters influence dengue incidence, for example: how much a stronger pendular migration contributes to starting a new epidemic.

Dengue is a disease of global concern and in spite of many decades of study in order to understand the dynamics of its transmission, many questions remain. Considering the essential role played by mathematical models in planning measures to prevent and combat dengue, it can be said that the results of this Thesis contributed to a better understanding of the role of climate fluctuations in dengue dynamics.

Bibliography

ABAD-FRANCH, F.; ZAMORA-PEREA, E.; LUZ, S. L. Mosquito-disseminated insecticide for citywide vector control and its potential to block arbovirus epidemics: entomological observations and modeling results from amazonian Brazil. *PLoS medicine*, Public Library of Science San Francisco, CA USA, v. 14, n. 1, p. e1002213, 2017. Citado 3 vezes nas páginas 50, 51, and 53.

ADAMS, B.; BOOTS, M. How important is vertical transmission in mosquitoes for the persistence of dengue? insights from a mathematical model. *Epidemics*, Elsevier, v. 2, n. 1, p. 1–10, 2010. Citado 4 vezes nas páginas 28, 67, 70, and 88.

ALTO, B. W.; JULIANO, S. A. Precipitation and temperature effects on populations of *aedes albopictus* (*Diptera: Culicidae*): implications for range expansion. *Journal of medical entomology*, Oxford University Press Oxford, UK, v. 38, n. 5, p. 646–656, 2001. Citado 4 vezes nas páginas 47, 48, 67, and 71.

ALVARES, C. A. et al. Köppen's climate classification map for Brazil. *Meteorologische Zeitschrift*, Stuttgart, v. 22, n. 6, p. 711–728, 2013. Citado 4 vezes nas páginas 11, 42, 43, and 44.

ALVES, L. D.; LANA, R. M.; COELHO, F. C. A framework for weather-driven dengue virus transmission dynamics in different Brazilian regions. *International Journal of Environmental Research and Public Health*, Multidisciplinary Digital Publishing Institute, v. 18, n. 18, p. 9493, 2021. Citado 2 vezes nas páginas 28 and 29.

ANDRAUD, M. et al. Dynamic epidemiological models for dengue transmission: a systematic review of structural approaches. *PloS one*, Public Library of Science, v. 7, n. 11, p. e49085, 2012. Citado 3 vezes nas páginas 27, 54, and 91.

BAR-ZEEV, W. et al. The effect of density on the larvae of a mosquito and its influence on fecundity. *Bulletin of the Research Council of Israel*, n. 3/4, p. 220–28, 1957. Citado 6 vezes nas páginas 48, 49, 67, 70, 88, and 92.

BELTRÁN-SILVA, S. et al. Clinical and differential diagnosis: Dengue, chikungunya and zika. *Revista Médica del Hospital General de México*, Elsevier, v. 81, n. 3, p. 146–153, 2018. Citado na página 90.

BHATT, S. et al. The global distribution and burden of dengue. *Nature*, Nature Publishing Group, v. 496, n. 7446, p. 504–507, 2013. Citado 3 vezes nas páginas 27, 35, and 38.

BOORMAN, J.; PORTERFIELD, J. et al. A simple technique for infection of mosquitoes with viruses. transmission of zika yirus. *Transactions of the Royal Society of Tropical Medicine and Hygiene*, London, v. 50, n. 3, 1956. Citado na página 53.

BOSIO, C. F. et al. Variation in the efficiency of vertical transmission of dengue-1 virus by strains of *aedes albopictus* (*diptera: culicidae*). *Journal of medical entomology*, Oxford University Press Oxford, UK, v. 29, n. 6, p. 985–989, 1992. Citado 3 vezes nas páginas 45, 46, and 77.

BRADY, O. J. et al. Modelling adult *aedes aegypti* and *aedes albopictus* survival at different temperatures in laboratory and field settings. *Parasites & vectors*, BioMed Central, v. 6, n. 1, p. 1–12, 2013. Citado na página 49.

BRASIL. *Censo Demográfico*. Instituto Brasileiro de Geografia e Estatística (IBGE), 2010. Disponível em: <https://www.ibge.gov.br/estatisticas/sociais/habitacao/9662-censo-demografico-2010.html?=&t=resultados>. Citado 6 vezes nas páginas 19, 56, 57, 58, 59, and 62.

BRASIL. *Base de dados*. [S.l.]: Minitério do turismo, 2020. Citado 4 vezes nas páginas 56, 57, 59, and 62.

BRASIL. *Conheça cidades e estados do Brasil*. Instituto Brasileiro de Geografia e Estatística (IBGE), 2020. Disponível em: <https://cidades.ibge.gov.br/?lang=&lista=uf&coduf=0&idtema=108&codv=V10>. Citado 3 vezes nas páginas 57, 58, and 59.

BRASIL. *Estimativas da população residente para os municípios e para as unidades da federação brasileiros com data de referência em 1º de julho de 2020*. Instituto Brasileiro de Geografia e Estatística (IBGE), 2020. Disponível em: <https://www.ibge.gov.br/estatisticas/sociais/populacao/9103-estimativas-de-populacao.html?=&t=o-que-e>. Citado 3 vezes nas páginas 57, 58, and 59.

BRASIL., M. da Saúde. Secretaria de Vigilância em Saúde. Departamento de V. E. *Sistema de Informação de Agravos de Notificação - Sinan*. Editora do Ministério da Saúde, 2007. Disponível em: <https://portalsinan.saude.gov.br/>. Citado na página 59.

BUCKNER, E. A.; ALTO, B. W.; LOUNIBOS, L. P. Vertical transmission of key west dengue-1 virus by *aedes aegypti* and *aedes albopictus* (*diptera: culicidae*) mosquitoes from florida. *Journal of medical entomology*, Oxford University Press Oxford, UK, v. 50, n. 6, p. 1291–1297, 2013. Citado na página 46.

BYTTEBIER, B.; MAJO, M. S. D.; FISCHER, S. Hatching response of *Aedes aegypti* (*Diptera: Culicidae*) eggs at low temperatures: Effects of hatching media and storage conditions. *Journal of medical entomology*, Oxford University Press Oxford, UK, v. 51, n. 1, p. 97–103, 2014. Citado na página 47.

CÂMARA, F. P. et al. Clima e epidemias de dengue no estado do Rio de Janeiro. *Revista da Sociedade Brasileira de Medicina Tropical*, SciELO Brasil, v. 42, n. 2, p. 137–140, 2009. Citado na página 56.

CAMPOS, R. de M. et al. Emergence of dengue virus 4 genotypes ii b and i in the city of Rio de Janeiro. *Journal of clinical virology: the official publication of the Pan American Society for Clinical Virology*, v. 56, n. 1, p. 86–88, 2013. Citado na página 41.

CANYON, D.; HII, J.; MÜLLER, R. Adaptation of *Aedes aegypti* (*Diptera: Culicidae*) oviposition behavior in response to humidity and diet. *Journal of insect physiology*, Elsevier, v. 45, n. 10, p. 959–964, 1999. Citado 2 vezes nas páginas 45 and 95.

CANYON, D.; HII, J.; MULLER, R. The frequency of host biting and its effect on oviposition and survival in *Aedes aegypti* (*Diptera: Culicidae*). *Bulletin of entomological research*, Cambridge University Press, v. 89, n. 1, p. 35–39, 1999. Citado na página 51.

CAPRARA, A. et al. Entomological impact and social participation in dengue control: a cluster randomized trial in Fortaleza, Brazil. *Transactions of the Royal Society of Tropical Medicine and Hygiene*, Oxford University Press, v. 109, n. 2, p. 99–105, 2015. Citado na página 56.

CHADEE, D. D.; CORBET, P. S.; TALBOT, H. Proportions of eggs laid by *Aedes aegypti* on different substrates within an ovitrap in Trinidad, West Indies. *Medical and veterinary entomology*, Wiley Online Library, v. 9, n. 1, p. 66–70, 1995. Citado 4 vezes nas páginas 43, 44, 45, and 95.

CHANPRASOPCHAI, P.; TANG, I. M.; PONGSUMPUN, P. Sir model for dengue disease with effect of dengue vaccination. *Computational and mathematical methods in medicine*, Hindawi, v. 2018, 2018. Citado na página 27.

CHÁVEZ, J. P. et al. An sir-dengue transmission model with seasonal effects and impulsive control. *Mathematical biosciences*, Elsevier, v. 289, p. 29–39, 2017. Citado na página 89.

CHOW, V. et al. Monitoring of dengue viruses in field-caught *Aedes aegypti* and *Aedes albopictus* mosquitoes by a type-specific polymerase chain reaction and cycle sequencing. *The American journal of tropical medicine and hygiene*, ASTMH, v. 58, n. 5, p. 578–586, 1998. Citado na página 46.

CHOWELL, G. et al. Estimation of the reproduction number of dengue fever from spatial epidemic data. *Mathematical biosciences*, Elsevier, v. 208, n. 2, p. 571–589, 2007. Citado na página 52.

CLEMENTS, A. N. et al. *The biology of mosquitoes: development, nutrition and reproduction*. [S.l.]: Chapman & Hall London, 1992. v. 1. Citado na página 47.

CODECO, C. et al. Infodengue: A nowcasting system for the surveillance of arboviruses in Brazil. *Revue d'Épidémiologie et de Santé Publique*, v. 66, p. S386, 2018. ISSN 0398-7620. European Congress of Epidemiology "Crises, epidemiological transitions and the role of epidemiologists". Disponível em: <http://www.sciencedirect.com/science/article/pii/S0398762018311088>. Citado 8 vezes nas páginas 13, 56, 57, 59, 62, 95, 113, and 114.

CONTE, C. H. Comércio e deslocamento pendular: posicionamentos sobre a rede urbana de foz do iguaçu. *Revista Geoaraguaia*, v. 3, n. 2, 2013. Citado na página 56.

COSTA, C. F. da et al. Transovarial transmission of denv in *Aedes aegypti* in the Amazon basin: a local model of xenomonitoring. *Parasites & vectors*, Springer, v. 10, n. 1, p. 1–9, 2017. Citado na página 45.

CRUZ, L. C. d. T. A. d. et al. Natural transovarial transmission of dengue virus 4 in *Aedes aegypti* from cuiabá, state of mato grosso, Brazil. *Revista da Sociedade Brasileira de Medicina Tropical*, SciELO Brasil, v. 48, n. 1, p. 18–25, 2015. Citado na página 46.

CRUZ, R. R. Estrategias para el control del dengue y del *Aedes aegypti* en las américas. *Revista Cubana de Medicina Tropical*, 1999, Editorial Ciencias Médicas, v. 54, n. 3, p. 189–201, 2002. Citado na página 38.

DEFTERLI, Ö. Modeling the impact of temperature on fractional order dengue model with vertical transmission. 2020. Citado na página 89.

DICK, O. B. et al. The history of dengue outbreaks in the americas. *The American journal of tropical medicine and hygiene*, ASTMH, v. 87, n. 4, p. 584–593, 2012. Citado 3 vezes nas páginas 40, 41, and 42.

DIENG, H. et al. The effects of simulated rainfall on immature population dynamics of *Aedes albopictus* and female oviposition. *International journal of biometeorology*, Springer, v. 56, n. 1, p. 113–120, 2012. Citado na página 91.

ERGULER, K. et al. Large-scale modelling of the environmentally-driven population dynamics of temperate *Aedes albopictus* (skuse). *PloS one*, Public Library of Science San Francisco, CA USA, v. 11, n. 2, p. e0149282, 2016. Citado na página 50.

ESTEVA, L.; YANG, H. M. Assessing the effects of temperature and dengue virus load on dengue transmission. *Journal of Biological Systems*, World Scientific, v. 23, n. 04, p. 1550027, 2015. Citado na página 89.

FARINELLI, E. C. et al. Low socioeconomic condition and the risk of dengue fever: a direct relationship. *Acta tropica*, Elsevier, v. 180, p. 47–57, 2018. Citado 2 vezes nas páginas 27 and 33.

FAULL, K. J.; WILLIAMS, C. R. Intraspecific variation in desiccation survival time of *Aedes aegypti* (l.) mosquito eggs of australian origin. *Journal of Vector Ecology*, Wiley Online Library, v. 40, n. 2, p. 292–300, 2015. Citado na página 46.

FAY, R.; PERRY, A. et al. Laboratory studies of ovipositional preferences of *Aedes aegypti*. *Mosquito News*, v. 25, n. 3, p. 276–281, 1965. Citado 2 vezes nas páginas 43 and 44.

FOCKS, D. et al. Dynamic life table model for *Aedes aegypti* (*Diptera: Culicidae*): simulation results and validation. *Journal of medical entomology*, Oxford University Press Oxford, UK, v. 30, n. 6, p. 1018–1028, 1993. Citado 6 vezes nas páginas 27, 28, 44, 47, 48, and 49.

FOCKS, D. A. et al. Transmission thresholds for dengue in terms of *Aedes aegypti* pupae per person with discussion of their utility in source reduction efforts. *The American journal of tropical medicine and hygiene*, ASTMH, v. 62, n. 1, p. 11–18, 2000. Citado 2 vezes nas páginas 49 and 50.

FOCKS, D. A. et al. A simulation model of the epidemiology of urban dengue fever: literature analysis, model development, preliminary validation, and samples of simulation results. *The American journal of tropical medicine and hygiene*, ASTMH, v. 53, n. 5, p. 489–506, 1995. Citado 3 vezes nas páginas 49, 52, and 53.

FREEMAN, P.; DOE, S.; SIEMIGINOWSKA, A. Sherpa: a mission-independent data analysis application. In: INTERNATIONAL SOCIETY FOR OPTICS AND PHOTONICS. *Astronomical Data Analysis*. [S.l.], 2001. v. 4477, p. 76–87. Citado na página 72.

FREGLY, A. B. C. *Data Science on AWS: Implementing End-to-End, Continuous AI and Machine Learning Pipelines*. 1. ed. [S.l.]: O'Reilly Media, 2021. ISBN 1492079391,9781492079392. Citado 2 vezes nas páginas 11 and 55.

FUNK, C. et al. *The climate hazards infrared precipitation with stations—a new environmental record for monitoring extremes. Sci Data. 2015; 2: 150066*. [S.l.]: Epub 2015/12/10. https://doi. org/10.1038/sdata. 2015.66 PMID: 26646728. Citado 3 vezes nas páginas 56, 57, and 61.

GAGNON, A. S.; BUSH, A. B.; SMOYER-TOMIC, K. E. Dengue epidemics and the el niño southern oscillation. *Climate Research*, v. 19, n. 1, p. 35–43, 2001. Citado 2 vezes nas páginas 34 and 90.

GOMES, A. d. C. et al. Duration of larval and pupal development stages of *Aedes albopictus* in natural and artificial containers. *Revista de saude publica*, SciELO Brasil, v. 29, n. 1, p. 15–19, 1995. Citado na página 48.

GÖTZ, T. et al. Modeling dengue data from semarang, indonesia. *Ecological complexity*, Elsevier, v. 30, p. 57–62, 2017. Citado na página 89.

GUARNER, J.; HALE, G. L. Four human diseases with significant public health impact caused by mosquito-borne flaviviruses: West nile, zika, dengue and yellow fever. In: ELSEVIER. *Seminars in diagnostic pathology*. [S.l.], 2019. v. 36, n. 3, p. 170–176. Citado na página 27.

GUBLER, D. J. Dengue and dengue hemorrhagic fever. *Clinical microbiology reviews*, Am Soc Microbiol, v. 11, n. 3, p. 480–496, 1998. Citado 6 vezes nas páginas 11, 36, 37, 38, 51, and 52.

GUZMAN, M. G. et al. Dengue infection. *Nature reviews Disease primers*, Nature Publishing Group, v. 2, n. 1, p. 1–25, 2016. Citado 3 vezes nas páginas 11, 36, and 37.

HALSTEAD, S. B. Dengue in the americas and southeast asia: do they differ? *Revista panamericana de salud publica*, SciELO Public Health, v. 20, p. 407–415, 2006. Citado na página 41.

HALSTEAD, S. B. Dengue. *The lancet*, Elsevier, v. 370, n. 9599, p. 1644–1652, 2007. Citado na página 35.

HARDWOOD, R.; HORSFALL, W. Development, structure, and function of covering of eggs of floodwater mosquitoes. *III Functions of coverings Ann Entomol Soc Am*, v. 52, p. 113–6, 1959. Citado na página 46.

HARRIS, C. R. et al. Array programming with NumPy. *Nature*, Springer Science and Business Media LLC, v. 585, n. 7825, p. 357–362, set. 2020. Disponível em: <https://doi.org/10.1038/s41586-020-2649-2>. Citado na página 72.

HASENACK, H.; FLORES, F. E. V. Relações entre temperatura do ar e variáveis do ambiente urbano de porto alegre, rs. *Pesquisas em Geociências*, v. 21, n. 1, p. 3–11, 1994. Citado na página 57.

HERMAN, J.; USHER, W. Salib: an open-source python library for sensitivity analysis. *Journal of Open Source Software*, v. 2, n. 9, p. 97, 2017. Citado na página 70.

HII, Y. L. et al. Forecast of dengue incidence using temperature and rainfall. *PLoS Negl Trop Dis*, Public Library of Science, v. 6, n. 11, p. e1908, 2012. Citado na página 28.

HUBER, J. H. et al. Seasonal temperature variation influences climate suitability for dengue, chikungunya, and zika transmission. *PLoS neglected tropical diseases*, Public Library of Science, v. 12, n. 5, p. e0006451, 2018. Citado 7 vezes nas páginas 27, 28, 50, 52, 53, 62, and 89.

JIMÉNEZ-MUÑOZ, J. C. et al. Record-breaking warming and extreme drought in the amazon rainforest during the course of el niño 2015–2016. *Scientific reports*, Nature Publishing Group, v. 6, p. 33130, 2016. Citado na página 90.

JOSHI, V.; MOURYA, D.; SHARMA, R. Persistence of dengue-3 virus through transovarial transmission passage in successive generations of *Aedes aegypti* mosquitoes. *The American journal of tropical medicine and hygiene*, ASTMH, v. 67, n. 2, p. 158–161, 2002. Citado 3 vezes nas páginas 36, 45, and 77.

KERMACK, W. O.; MCKENDRICK, A. G. A contribution to the mathematical theory of epidemics. *Proceedings of the royal society of london. Series A, Containing papers of a mathematical and physical character*, The Royal Society London, v. 115, n. 772, p. 700–721, 1927. Citado 2 vezes nas páginas 53 and 54.

KERMACK, W. O.; MCKENDRICK, A. G. Contributions to the mathematical theory of epidemics. iii.—further studies of the problem of endemicity. *Proceedings of the Royal Society of London. Series A, Containing Papers of a Mathematical and Physical Character*, The Royal Society London, v. 141, n. 843, p. 94–122, 1933. Citado na página 54.

KRAEMER, M. U. et al. Past and future spread of the arbovirus vectors *Aedes aegypti* and *Aedes albopictus*. *Nature microbiology*, Nature Publishing Group, v. 4, n. 5, p. 854–863, 2019. Citado na página 28.

KUNO, G. et al. Phylogeny of the genus flavivirus. *Journal of virology*, Am Soc Microbiol, v. 72, n. 1, p. 73–83, 1998. Citado na página 35.

LAI, Y.-H. The climatic factors affecting dengue fever outbreaks in southern taiwan: an application of symbolic data analysis. *Biomedical engineering online*, BioMed Central, v. 17, n. 2, p. 1–14, 2018. Citado na página 33.

LANA, R. M. et al. Assessment of a trap based *Aedes aegypti* surveillance program using mathematical modeling. *PLoS One*, Public Library of Science San Francisco, CA USA, v. 13, n. 1, p. e0190673, 2018. Citado na página 50.

LAURA, L. et al. Biological and mechanical transmission models of dengue fever. *Communication in Biomathematical Sciences*, v. 2, n. 1, p. 12–22, 2019. Citado na página 27.

LEQUIME, S.; PAUL, R. E.; LAMBRECHTS, L. Determinants of arbovirus vertical transmission in mosquitoes. *PLoS pathogens*, Public Library of Science San Francisco, CA USA, v. 12, n. 5, p. e1005548, 2016. Citado na página 77.

LESSLER, J. T. et al. Times to key events in the course of zika infection and their implications: a systematic review and pooled analysis. *Bull World Health Organ*, v. 1, 2016. Citado 2 vezes nas páginas 51 and 70.

LIMA, T. et al. A framework for modeling and simulating *Aedes aegypti* and dengue fever dynamics. In: IEEE. *Proceedings of the Winter Simulation Conference 2014*. [S.l.], 2014. p. 1481–1492. Citado 2 vezes nas páginas 27 and 28.

LIMA, V. H. Ferreira-de; LIMA-CAMARA, T. N. Natural vertical transmission of dengue virus in *Aedes aegypti* and *Aedes albopictus*: a systematic review. *Parasites & vectors*, BioMed Central, v. 11, n. 1, p. 1–8, 2018. Citado na página 45.

LOWE, R.; CHIROMBO, J.; TOMPKINS, A. M. Relative importance of climatic, geographic and socio-economic determinants of malaria in malawi. *Malaria journal*, Springer, v. 12, n. 1, p. 416, 2013. Citado 2 vezes nas páginas 27 and 28.

MAGORI, K. et al. Skeeter buster: a stochastic, spatially explicit modeling tool for studying *Aedes aegypti* population replacement and population suppression strategies. *PLoS neglected tropical diseases*, Public Library of Science, v. 3, n. 9, 2009. Citado 3 vezes nas páginas 50, 67, and 70.

MAIDANA, N.; YANG, H. A spatial model to describe the dengue propagation. *TEMA (São Carlos)*, v. 8, n. 1, p. 83–92, 2007. Citado na página 50.

MAPS, G. *TerraMetrics, Dados do mapa*. [S.l.]: Retrieved from https://www.google.com/maps/@-14.4117221,-45.4088648,4770598m/data=!3m1!1e3, 2021. Citado 2 vezes nas páginas 12 and 60.

MARTINEZ-ROMERO, N. et al. Natural gas network optimization and sensibility analysis. In: SOCIETY OF PETROLEUM ENGINEERS. *SPE International Petroleum Conference and Exhibition in Mexico*. [S.l.], 2002. Citado 2 vezes nas páginas 70 and 73.

MCLEAN, D. et al. Dengue virus transmission by mosquitoes incubated at low temperatures. *Mosq News*, v. 35, p. 322–327, 1975. Citado na página 51.

MELTZER, M. I. et al. Using disability-adjusted life years to assess the economic impact of dengue in puerto rico: 1984-1994. *The American journal of tropical medicine and hygiene*, ASTMH, v. 59, n. 2, p. 265–271, 1998. Citado na página 39.

MESSINA, J. P. et al. The current and future global distribution and population at risk of dengue. *Nature microbiology*, Nature Publishing Group, v. 4, n. 9, p. 1508–1515, 2019. Citado na página 33.

MITCHELL, C.; MILLER, B. Vertical transmission of dengue viruses by strains of *Aedes albopictus* recently introduced into Brazil. *Journal of the American Mosquito Control Association*, v. 6, n. 2, p. 251–253, 1990. Citado 2 vezes nas páginas 36 and 45.

MORDECAI, E. A. et al. Detecting the impact of temperature on transmission of zika, dengue, and chikungunya using mechanistic models. *PLoS neglected tropical diseases*, Public Library of Science, v. 11, n. 4, p. e0005568, 2017. Citado 9 vezes nas páginas 45, 48, 51, 53, 67, 71, 88, 91, and 92.

MORIN, C. W.; COMRIE, A. C.; ERNST, K. Climate and dengue transmission: evidence and implications. *Environmental health perspectives*, National Institute of Environmental Health Sciences, v. 121, n. 11-12, p. 1264–1272, 2013. Citado na página 42.

MOURA, M. C. B. d. M. et al. Spatio-temporal dynamics of *Aedes aegypti* and *Aedes albopictus* oviposition in an urban area of northeastern Brazil. *Tropical Medicine & International Health*, Wiley Online Library, v. 25, n. 12, p. 1510–1521, 2020. Citado na página 47.

NATAL, D. Bioecologia do *Aedes aegypti*. *Biológico*, v. 64, n. 2, p. 205–207, 2002. Citado na página 28.

NEIRA, M. et al. Estimation of *Aedes aegypti* (*Diptera: Culicidae*) population size and adult male survival in an urban area in panama. *Memórias do Instituto Oswaldo Cruz*, SciELO Brasil, v. 109, n. 7, p. 879–886, 2014. Citado 4 vezes nas páginas 50, 66, 67, and 70.

NELSON, M. J. et al. *Aedes aegypti*: biología y ecología. 1986. Citado 5 vezes nas páginas 28, 35, 48, 49, and 50.

NEWTON, E. A.; REITER, P. A model of the transmission of dengue fever with an evaluation of the impact of ultra-low volume (ulv) insecticide applications on dengue epidemics. *The American journal of tropical medicine and hygiene*, ASTMH, v. 47, n. 6, p. 709–720, 1992. Citado na página 52.

NISHIURA, H.; HALSTEAD, S. B. Natural history of dengue virus (denv)—1 and denv—4 infections: reanalysis of classic studies. *The Journal of infectious diseases*, The University of Chicago Press, v. 195, n. 7, p. 1007–1013, 2007. Citado na página 52.

NOGUEIRA, R. M. R. et al. Dengue virus type 3 in Rio de Janeiro, Brazil. *Memórias do Instituto Oswaldo Cruz*, SciELO Brasil, v. 96, n. 7, p. 925–926, 2001. Citado na página 41.

NOGUEIRA, R. M. R. et al. Dengue epidemic in the state of Rio de Janeiro, Brazil, 1990–1: co-circulation of dengue 1 and dengue 2 serotypes. *Epidemiology & Infection*, Cambridge University Press, v. 111, n. 1, p. 163–170, 1993. Citado na página 41.

ORGANIZATION, P. A. H. Pan american health organization. *Pan American Health Organization*, 2022. Disponível em: <https://www3.paho.org/data/index.php/es/>. Citado 3 vezes nas páginas 11, 38, and 39.

ORGANIZATION, W. H. *International health regulations (2005).* [S.l.]: World Health Organization, 2008. Citado na página 33.

ORGANIZATION, W. H. *Dengue guidelines for diagnosis, treatment, prevention and control : new edition*. [S.l.]: World Health Organization, 2009. WHO/HTM/NTD/DEN/2009.1 p. Citado 2 vezes nas páginas 67 and 70.

ORGANIZATION, W. H. *Dengue Guidelines for Diagnosis, Treatment, Prevention and Control*. New. World Health Organization, 2010. ISBN 9241547871,9789241547871. Disponível em: <http://gen.lib.rus.ec/book/index.php?md5=0f988f96437f2d6485e2fd7424df0a13>. Citado na página 38.

ORGANIZATION, W. H. et al. National guidelines for clinical management of dengue fever. *India: World Health Organization*, 2015. Citado 9 vezes nas páginas 35, 36, 39, 40, 42, 49, 51, 52, and 53.

OSORIO, S. R. et al. A simulation model for the chikungunya with vectorial capacity. *Applied Mathematical Sciences*, v. 9, n. 140, p. 6953–6960, 2015. Citado na página 89.

OTERO, M.; SOLARI, H. G. Stochastic eco-epidemiological model of dengue disease transmission by *Aedes aegypti* mosquito. *Mathematical biosciences*, Elsevier, v. 223, n. 1, p. 32–46, 2010. Citado na página 52.

OTERO, M.; SOLARI, H. G.; SCHWEIGMANN, N. A stochastic population dynamics model for *Aedes aegypti*: formulation and application to a city with temperate climate. *Bulletin of mathematical biology*, Springer, v. 68, n. 8, p. 1945–1974, 2006. Citado 2 vezes nas páginas 27 and 28.

PALAMARA, G. M. et al. Inferring the temperature dependence of population parameters: the effects of experimental design and inference algorithm. *Ecology and evolution*, Wiley Online Library, v. 4, n. 24, p. 4736–4750, 2014. Citado na página 50.

PERIS, A. F.; LUGNANI, A. C. Um estudo sobre o eixo cascavel–foz do iguaçu na região oeste do paraná. *Revista Paranaense de Desenvolvimento-RPD*, n. 104, p. 79–102, 2011. Citado na página 57.

PETROVA, D. et al. The 2018–2019 weak el niño: predicting the risk of a dengue outbreak in machala, ecuador. *International Journal of Climatology*, Wiley Online Library, 2020. Citado na página 90.

PHAIJOO, G. R.; GURUNG, D. B. Modeling impact of temperature and human movement on the persistence of dengue disease. *Computational and mathematical methods in medicine*, Hindawi, v. 2017, 2017. Citado na página 89.

POLWIANG, S. The seasonal reproduction number of dengue fever: impacts of climate on transmission. *PeerJ*, PeerJ Inc., v. 3, p. e1069, 2015. Citado 3 vezes nas páginas 34, 51, and 53.

RABELO, A. C. L. et al. Characterization of dengue cases confirmed using the database linkage technique: assessment of virus circulation in belo horizonte, Brazil, 2009-2014. *Epidemiologia e Serviços de Saúde*, SciELO Brasil, v. 29, 2020. Citado na página 92.

RACLOZ, V. et al. Surveillance of dengue fever virus: a review of epidemiological models and early warning systems. *PLoS Negl Trop Dis*, Public Library of Science, v. 6, n. 5, p. e1648, 2012. Citado na página 27.

RASHKOV, P. et al. On the role of vector modeling in a minimalistic epidemic model. *Mathematical Biosciences and Engineering*, Arizona State University, v. 16, n. 5, p. 4314–4338, 2019. Citado na página 89.

Rio de Janeiro, G. do Estado do. *Informações de Saúde*. [S.l.]: Secretaria de Saúde, 2020. Citado 3 vezes nas páginas 59, 61, and 67.

ROSSUM, G. V.; JR, F. L. D. *Python tutorial*. [S.l.]: Centrum voor Wiskunde en Informatica Amsterdam, The Netherlands, 1995. Citado na página 72.

RUEDA, L. et al. Temperature-dependent development and survival rates of culex quinquefasciatus and *Aedes aegypti* (*Diptera: Culicidae*). *Journal of medical entomology*, Oxford University Press Oxford, UK, v. 27, n. 5, p. 892–898, 1990. Citado na página 27.

SABIN, A. B.; SCHLESINGER, R. W. Production of immunity to dengue with virus modified by propagation in mice. *Science*, American Association for the Advancement of Science, v. 101, n. 2634, p. 640–642, 1945. Citado na página 40.

SAIFUR, R. G. et al. The effects of moisture on ovipositional responses and larval eclosion of *Aedes albopictus*. *Journal of the American Mosquito Control Association*, BioOne, v. 26, n. 4, p. 373–380, 2010. Citado na página 47.

SALLES, T. S. et al. History, epidemiology and diagnostics of dengue in the american and Brazilian contexts: a review. *Parasites & vectors*, BioMed Central, v. 11, n. 1, p. 1–12, 2018. Citado 2 vezes nas páginas 11 and 41.

SCHAPER, S.; HERNÁNDEZ-CHAVARRÍA, F. Scanning electron microscopy of the four larval instars of the dengue fever vector *Aedes aegypti* (*Diptera: Culicidae*). *Revista de biología tropical*, http://creativecommons. org/licenses/by/3.0, v. 54, n. 3, p. 847–852, 2006. Citado na página 47.

SCHATZMAYR, H. G. et al. An outbreak of dengue virus at Rio de Janeiro-1986. Instituto Oswaldo Cruz, 1986. Citado na página 41.

SERUFO, J. C. et al. Isolation of dengue virus type 1 from larvae of *Aedes albopictus* in campos altos city, state of minas gerais, Brazil. *Memórias do Instituto Oswaldo Cruz*, v. 88, n. 3, p. 503–504, 1993. Citado 2 vezes nas páginas 36 and 45.

SERVIÇOS., M. da Saúde. Secretaria de Vigilância em Saúde. Coordenação-Geral de Desenvolvimento da Epidemiologia em. *Guia de Vigilância em Saúde: volume único*. [S.l.]: Brasil, 2019. Citado na página 35.

SEVERO, O. P. Eradication of the *Aedes aegypti* mosquito from the americas. 1955. Citado na página 41.

SIDE, S.; NOORANI, M. S. M. A sir model for spread of dengue fever disease (simulation for south sulawesi, indonesia and selangor, malaysia). *World Journal of Modelling and Simulation*, v. 9, n. 2, p. 96–105, 2013. Citado 2 vezes nas páginas 27 and 28.

SOTA, T.; MOGI, M. Interspecific variation in desiccation survival time of aedes (stegomyia) mosquito eggs is correlated with habitat and egg size. *Oecologia*, Springer, v. 90, n. 3, p. 353–358, 1992. Citado na página 46.

SUAYA, J. A. et al. Cost of dengue cases in eight countries in the americas and asia: a prospective study. *The American journal of tropical medicine and hygiene*, ASTMH, v. 80, n. 5, p. 846–855, 2009. Citado 3 vezes nas páginas 35, 39, and 40.

TAUIL, P. L. Urbanização e ecologia do dengue. *Cadernos de Saúde Pública*, SciELO Public Health, v. 17, p. S99–S102, 2001. Citado na página 35.

TIDMAN, R.; ABELA-RIDDER, B.; CASTAÑEDA, R. R. de. The impact of climate change on neglected tropical diseases: a systematic review. *Transactions of the Royal Society of Tropical Medicine and Hygiene*, Oxford University Press, v. 115, n. 2, p. 147–168, 2021. Citado 4 vezes nas páginas 27, 29, 33, and 34.

TIPAYAMONGKHOLGUL, M. et al. Effects of the el niño-southern oscillation on dengue epidemics in thailand, 1996-2005. *BMC public health*, BioMed Central, v. 9, n. 1, p. 1–15, 2009. Citado na página 90.

TRAN, A. et al. A rainfall-and temperature-driven abundance model for *Aedes albopictus* populations. *International journal of environmental research and public health*, Multidisciplinary Digital Publishing Institute, v. 10, n. 5, p. 1698–1719, 2013. Citado na página 50.

TRPIŠ, M. Dry season survival of *Aedes aegypti* eggs in various breeding sites in the dar es salaam area, tanzania. *Bulletin of the World Health Organization*, World Health Organization, v. 47, n. 3, p. 433, 1972. Citado na página 28.

TUN-LIN, W.; BURKOT, T.; KAY, B. Effects of temperature and larval diet on development rates and survival of the dengue vector *Aedes aegypti* in north queensland, australia. *Medical and veterinary entomology*, Wiley Online Library, v. 14, n. 1, p. 31–37, 2000. Citado na página 27.

URBANSKI, J. M. et al. The molecular physiology of increased egg desiccation resistance during diapause in the invasive mosquito, *Aedes albopictus*. *Proceedings of the Royal Society B: Biological Sciences*, The Royal Society, v. 277, n. 1694, p. 2683–2692, 2010. Citado na página 46.

WAGENMAKERS, E.-J.; FARRELL, S. Aic model selection using akaike weights. *Psychonomic bulletin & review*, Springer, v. 11, n. 1, p. 192–196, 2004. Citado na página 72.

WAN, Z.; HOOK, S.; HULLEY, G. Mod11a2 modis/terra land surface temperature/emissivity 8-day l3 global 1km sin grid v006. *NASA EOSDIS Land Processes DAAC*, v. 10, 2015. Citado 5 vezes nas páginas 56, 57, 58, 59, and 61.

WATTS, D. M. et al. Effect of temperature on the vector efficiency of *Aedes aegypti* for dengue 2 virus. *The American journal of tropical medicine and hygiene*, ASTMH, v. 36, n. 1, p. 143–152, 1987. Citado 2 vezes nas páginas 27 and 51.

WIJEYARATNE, P. et al. Development and survival of a natural population of *Aedes aegypti*. *Mosquito News*, v. 34, n. 1, p. 36–42, 1974. Citado na página 48.

WILDER-SMITH, A. The expanding geographic range of dengue in australia. *The Medical Journal of Australia*, v. 215, n. 4, p. 171–172, 2021. Citado na página 33.

WILDER-SMITH, A.; GUBLER, D. J. Geographic expansion of dengue: the impact of international travel. *Medical Clinics of North America*, Elsevier, v. 92, n. 6, p. 1377–1390, 2008. Citado na página 38.

XIAO, F.-Z. et al. The effect of temperature on the extrinsic incubation period and infection rate of dengue virus serotype 2 infection in *Aedes albopictus*. *Archives of virology*, Springer, v. 159, n. 11, p. 3053–3057, 2014. Citado na página 52.

YANG, H. et al. Assessing the effects of temperature on the population of *Aedes aegypti*, the vector of dengue. *Epidemiology & Infection*, Cambridge University Press, v. 137, n. 8, p. 1188–1202, 2009. Citado na página 45.

YANG, H. M. et al. Fitting the incidence data from the city of campinas, Brazil, based on dengue transmission modellings considering time-dependent entomological parameters. *PloS one*, Public Library of Science San Francisco, CA USA, v. 11, n. 3, p. e0152186, 2016. Citado 2 vezes nas páginas 51 and 53.

YANG, H. M. et al. Follow up estimation of *Aedes aegypti* entomological parameters and mathematical modellings. *Biosystems*, Elsevier, v. 103, n. 3, p. 360–371, 2011. Citado na página 48.

YANG, H. M. et al. Assessing the influence of quiescence eggs on the dynamics of mosquito *Aedes aegypti*. *Applied Mathematics*, Scientific Research Publishing, v. 5, n. 17, p. 2696, 2014. Citado na página 46.

ZASLAVSKY, R.; GOULART, B. N. G. d. Pendulum migration and healthcare in border area. *Ciência & Saúde Coletiva*, SciELO Public Health, v. 22, p. 3981–3986, 2017. Citado na página 65.

ZEIDLER, J. D. et al. Vírus dengue em larvas de *Aedes aegypti* e sua dinâmica de infestação, Roraima, Brasil. *Revista de Saúde Pública*, SciELO Brasil, v. 42, n. 6, p. 986–991, 2008. Citado 2 vezes nas páginas 45 and 95.

Annex

ANNEX A – Environmental variables

All the Figures were created using the Matplotlib library of Python 3 programming language. Figures 19 and 20 show environment variables. Figure S3, S4 and S5 illustrate the behavior of the functions used in the article. Figures S6 to S14 show results derived from the sensitivity analysis. Lastly, Figure S15 and S16 illustrate the moment when Chikungunya and Zika cases were first reported in Rio de Janeiro and Fortaleza municipalities, respectively.

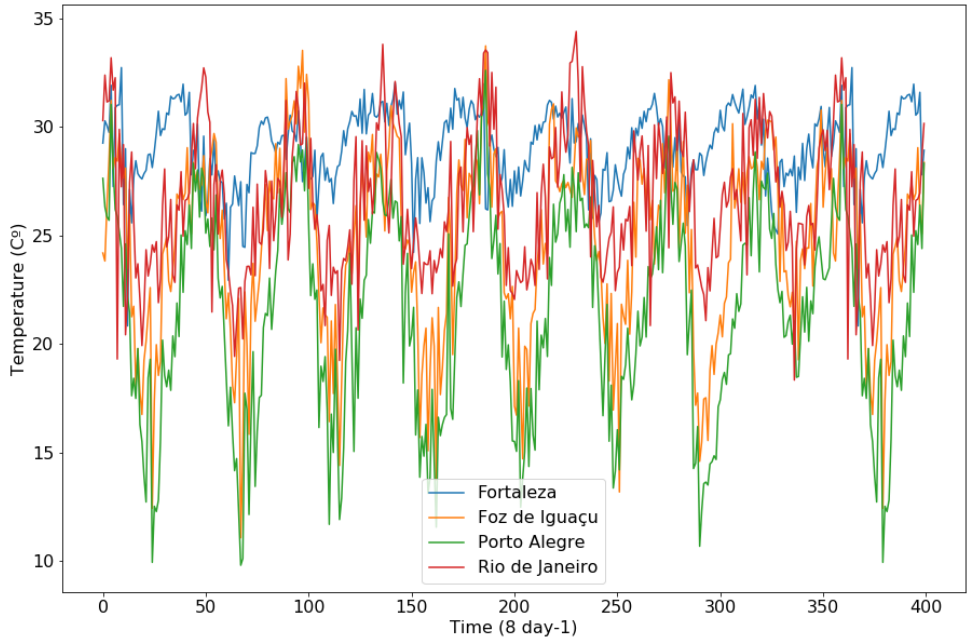

Figure 19 – Average temperature per 8 days from 2010 to 2019 in Fortaleza (Blue), Foz de Iguaçu (Orange), Porto Alegre (Green) and Rio de Janeiro (Red) municipalities, Brazil.

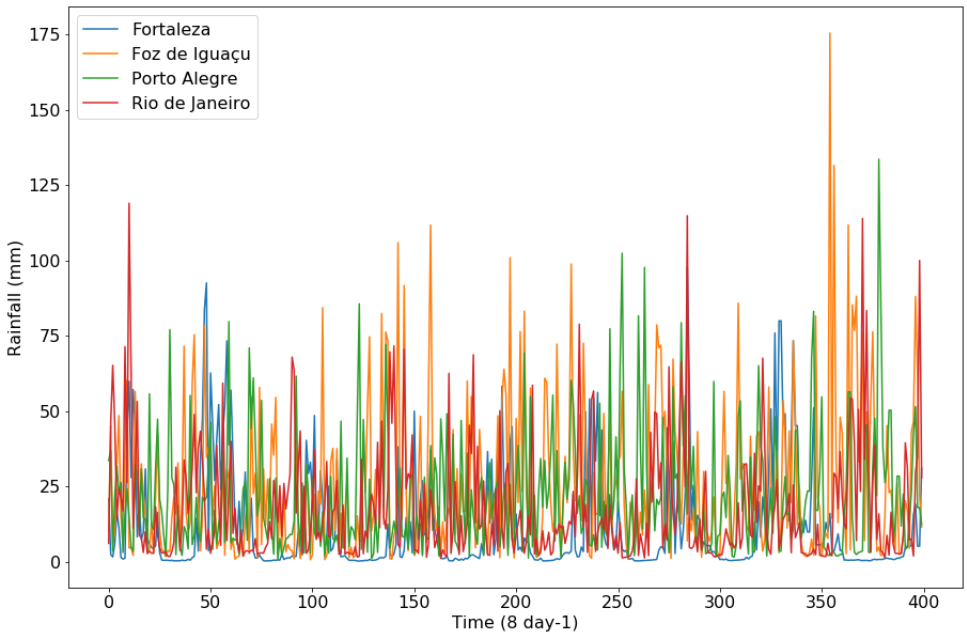

Figure 20 – Mean rainfall per 8 days from 2010 to 2019 in Fortaleza (Blue), Foz de Iguaçu (Orange), Porto Alegre (Green) and Rio de Janeiro (Red) municipalities, Brazil.

ANNEX B – Chikungunya and Zika cases

All the Figures were created using the Matplotlib library of Python 3 programming language. Figure 21 and 22 illustrate the moment when Chikungunya and Zika cases were first reported in Rio de Janeiro and Fortaleza municipalities, respectively.

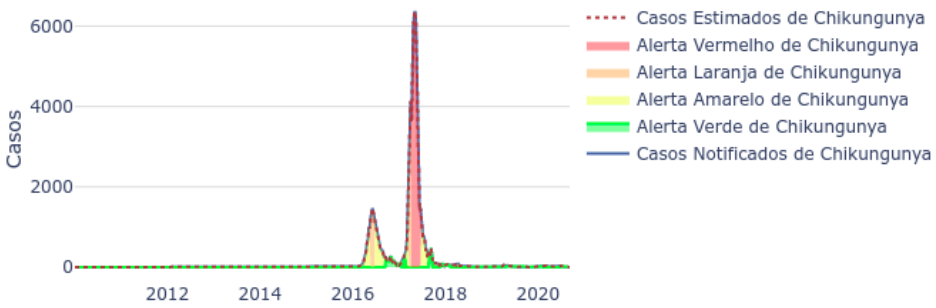

Figure 21 – Chikungunya cases in Fortaleza from 2010 to 2020 according to InfoDengue data (CODECO et al., 2018)

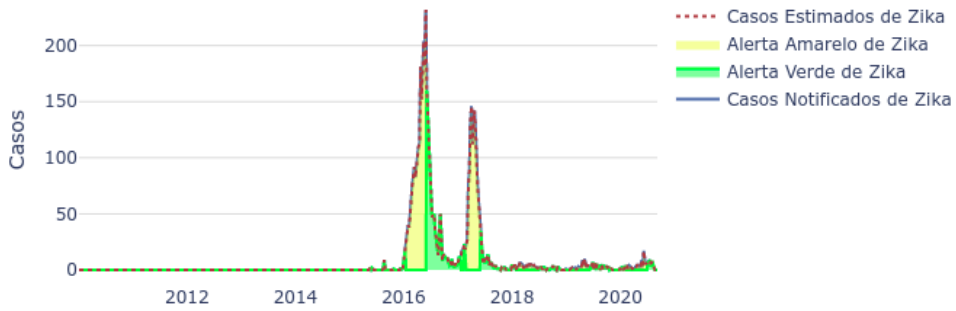

Figure 22 – Zika cases in Rio de Janeiro from 2010 to 2020 according to InfoDengue data (CODECO et al., 2018)

ANNEX C – Functions behavior

All the Figures were created using the Matplotlib library of Python 3 programming language. Figure 23 and 24 illustrate the behavior of the functions used in the article.

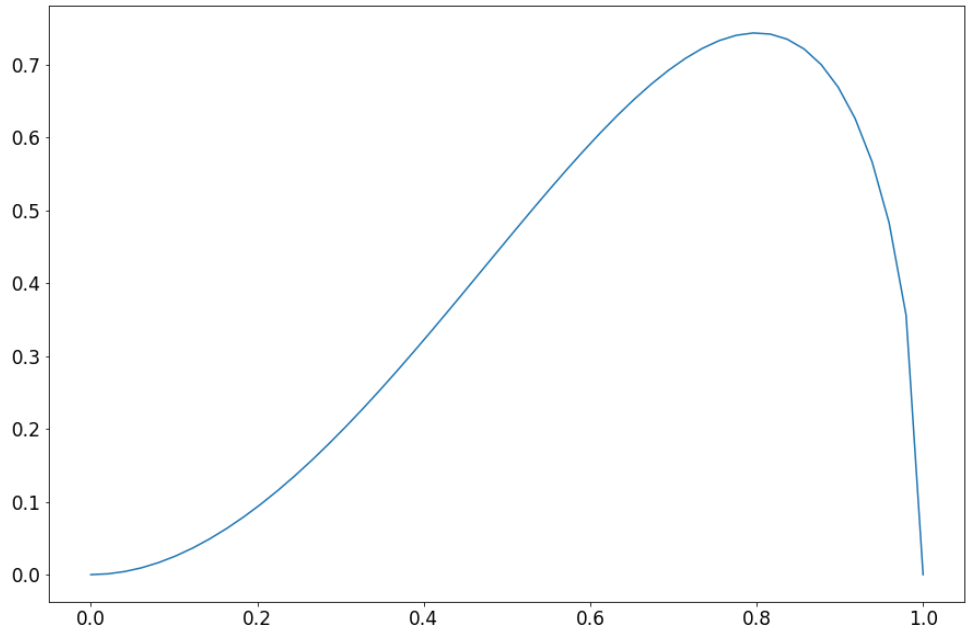

Figure 23 – Brieré curve of the equation $2.59R(R-0)((1-R)^{\frac{1}{2}}$

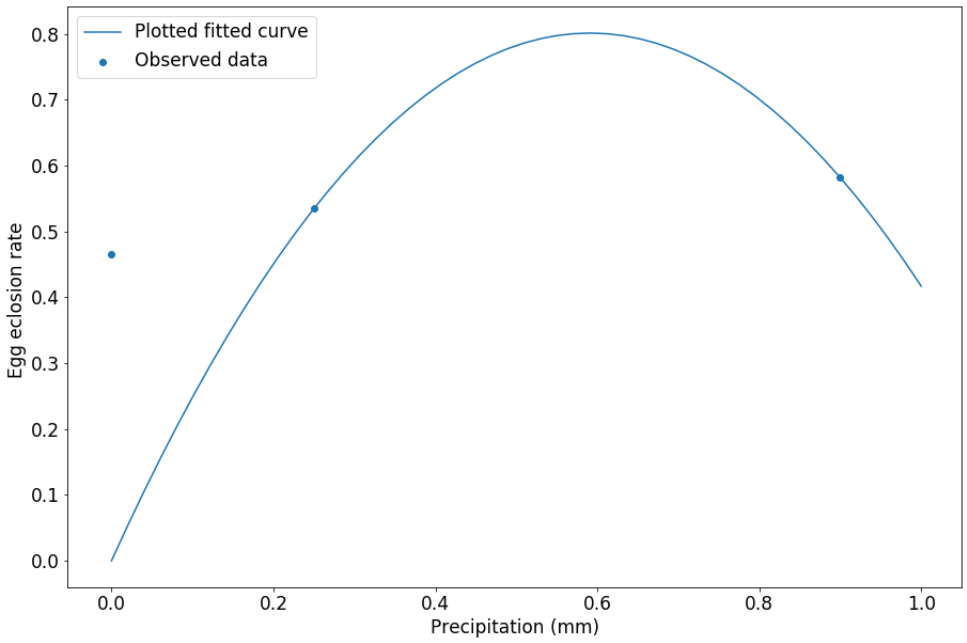

Figure 24 – Relation between egg eclosion rate (day) and rainfall represented by the quadratic function: $-2.29574834R^2 + 2.71268315b$

ANNEX D – SIR model

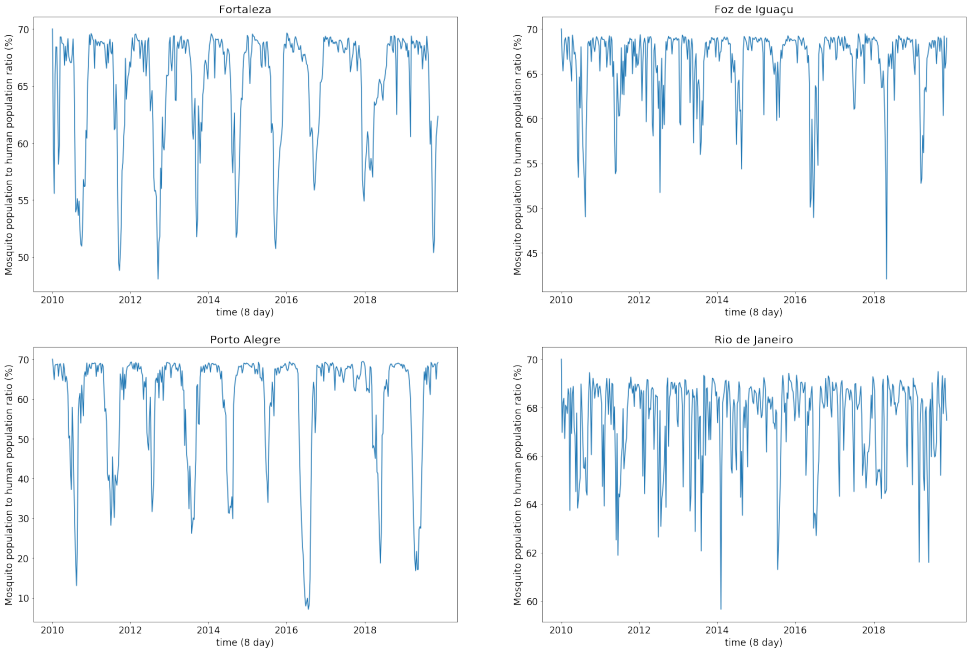

Figure 25 – Simulations of adult populations of *Ae. aegypti* from 2010 to 2019 for Fortaleza, Foz de Iguaçu, Porto Alegre and Rio de Janeiro municipalities.

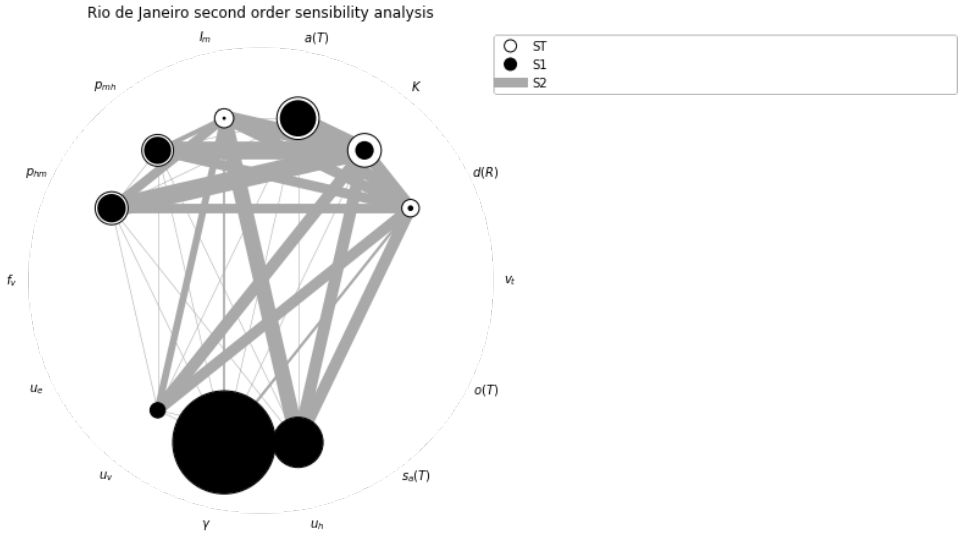

Figure 26 – Porto Alegre first, second and total order sensitivity analysis: interaction between $O_t(T)$(0.5-2), v_t(0-0.3), K (0.5, 3), $a(T)$ (0.5-2), i_m (0.00001-0.01), p_{mh} (0.5-2), p_{hm} (0.5-2), f_v (0.3-0.7), u_e (0.01-0.15), u_v (0.3-0.7), γ (0.4-1.6), u_h (0.00001-0,001), $sa(T)$ (0.5-2) and model output sum of square errors (SSE).

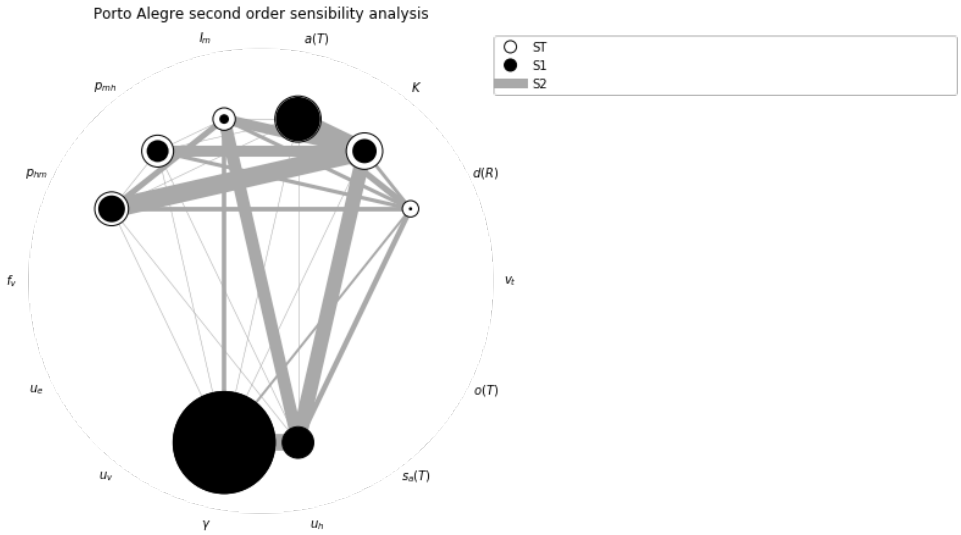

Figure 27 – Rio de Janeiro first, second and total order sensitivity analysis: interaction between $O_t(T)$(0.5-2), v_t(0-0.3), K (0.5, 3), $a(T)$ (0.5-2), i_m (0.00001-0.01), p_{mh} (0.5-2), p_{hm} (0.5-2), f_v (0.3-0.7), u_e (0.01-0.15), u_v (0.3-0.7), γ (0.4-1.6), u_h (0.00001-0,001), $sa(T)$ (0.5-2) and model output sum of square errors (SSE).

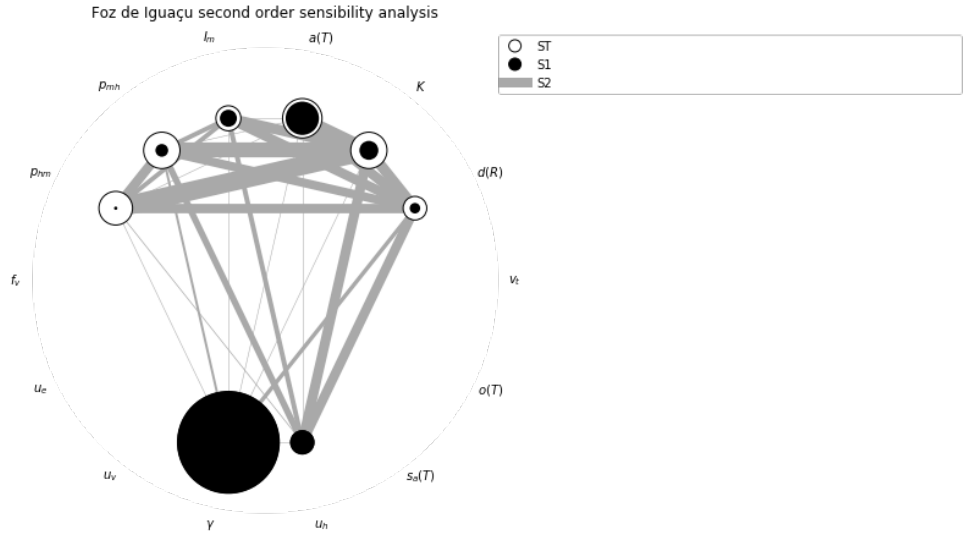

Figure 28 – Foz de Iguaçu first, second and total order sensitivity analysis: interaction between $O_t(T)$(0.5-2), v_t(0-0.3), K (0.5, 3), $a(T)$ (0.5-2), i_m (0.00001-0.01), p_{mh} (0.5-2), p_{hm} (0.5-2), f_v (0.3-0.7), u_e (0.01-0.15), u_v (0.3-0.7), γ (0.4-1.6), u_h (0.00001-0,001), $sa(T)$ (0.5-2) and model output sum of square errors (SSE).

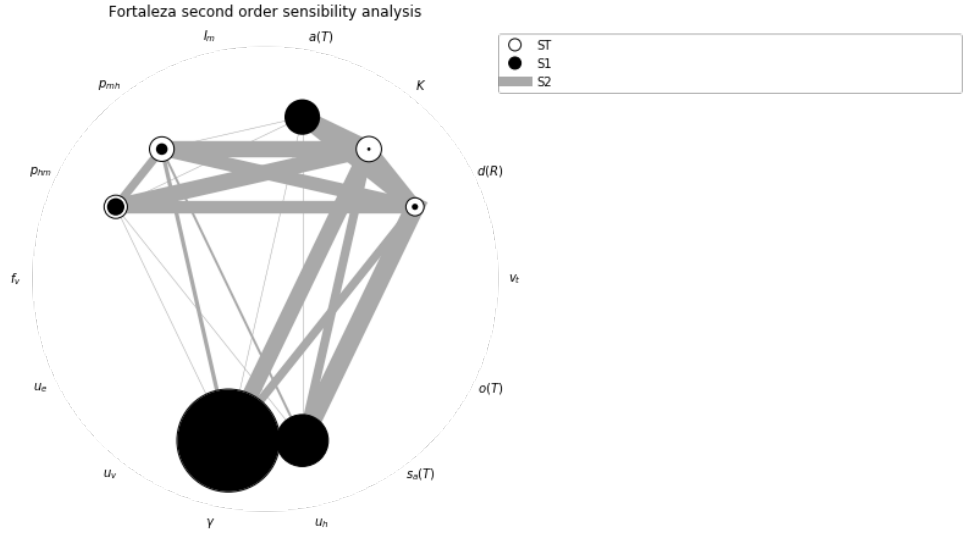

Figure 29 – Fortaleza first, second and total order sensitivity analysis: interaction between $O_t(T)$(0.5-2), v_t(0-0.3), K (0.5, 3), $a(T)$ (0.5-2), i_m (0.00001-0.01), p_{mh} (0.5-2), p_{hm} (0.5-2), f_v (0.3-0.7), u_e (0.01-0.15), u_v (0.3-0.7), γ (0.4-1.6), u_h (0.00001-0,001), $sa(T)$ (0.5-2) and model output sum of square errors (SSE)

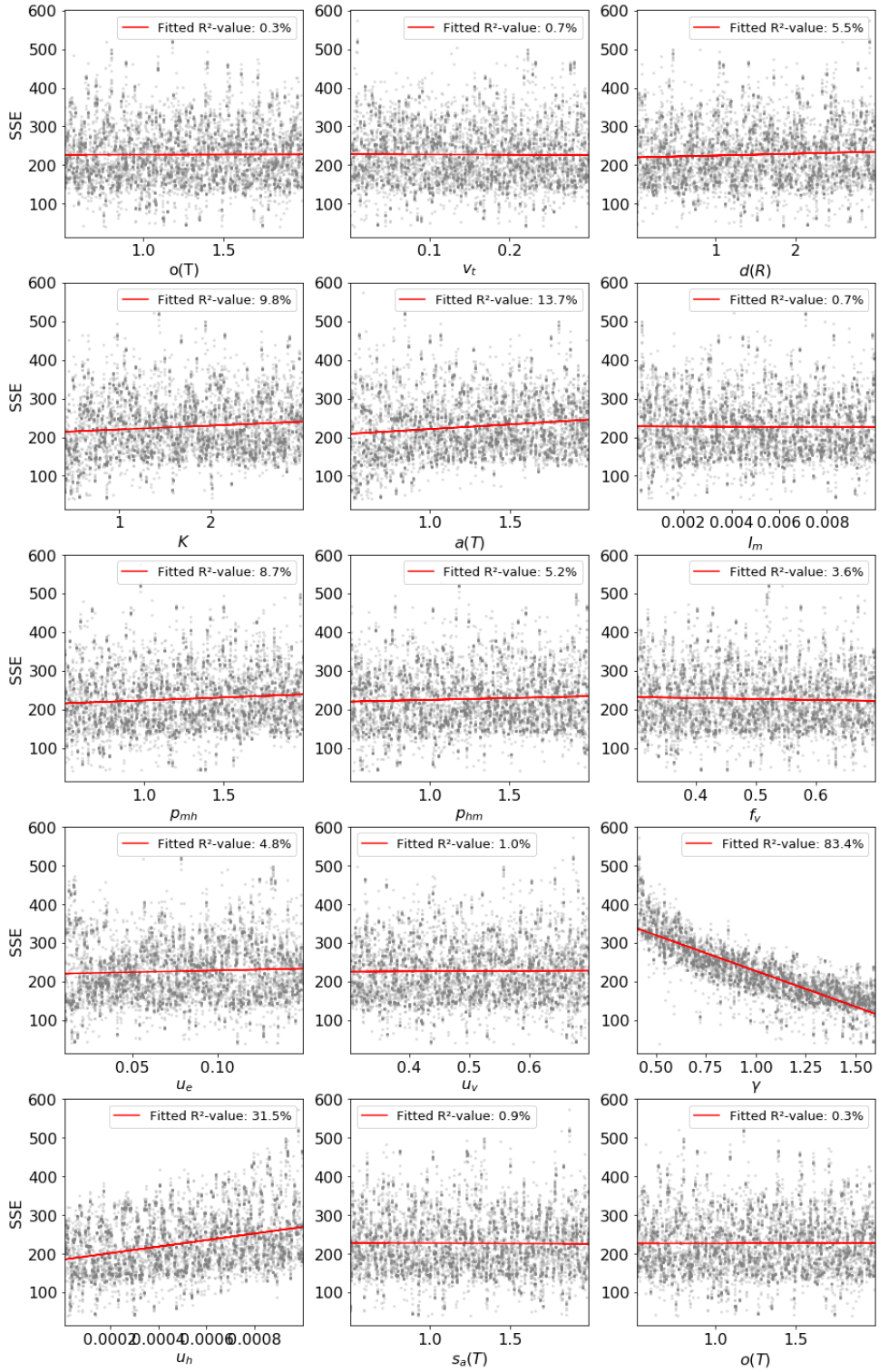

Figure 30 – Sensitivity Analysis residues regarding sum of square errors (SSE) from model simulations and simulations parameters with the respecting range of possibilities: $O_t(T)$(0.5-2), v_t(0-0.3), K (0.5, 3), $a(T)$ (0.5-2), i_m (0.00001-0.01), p_{mh} (0.5-2), p_{hm} (0.5-2), f_v (0.3-0.7), u_e (0.01-0.15), u_v (0.3-0.7), γ (0.4-1.6), u_h (0.00001-0,001), $sa(T)$ (0.5-2) ; for Rio de Janeiro

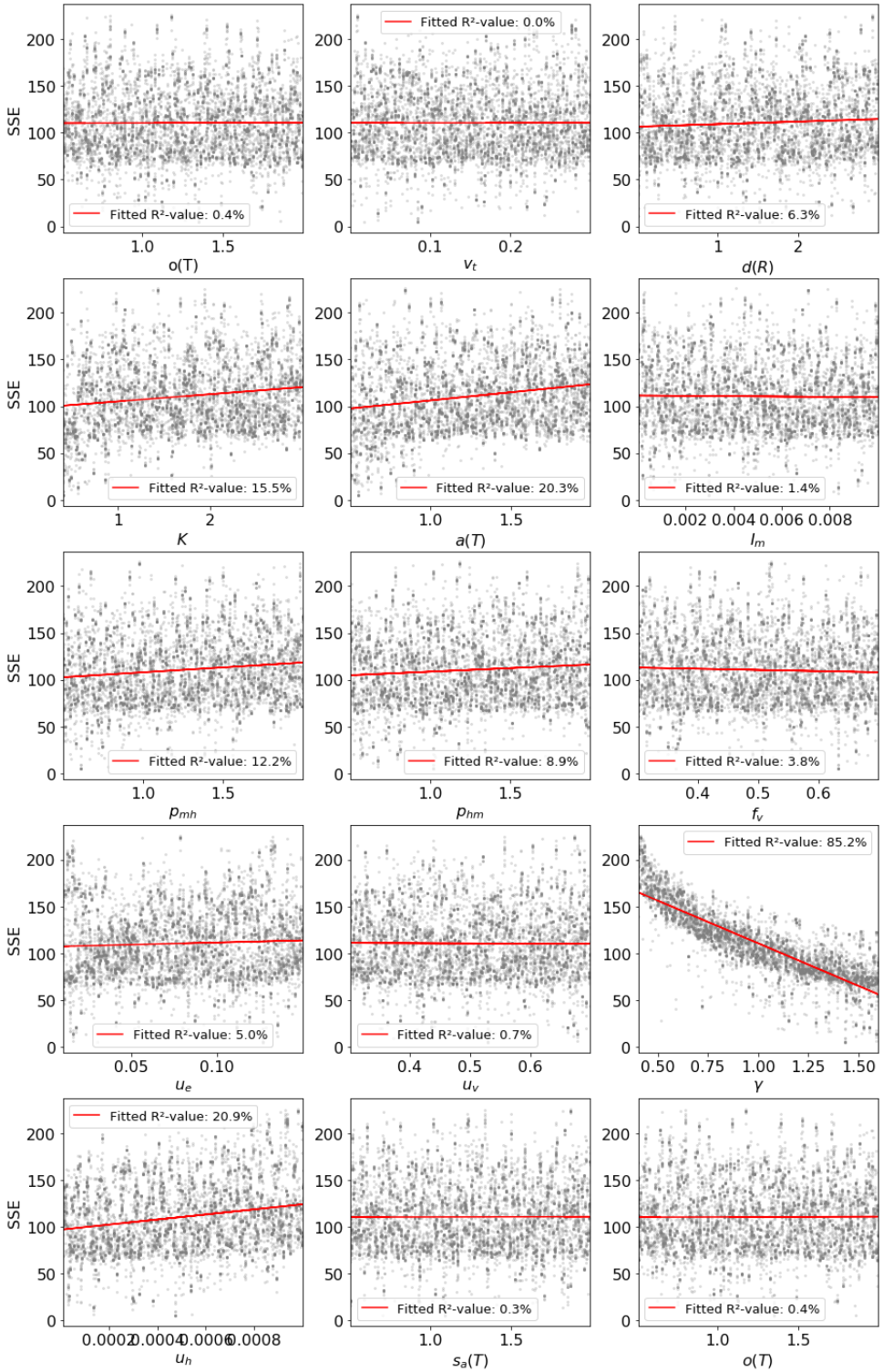

Figure 31 – Sensitivity Analysis residues regarding sum of square errors (SSE) from model simulations and simulations parameters with the respecting range of possibilities: $O_t(T)$(0.5-2), v_t(0-0.3), K (0.5, 3), $a(T)$ (0.5-2), i_m (0.00001-0.01), p_{mh} (0.5-2), p_{hm} (0.5-2), f_v (0.3-0.7), u_e (0.01-0.15), u_v (0.3-0.7), γ (0.4-1.6), u_h (0.00001-0,001), $sa(T)$ (0.5-2) ; for Porto Alegre

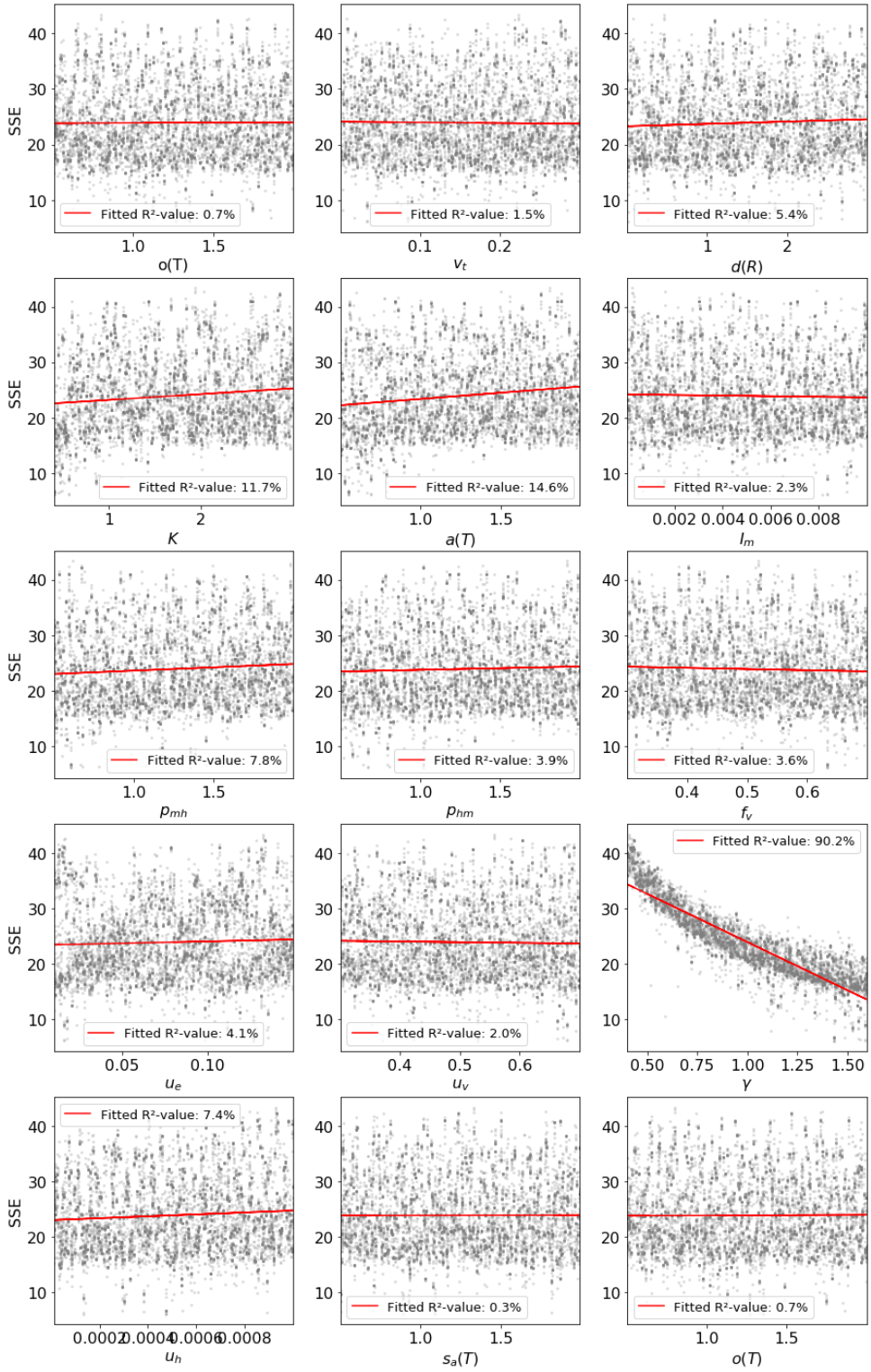

Figure 32 – Sensitivity Analysis residues regarding sum of square errors (SSE) from model simulations and simulations parameters with the respecting range of possibilities: $O_t(T)$(0.5-2), v_t(0-0.3), K (0.5, 3), $a(T)$ (0.5-2), i_m (0.00001-0.01), p_{mh} (0.5-2), p_{hm} (0.5-2), f_v (0.3-0.7), u_e (0.01-0.15), u_v (0.3-0.7), γ (0.4-1.6), u_h (0.00001-0,001), $sa(T)$ (0.5-2) ; for Foz de Iguaçu

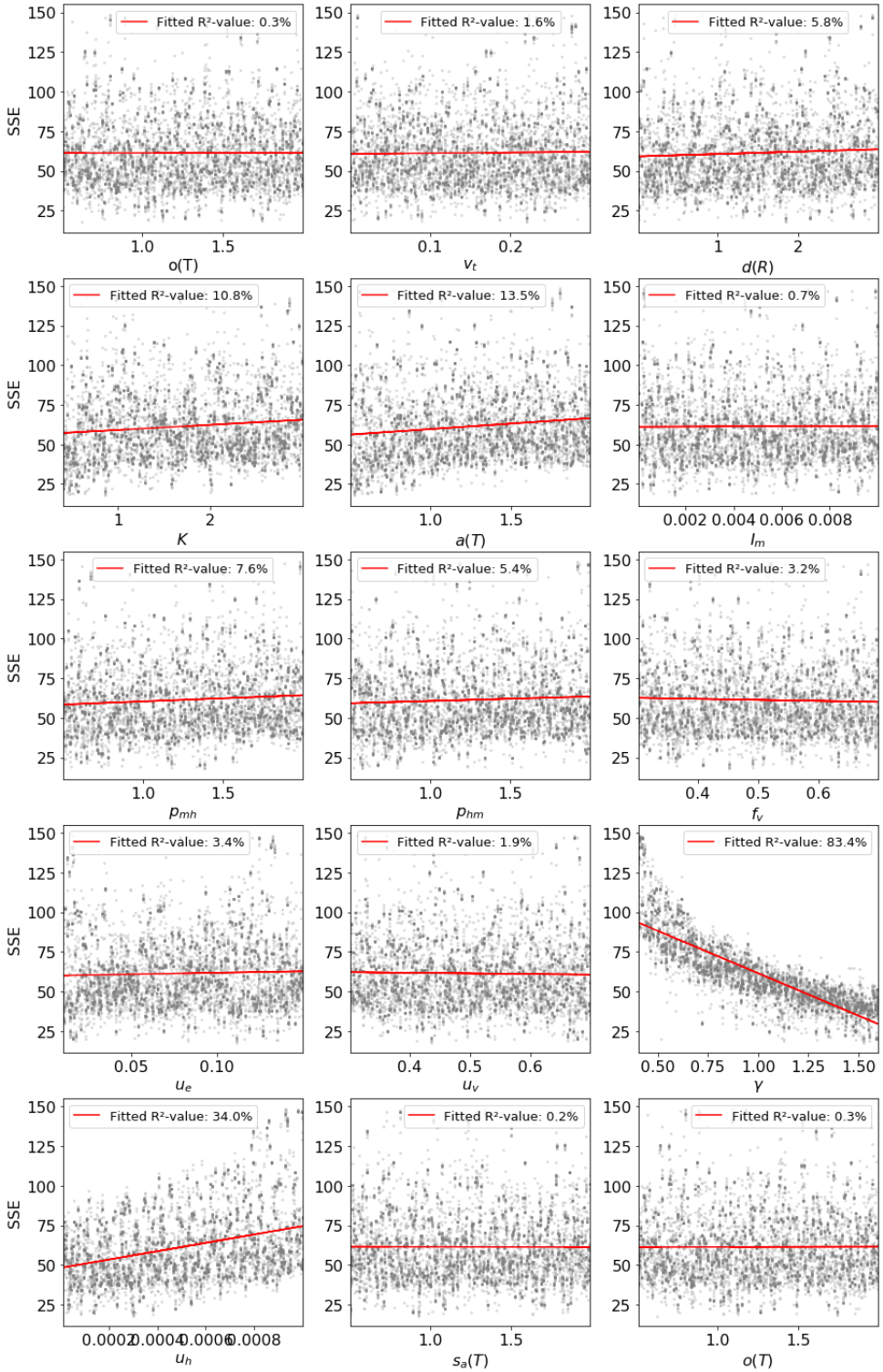

Figure 33 – Sensitivity Analysis residues regarding sum of square errors (SSE) from model simulations and simulations parameters with the respecting range of possibilities: $O_t(T)$(0.5-2), v_t(0-0.3), K (0.5, 3), $a(T)$ (0.5-2), i_m (0.00001-0.01), p_{mh} (0.5-2), p_{hm} (0.5-2), f_v (0.3-0.7), u_e (0.01-0.15), u_v (0.3-0.7), γ (0.4-1.6), u_h (0.00001-0,001), $sa(T)$ (0.5-2) ; for Fortaleza

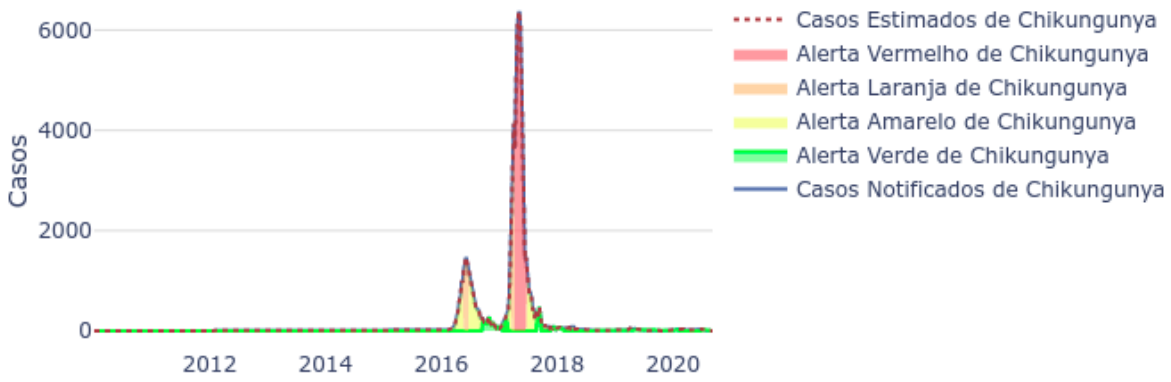

Figure 34 – Chikungunya incidence in Fortaleza from 2010 to 2020 according to Infodengue data

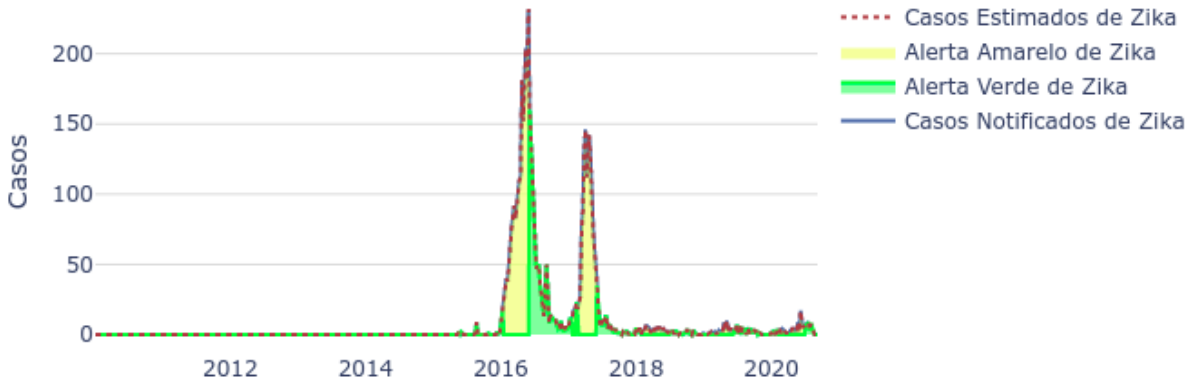

Figure 35 – Zika incidence in Rio de Janeiro from 2010 to 2020 according to Infodengue data

ANNEX E – Sensitivity analysis for model SI-SEI-SEIR

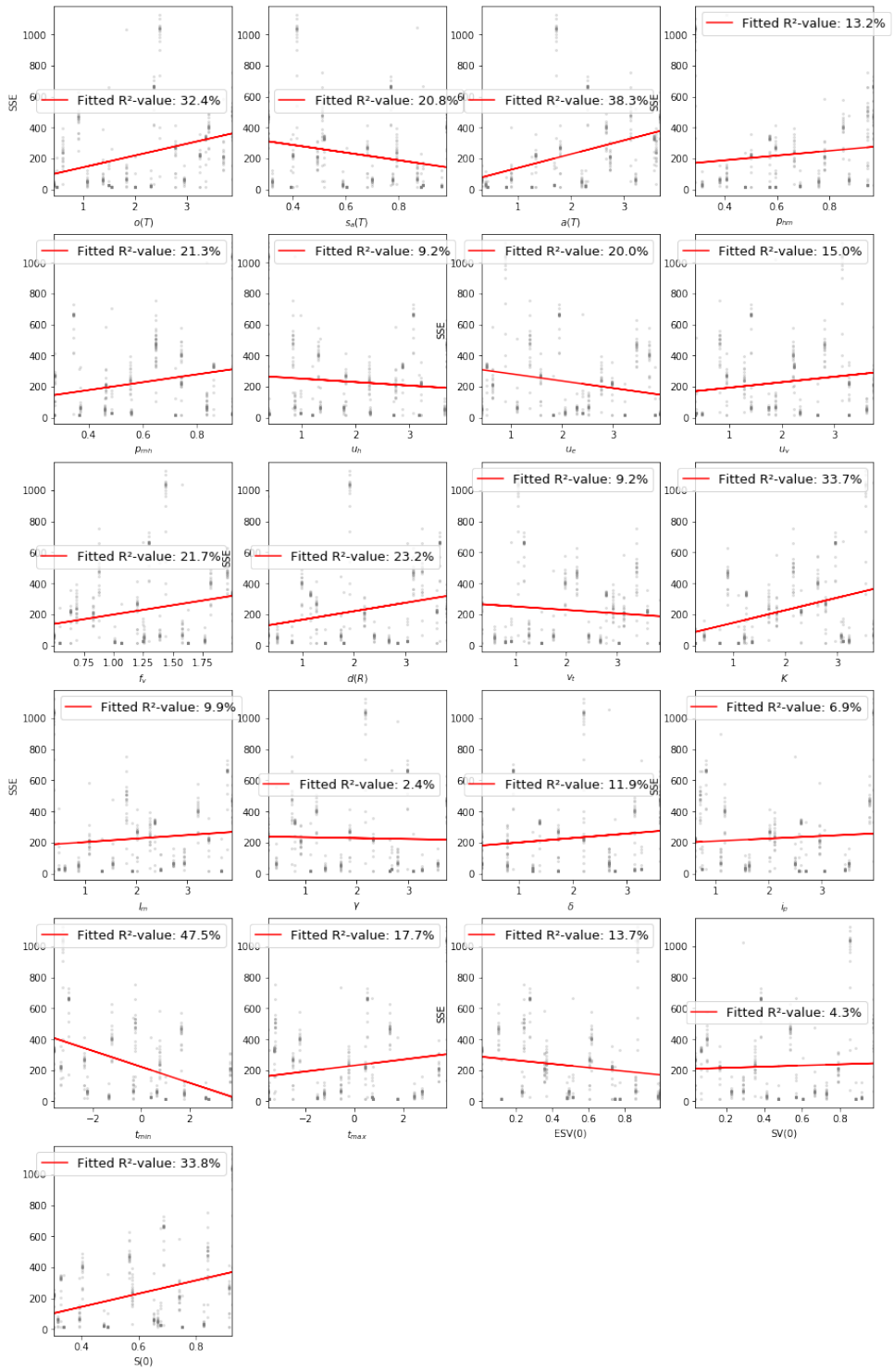

Figure 36 – Sensitivity Analysis residues regarding sum of square errors (SSE) from model simulations and simulations parameters with the respecting range of possibilities: $O_t(T)$(0.25-4), v_t(0.25-0.4), K (0.25, 4), $a(T)$ (0.25-4), i_m (0.25-4), p_{mh} (0.25-1), p_{hm} (0.25-1), f_v (0.25-1.5), u_e (0.25-4), u_v (0.25-4), δ (0.25-4), γ (0.25-4), i_p (0.25-4), u_h (0.25-4), $sa(T)$ (0.25-4) ; for Rio de Janeiro

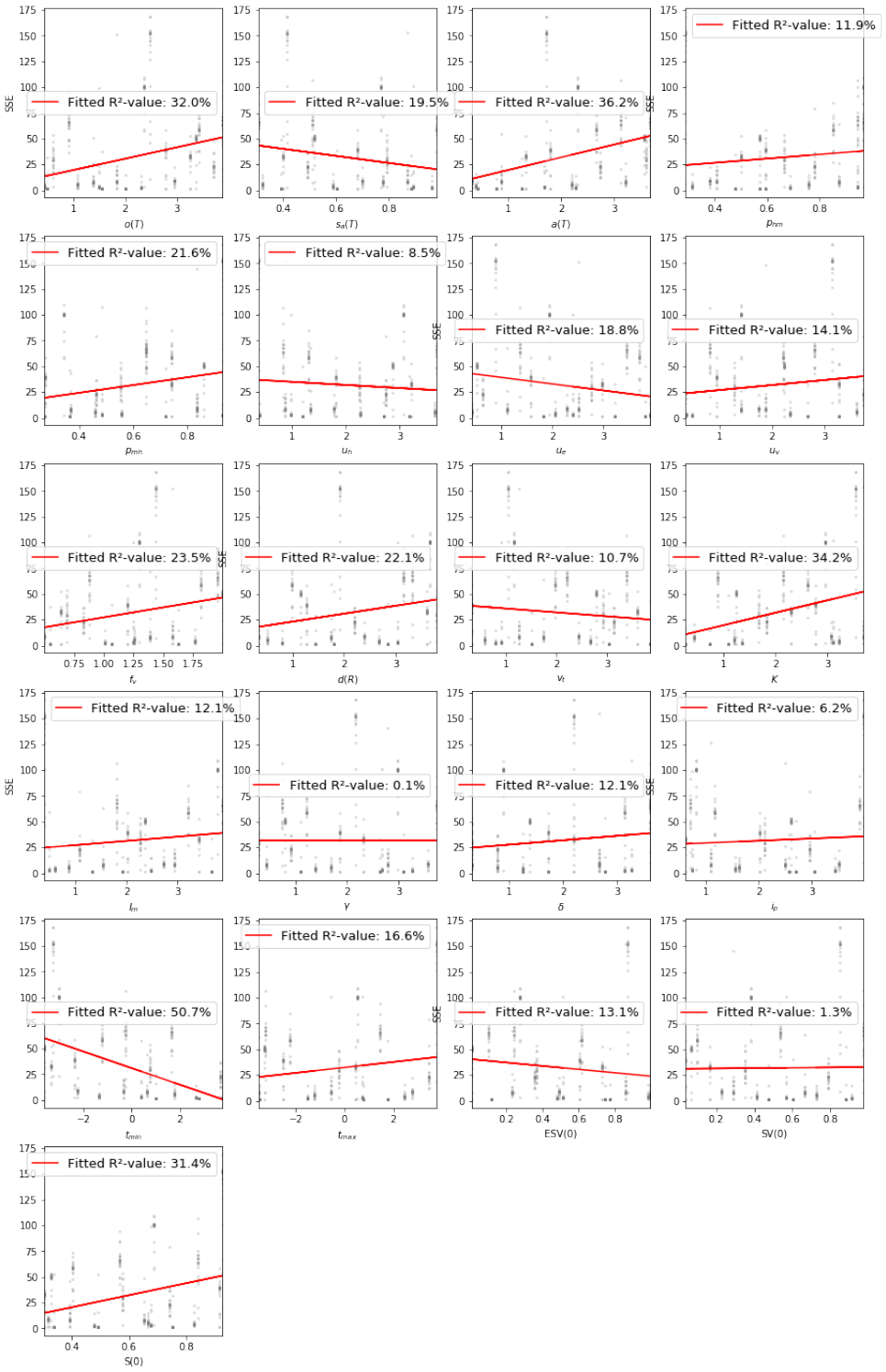

Figure 37 – Sensitivity Analysis residues regarding sum of square errors (SSE) from model simulations and simulations parameters with the respecting range of possibilities: $O_t(T)$(0.25-4), v_t(0.25-0.4), K (0.25, 4), $a(T)$ (0.25-4), i_m (0.25-4), p_{mh} (0.25-1), p_{hm} (0.25-1), f_v (0.25-1.5), u_e (0.25-4), u_v (0.25-4), δ (0.25-4), γ (0.25-4), i_p (0.25-4), u_h (0.25-4), $sa(T)$ (0.25-4) ; for São Gonçalo

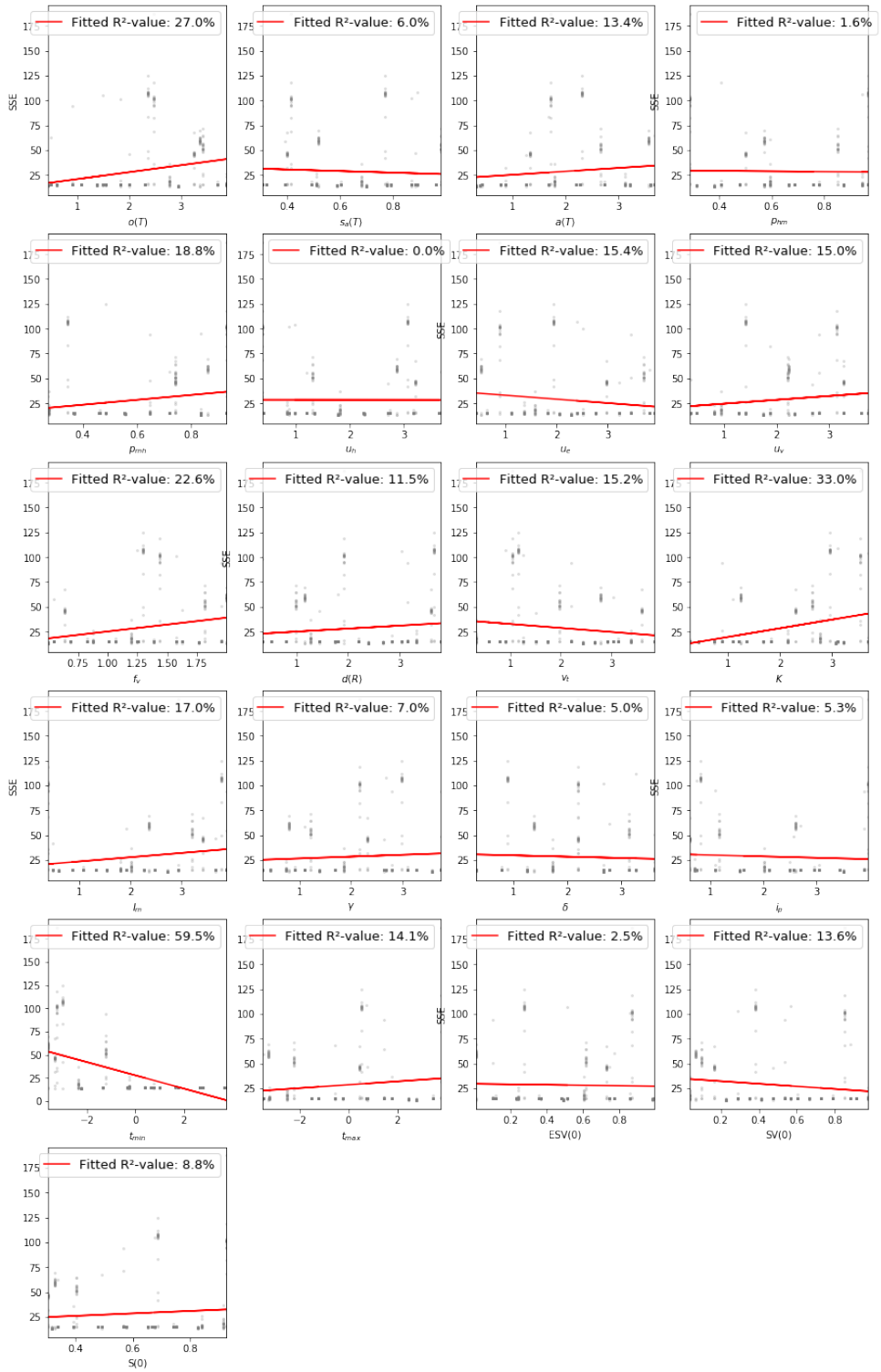

Figure 38 – Sensitivity Analysis residues regarding sum of square errors (SSE) from model simulations and simulations parameters with the respecting range of possibilities: $O_t(T)$(0.25-4), v_t(0.25-0.4), K (0.25, 4), $a(T)$ (0.25-4), i_m (0.25-4), p_{mh} (0.25-1), p_{hm} (0.25-1), f_v (0.25-1.5), u_e (0.25-4), u_v (0.25-4), δ (0.25-4), γ (0.25-4), i_p (0.25-4), u_h (0.25-4), $sa(T)$ (0.25-4) ; for Belo Horizonte

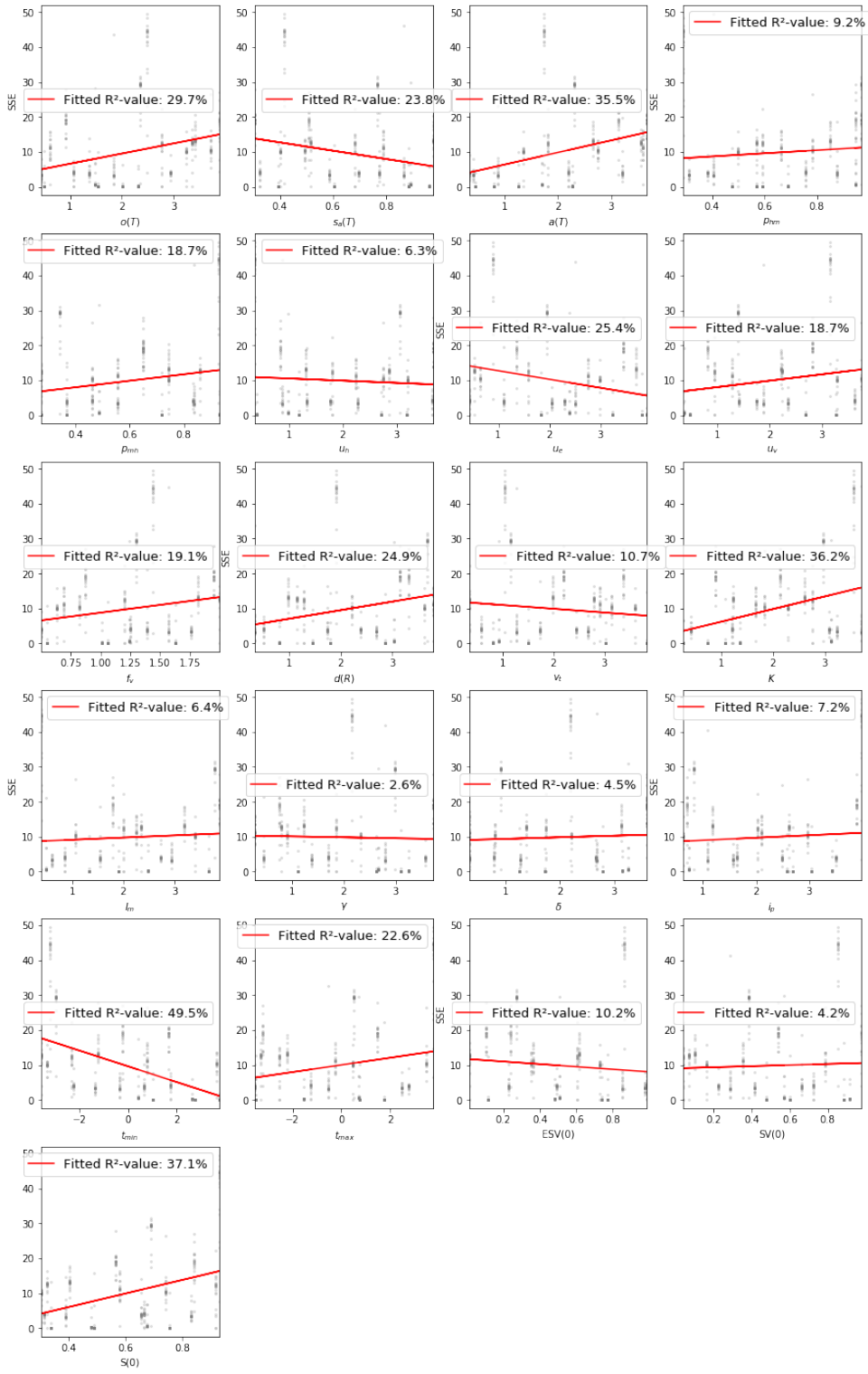

Figure 39 – Sensitivity Analysis residues regarding sum of square errors (SSE) from model simulations and simulations parameters with the respecting range of possibilities: $O_t(T)$(0.25-4), v_t(0.25-0.4), K (0.25, 4), $a(T)$ (0.25-4), i_m (0.25-4), p_{mh} (0.25-1), p_{hm} (0.25-1), f_v (0.25-1.5), u_e (0.25-4), u_v (0.25-4), δ (0.25-4), γ (0.25-4), i_p (0.25-4), u_h (0.25-4), $sa(T)$ (0.25-4) ; for Caucaia

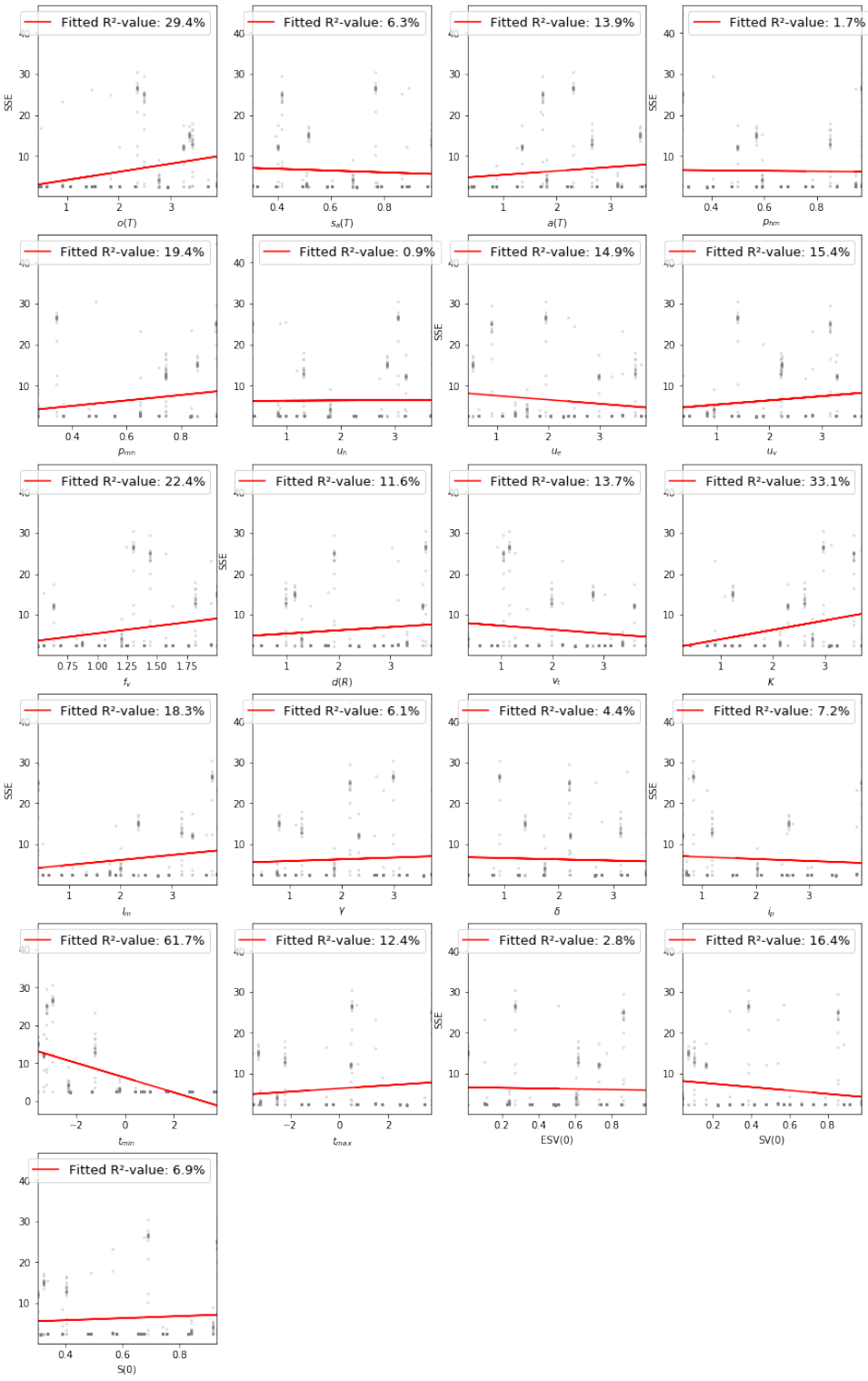

Figure 40 – Sensitivity Analysis residues regarding sum of square errors (SSE) from model simulations and simulations parameters with the respecting range of possibilities: $O_t(T)$(0.25-4), v_t(0.25-0.4), K (0.25, 4), $a(T)$ (0.25-4), i_m (0.25-4), p_{mh} (0.25-1), p_{hm} (0.25-1), f_v (0.25-1.5), u_e (0.25-4), u_v (0.25-4), δ (0.25-4), γ (0.25-4), i_p (0.25-4), u_h (0.25-4), $sa(T)$ (0.25-4) ; for Contagem

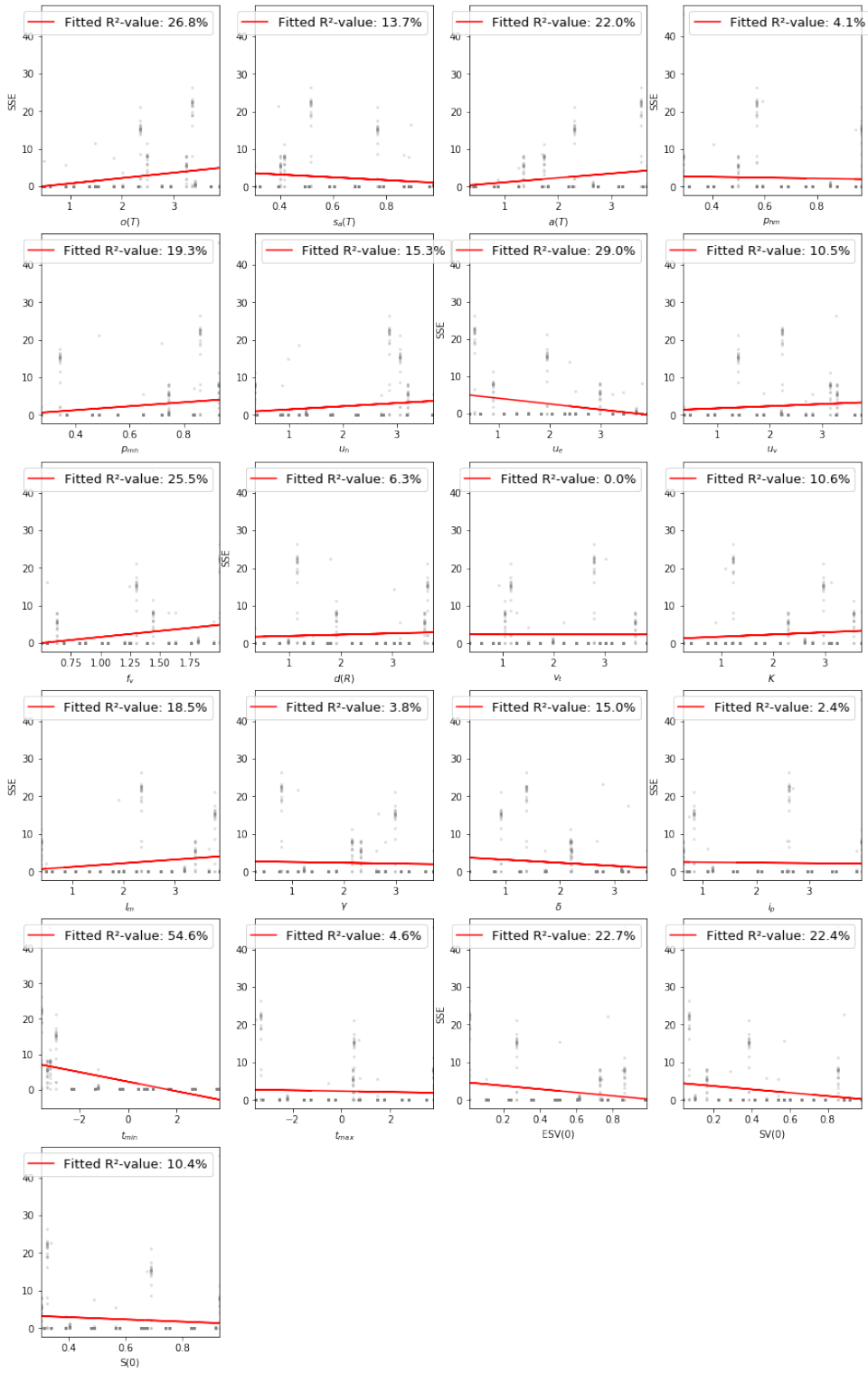

Figure 41 – Sensitivity Analysis residues regarding sum of square errors (SSE) from model simulations and simulations parameters with the respecting range of possibilities: $O_t(T)$(0.25-4), v_t(0.25-0.4), K (0.25, 4), $a(T)$ (0.25-4), i_m (0.25-4), p_{mh} (0.25-1), p_{hm} (0.25-1), f_v (0.25-1.5), u_e (0.25-4), u_v (0.25-4), δ (0.25-4), γ (0.25-4), i_p (0.25-4), u_h (0.25-4), $sa(T)$ (0.25-4) ; for Curitiba

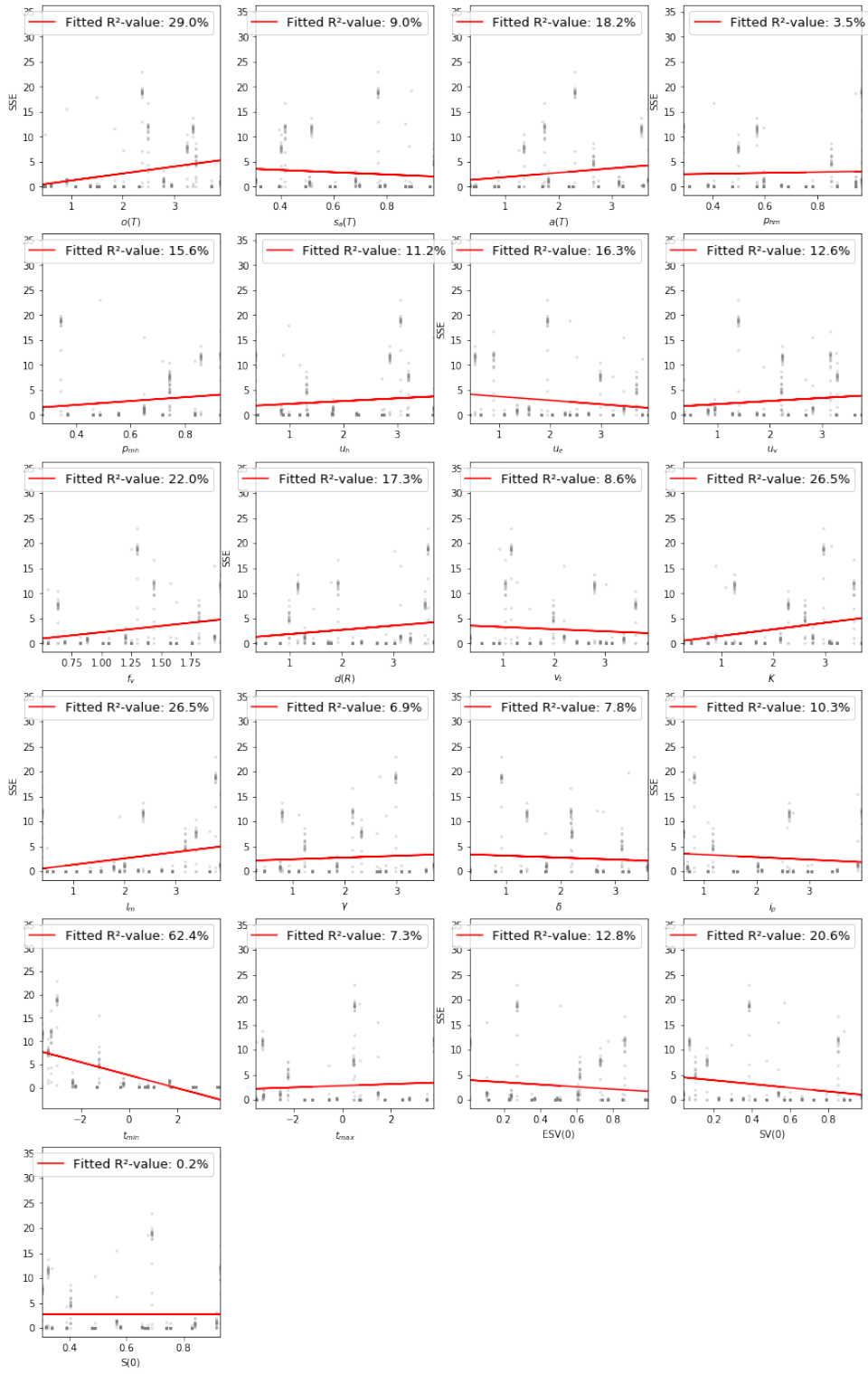

Figure 42 – Sensitivity Analysis residues regarding sum of square errors (SSE) from model simulations and simulations parameters with the respecting range of possibilities: $O_t(T)$(0.25-4), v_t(0.25-0.4), K (0.25, 4), $a(T)$ (0.25-4), i_m (0.25-4), p_{mh} (0.25-1), p_{hm} (0.25-1), f_v (0.25-1.5), u_e (0.25-4), u_v (0.25-4), δ (0.25-4), γ (0.25-4), i_p (0.25-4), u_h (0.25-4), $sa(T)$ (0.25-4) ; for Florianópolis

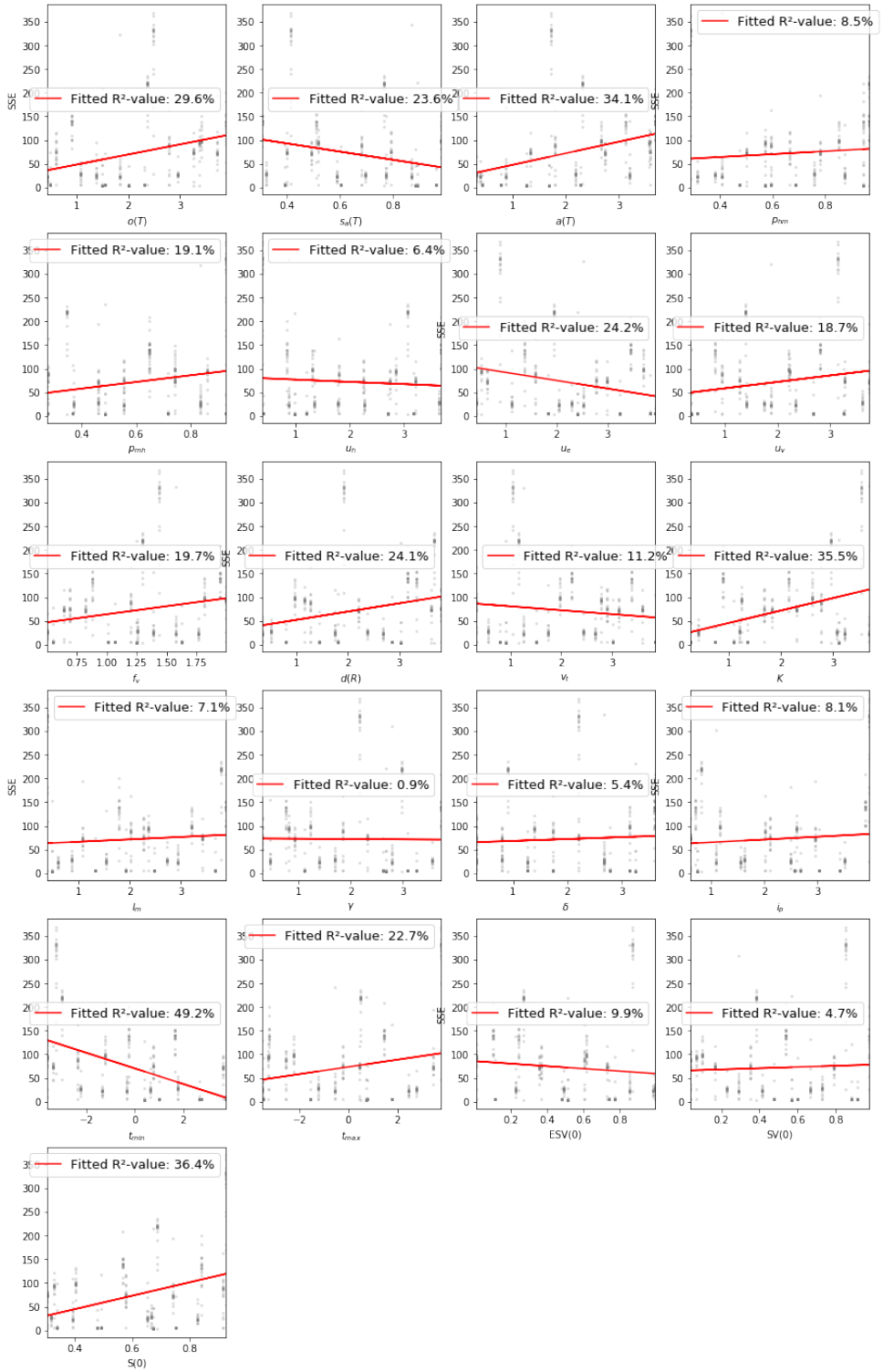

Figure 43 – Sensitivity Analysis residues regarding sum of square errors (SSE) from model simulations and simulations parameters with the respecting range of possibilities: $O_t(T)$(0.25-4), v_t(0.25-0.4), K (0.25, 4), $a(T)$ (0.25-4), i_m (0.25-4), p_{mh} (0.25-1), p_{hm} (0.25-1), f_v (0.25-1.5), u_e (0.25-4), u_v (0.25-4), δ (0.25-4), γ (0.25-4), i_p (0.25-4), u_h (0.25-4), $sa(T)$ (0.25-4) ; for Fortaleza

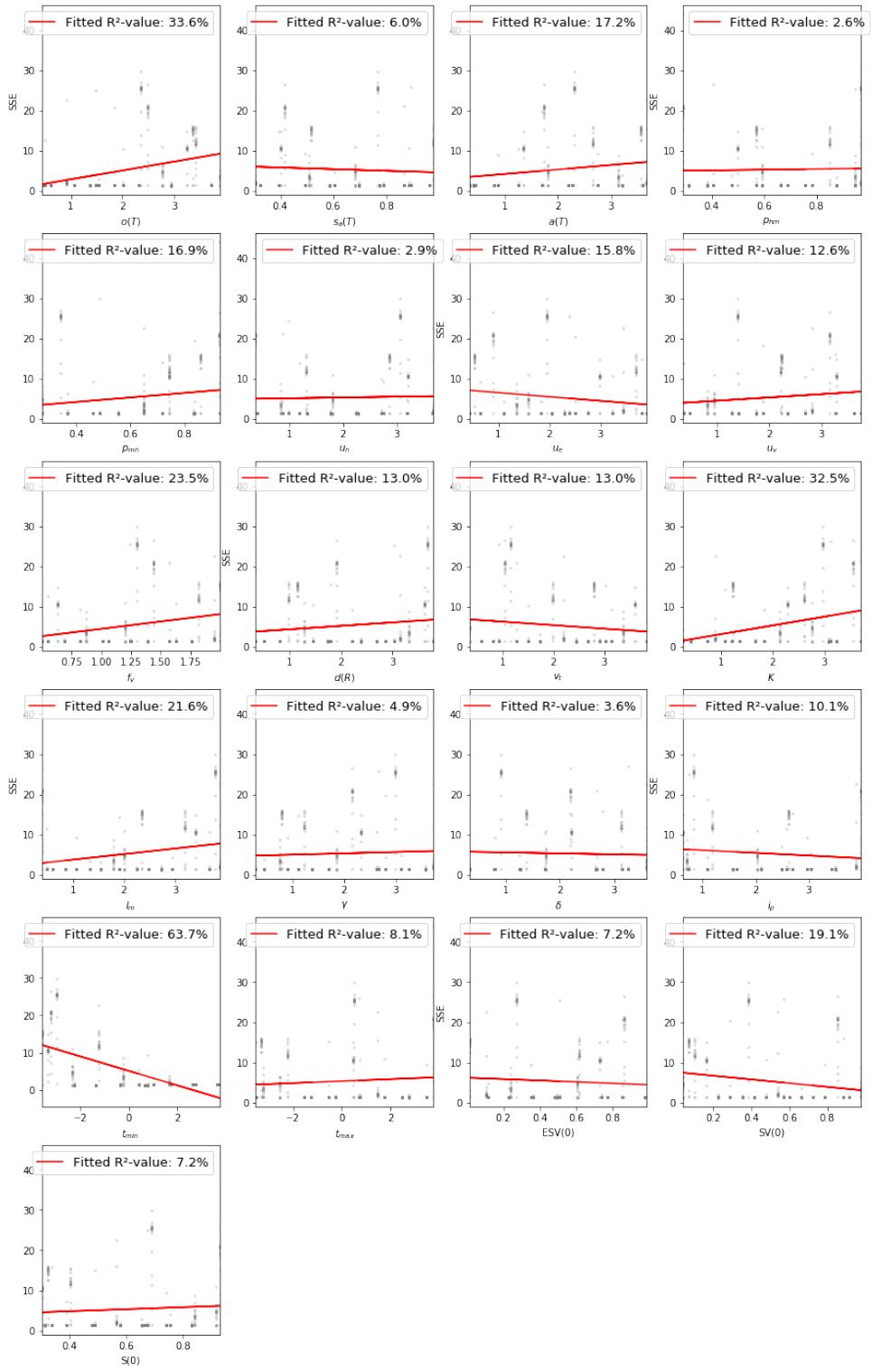

Figure 44 – Sensitivity Analysis residues regarding sum of square errors (SSE) from model simulations and simulations parameters with the respecting range of possibilities: $O_t(T)$(0.25-4), v_t(0.25-0.4), K (0.25, 4), $a(T)$ (0.25-4), i_m (0.25-4), p_{mh} (0.25-1), p_{hm} (0.25-1), f_v (0.25-1.5), u_e (0.25-4), u_v (0.25-4), δ (0.25-4), γ (0.25-4), i_p (0.25-4), u_h (0.25-4), $sa(T)$ (0.25-4) ; for Londrina

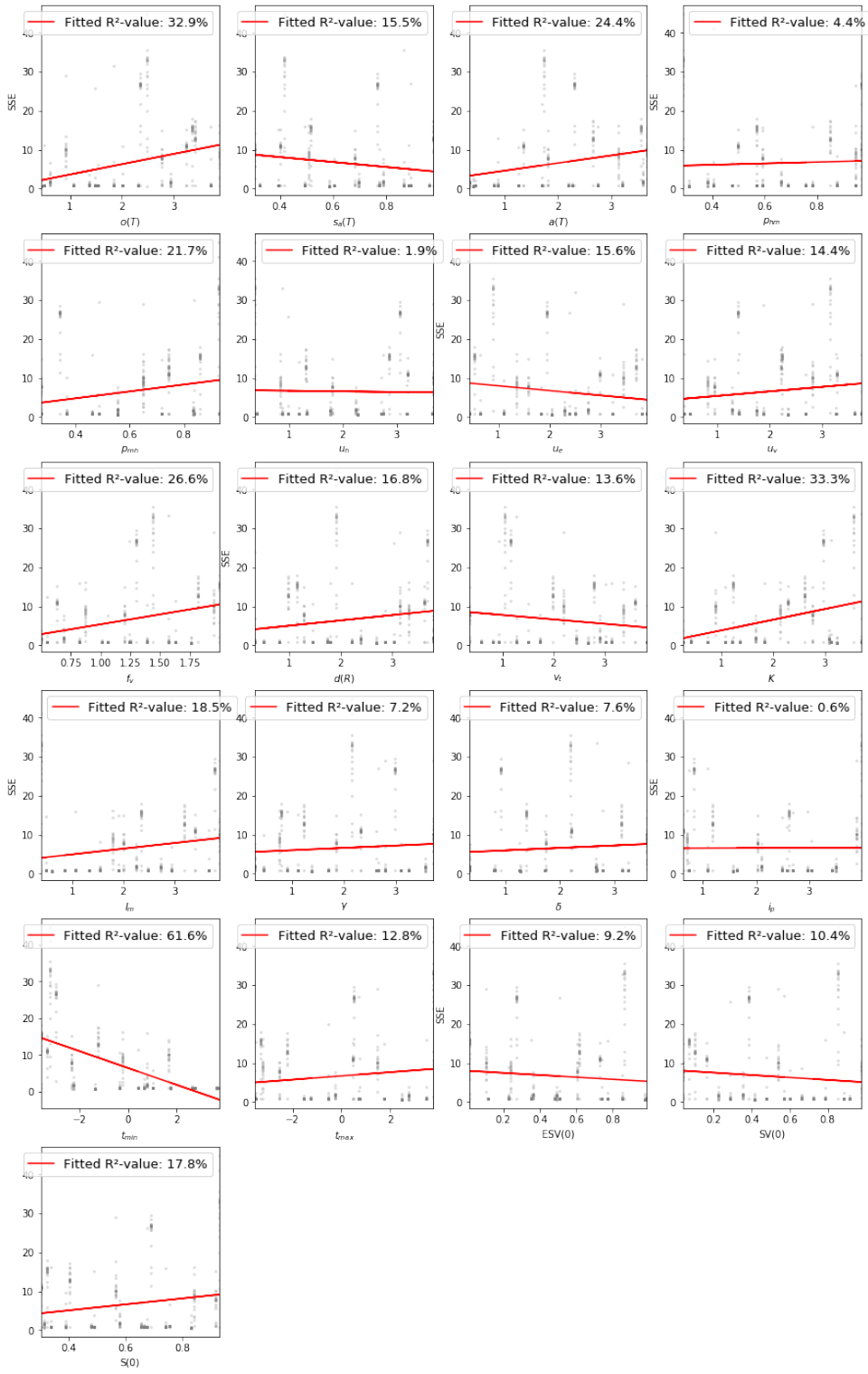

Figure 45 – Sensitivity Analysis residues regarding sum of square errors (SSE) from model simulations and simulations parameters with the respecting range of possibilities: $O_t(T)$(0.25-4), v_t(0.25-0.4), K (0.25, 4), $a(T)$ (0.25-4), i_m (0.25-4), p_{mh} (0.25-1), p_{hm} (0.25-1), f_v (0.25-1.5), u_e (0.25-4), u_v (0.25-4), δ (0.25-4), γ (0.25-4), i_p (0.25-4), u_h (0.25-4), $sa(T)$ (0.25-4) ; for Serra

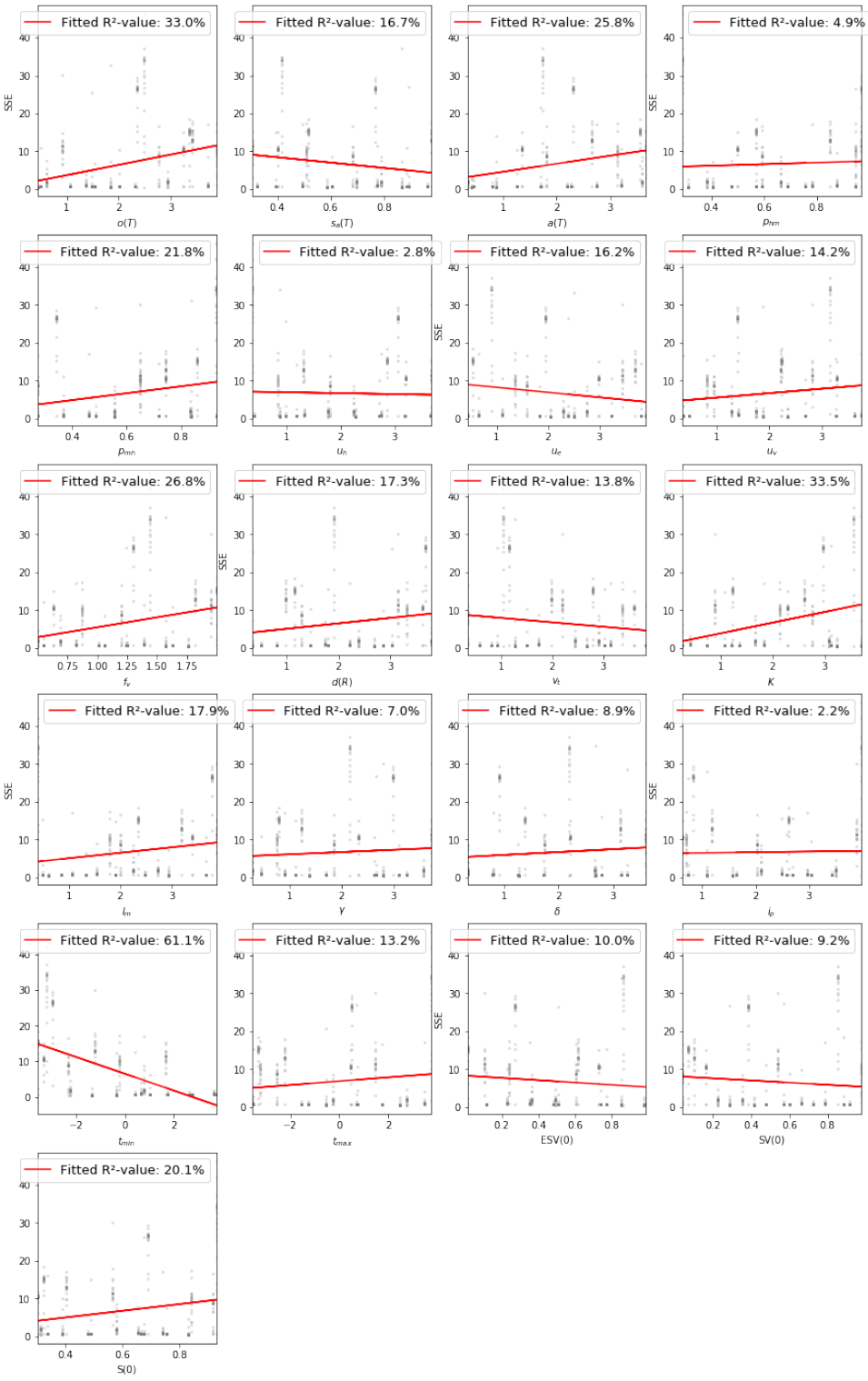

Figure 46 – Sensitivity Analysis residues regarding sum of square errors (SSE) from model simulations and simulations parameters with the respecting range of possibilities: $O_t(T)$(0.25-4), v_t(0.25-0.4), K (0.25, 4), $a(T)$ (0.25-4), i_m (0.25-4), p_{mh} (0.25-1), p_{hm} (0.25-1), f_v (0.25-1.5), u_e (0.25-4), u_v (0.25-4), δ (0.25-4), γ (0.25-4), i_p (0.25-4), u_h (0.25-4), $sa(T)$ (0.25-4) ; for Vila Velha

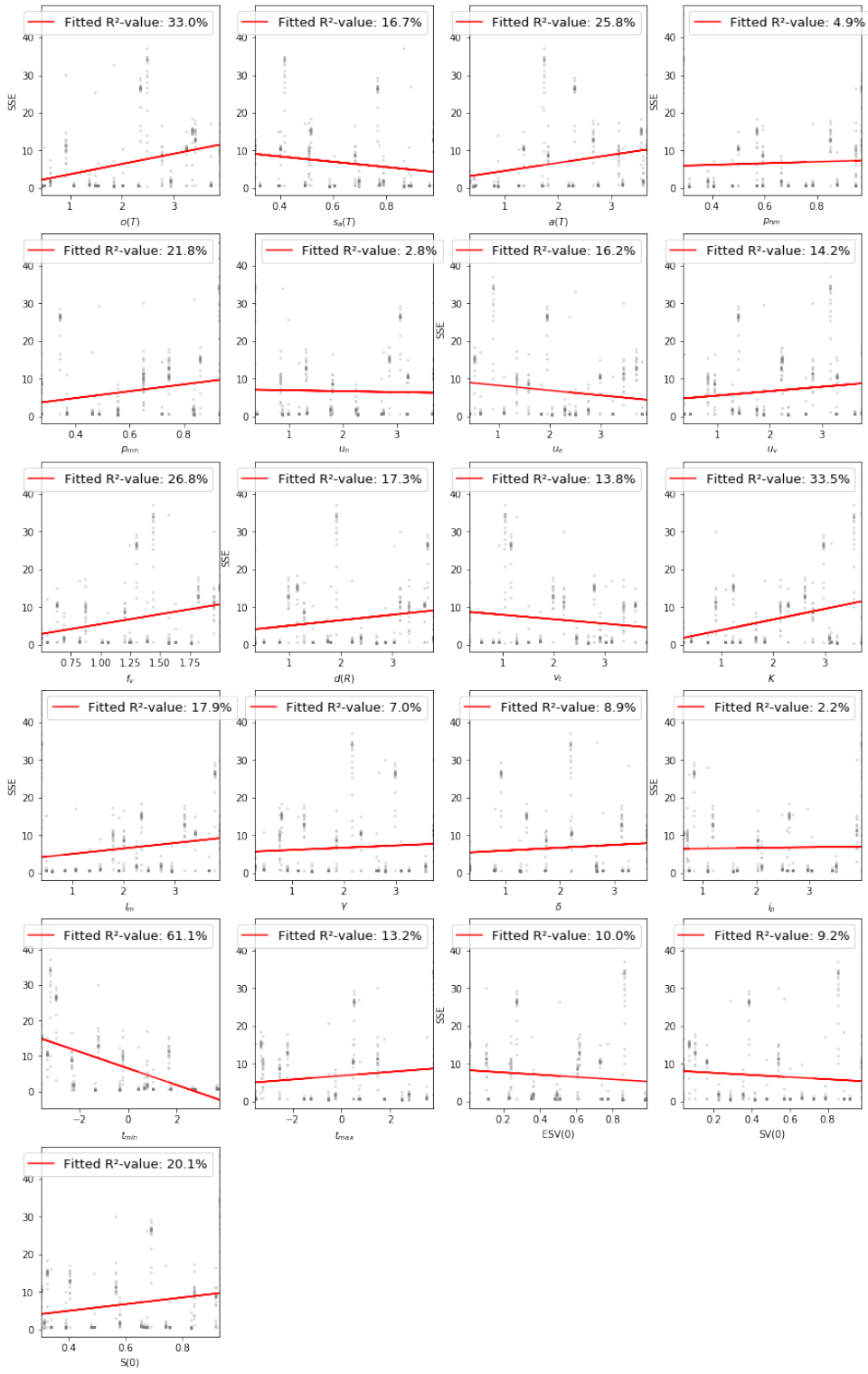

Figure 47 – Sensitivity Analysis residues regarding sum of square errors (SSE) from model simulations and simulations parameters with the respecting range of possibilities: $O_t(T)$(0.25-4), v_t(0.25-0.4), K (0.25, 4), $a(T)$ (0.25-4), i_m (0.25-4), p_{mh} (0.25-1), p_{hm} (0.25-1), f_v (0.25-1.5), u_e (0.25-4), u_v (0.25-4), δ (0.25-4), γ (0.25-4), i_p (0.25-4), u_h (0.25-4), $sa(T)$ (0.25-4) ; for Joinville